12-2015

Fluvial Deposition, El Nino and Landscape Construction in Northern Coastal Peru

Paul M. Pluta
University of Maine

FLUVIAL DEPOSITION, EL NIÑO AND LANDSCAPE CONSTRUCTION IN NORTHERN COASTAL PERU

By

Paul M. Pluta

B.A. Temple University, 2010

A THESIS

Submitted in Partial Fulfillment of the

Requirements for the Degree of

Master of Science

(in Quaternary and Climate Studies)

The Graduate School

The University of Maine

December 2015

Advisory Committee:

Daniel H. Sandweiss, Professor of Anthropology and Quaternary and Climate Studies, Co-Advisor

Alice R. Kelley, Assistant Research Professor of Quaternary and Climate Studies, Instructor of Earth and Climate Sciences, Co-Advisor

Gregory Zaro, Associate Professor of Anthropology and Climate Change

Daniel F. Belknap, Professor of Earth and Climate Sciences

FLUVIAL DEPOSITION, EL NIÑO AND LANDSCAPE CONSTRUCTION IN NORTHERN COASTAL PERU

By Paul M. Pluta

Thesis Co-Advisors: Dr. Daniel H. Sandweiss and Dr. Alice R. Kelley

An Abstract of the Thesis Presented
in Partial Fulfillment of the Requirements for the
Degree of Master of Science
(in Quaternary and Climate Studies)
December 2015

The El Niño global climate anomaly is a major cause of weather variation that can have far-reaching effects on human populations around the world. Northern coastal Peru is an area of historically major impacts where strong El Niño events have resulted in catastrophic flooding and mass wasting, leading to significant social disruption. There is a growing body of literature on the prehistoric chronology of El Niño and how it affected human populations of the past, but more work is needed. In order to address the timing and characteristics of past El Niño events I investigated the alluvial sedimentary sequences at two archaeological sites of the Moche Period, San José de Moro and Huaca del Sol, to infer patterns of past El Niño flooding. Both sites are located adjacent to braided rivers and are constructed on floodplains composed of thick alluvial sequences that are reflective of some aspects of the region's past climate.

San José de Moro is located along the Chamán River, just north of the city of Chepén. Due to the limited size of the river's drainage basin and the extremely dry nature of the regional environment, flooding is limited to periods of El Niño rainfall and all alluvial deposits at San José de Moro are thus thought to be El Niño related. The

exposed sedimentary sequence at the site reveals a prominent shift from broad, relatively flat floodplain deposits to cross-bedded, channelized deposits, which may have resulted from several causes, including channel avulsion, a change in stream character related to vegetation stabilization, a change in river base level, stream capture, or a change in climate resulting in an increase in the intensity or frequency of precipitation events. An increase in precipitation may be related to an increase in El Niño activity.

Huaca del Sol is located along the Moche River, near the city of Trujillo. The Moche River has a much larger drainage basin and extends much higher into the Andes Mountains than the Chamán River. Because of this, flooding may be caused by non-El Niño events but El Niño is still one of the major sources of flooding within the drainage. At Huaca del Sol the stratigraphic sequence has significant textural variation throughout, and is consistent with a pattern of regular shifting and avulsion characteristic of braided streams. There is thus no clear evidence of any environmental changes having a significant effect on the stratigraphic sequence at the site.

Both San José de Moro and Huaca del Sol are located on floodplain surfaces created at least in part by El Niño-driven aggradation that produced broad, elevated areas with decreased risk of El Niño flooding. The presence of these sites on this landscape shows that this environment was attractive for both occupation and ceremonialism. These results demonstration that in addition to being a cause of weather variation and catastrophism, El Niño should also be seen as a constructor of favorable landscapes that is essential to understanding the physical setting of prehistoric human settlements in northern coastal Peru.

ACKNOWLEDGEMENTS

This thesis was made possible by financial support from the National Science Foundation Award ARC-1152156 to Jeffrey Quilter (Harvard University). I am greatly indebted to Dr. Quilter for allowing me to pursue my research under his grant.

Thanks to Dr. Luis Jaime Castillo Butters and the rest of the crew at El Proyecto Arqueológico San José de Moro as well as Dr. Santiago Uceda Castillo and the crew at Huaca del Sol for welcoming me to their sites and providing assistance throughout the fieldwork process. María Claudia Herrera of El Proyecto Arqueológico San José de Moro was particularly helpful, offering her help in the field, as well as providing resources, information and moral support throughout the entirety of this project.

I would also like to thank Ana Cecilia Mauricio and Sofya Yelizarova for their invaluable assistance in the field. Dr. Joseph Kelley, Dr. Martin Yates and Kara Jacobacci were all enormous help with various aspects of the laboratory analysis. Dr. David Keefer graciously offered his knowledge and advice in support of my thesis. Jessica Whelpley and Jamie Fornier Wren both provided assistance in the lab as well as intelligent feedback and greatly needed moral support throughout the writing process. My committee members, Dr. Gregory Zaro and Dr. Daniel Belknap were both excellent sources of support and advice. Greg always provided a smiling face and thoughtful guidance whenever I came to him with questions or issues. Dan's help showing me my way around the Sedimentology Lab was key to the research of this thesis, and he was very helpful in assisting me in interpreting the results of my analysis.

I am extraordinarily grateful to my advisors Dr. Daniel Sandweiss and Dr. Alice Kelley. Both Dan and Alice took the time out of their busy schedules to thoughtfully guide me in my education, and I learned an immense amount from both. They have shown great dedication to my success, patience with my shortcomings and made sure that I got the most out of my time at the University of Maine. Either Dan or Alice alone would have made an excellent advisor, to have both was more than any burgeoning scholar and scientist could hope for.

Finally, thanks to my friends and family, especially my parents, for all of their love and support.

TABLE OF CONTENTS

LIST OF TABLES

LIST OF FIGURES

CHAPTER 1

INTRODUCTION AND BACKGROUND

Introduction

The effects of the El Niño climate phenomenon are widely felt, echoing in varying manners and intensities around the globe, and the phenomenon is known to have significant and, at times, devastating effects on human populations. Nowhere is this more apparent than northern coastal Peru, where an increase in sea-surface temperature impacts the productivity of local fisheries and can lead to torrential rainfall, resulting in flooding and debris flows in an area that rarely sees more than a few centimeters of rain in a normal, non-El Niño year.

There is a growing body of literature of the past chronology of El Niño, but more work is needed. The level of social disruption it causes in modern times suggests that it was of enormous significance to anyone living on the coastal plain of prehistoric Peru. The potential impact of El Niño is important to understand in light of the unique cultural trajectories of the region. This thesis project was born out of the goal of adding to our knowledge of El Niño's past by looking at flood deposits as proxies for prehistoric El Niño events.

In approaching this objective the author, along with Dr. Daniel Sandweiss, Dr. Alice Kelley and the enthusiastic assistance of many others, investigated the fluvial sedimentary sequences underlying the Moche occupations at two important archaeological sites: San José de Moro, located along the Chamán River, and Huaca del Sol, in the Moche River Valley. Stratigraphic profiles were exposed and analyzed at both of these sites. Sections were carefully drawn and described, and a column sample was collected from each profile. The author carried out textural analyses in the University of Maine sedimentology laboratory to provide information for a more thorough and detailed interpretation.

Results at San José de Moro show an abrupt shift from broad, fine-grained floodplain deposits to coarser-grained, cross-bedded channelized deposits that may indicate a change in channel location or an increase in flood velocity, either potentially resulting from a significant increase in the strength of El Niño events or one of several other sources. We also discovered evidence for agriculture at San José de Moro in the form of agricultural furrows directly below the earliest recognized Moche occupation and probable maize starch grains within and below the furrows. At Huaca del Sol the profile consisted of alternating strata of fine and course sediments, consistent with braided river channels undergoing avulsion during events of high flow. There is no strong evidence for any climatic or environmental changes within the profile. There were also several manuports in the profile as far as 2.45 m below the earliest recognized Moche occupation. The data from both sites indicate they exist on surfaces created at least in part by El Niño-driven aggradation that produced broad, elevated areas with reduced risk of El Niño flooding. In the Cháman drainage, El Niño flooding is the only source of surface-driven flow. At Huaca del Sol, high-flow events correspond to El Niño flooding combined with annual seasonal rains and glacial melt. These sites, therefore, show El Niño to be an important part of the story of landscape development in coastal Peru that is integral to understanding the physical setting of prehistoric human settlements in this region.

Outline of Thesis

The five chapters in this thesis present alluvial sequences from two major archaeological sites, contextual information necessary to the interpretation of these sites and an explanation of their implications on paleoclimate and the prehistoric inhabitants of coastal Peru. The present chapter, Chapter One, provides an introduction to the research questions and approach of this thesis. It covers relevant background information on the environmental and cultural context of the study area. Chapter Two details the field and laboratory methods used in the study. Chapters Three and Four present the results of analysis at San José de Moro and Huaca del Sol, respectively. Finally, Chapter Five discusses the implications of the results, presents the conclusions of the study and suggests directions for future work.

Background

The coastal desert of Peru consists of a narrow coastal plain running northwest to southeast, sandwiched between the immense Andes Mountain Range and the Pacific Ocean. It is characterized by extreme aridity, only broken by the rivers that drain the slopes of the western Andes. These rivers cross the desert at an orientation perpendicular to the coastline and flow into the Pacific Ocean. The vast wall of mountains to the east creates a rain shadow that blocks the movement of precipitation from the Atlantic Ocean/Amazon Basin. Under non-El Niño conditions the cold waters of the Humboldt Current cool the air at sea level, resulting in a thermal inversion that can produce substantial amounts of fog and stratus clouds but does not produce significant rainfall. The limited precipitation that is produced increases gradually with elevation up the slopes of the Andes. In the austral summer, solar radiation reflects off the desert coast's barren ground surface, causing humid air to rise as it moves inland with onshore winds. This humid air cools at higher altitudes along the slopes of the Andes, where it can condense and fall as seasonal rainfall in the highlands. In contrast, cooler temperatures during the austral winter keep humid air from rising more than a few hundred meters, resulting in dense fog and clouds that hover over the coast but yield little to no rainfall. In the Chamán River basin average annual precipitation ranges from 50 mm in the lower valley to 400 mm near its source (Vílchez et al. 2007). The larger Moche River basin ranges in average annual precipitation from a few millimeters along the coast to 1200 mm at its source (MINEM 1997).[1] During El Niño conditions, however, the western side of the Andes in Peru can receive significantly more precipitation. For example, in the Jequetepeque Valley, in which the Chamán River is located, El Niño has been calculated to increase precipitation by as much as 564 mm in some places (Vílchez el al. 2007). In the Moche Valley one location has recorded 1340 mm more during an El Niño year than it has on its peak non El Niño year (MINEM 1997).

The archaeological site of San José de Moro is located along the bank of the braided Chamán River in the northern Jequetepeque Valley, approximately 5 km north of the city of Chepén, La Libertad (Figure 1.1). Because of its position in the river's floodplain, the depositional environment at San José de Moro is dominated by fluvial processes. The Chamán River is a braided stream that receives very little to no flow

[1] Although it is not explicitly stated in either MINEM (1997) or Vílchez et al. (2007), these annual averages presumably include El Niño years. If this assumption is correct then the average annual precipitation would almost certainly be lower if El Niño years were removed from the calculations. Furthermore, Vílchez et al. (2007) indicate that there are only two stations where precipitation is recorded in the Chamán River's drainage basin. One is in San Gregorio, which appears to be very near the basin's uppermost point, from which the maximum average annual precipitation in the range was collected. The location of the lower elevation station is not given other than being in "the valley." Stations in the Jequetepeque's lower drainage basin have average annual precipitation values as low as 29.6 mm. For this reason I believe it is possible that the actual lowest annual average precipitation value in the Chamán basin is even lower than 50 mm.

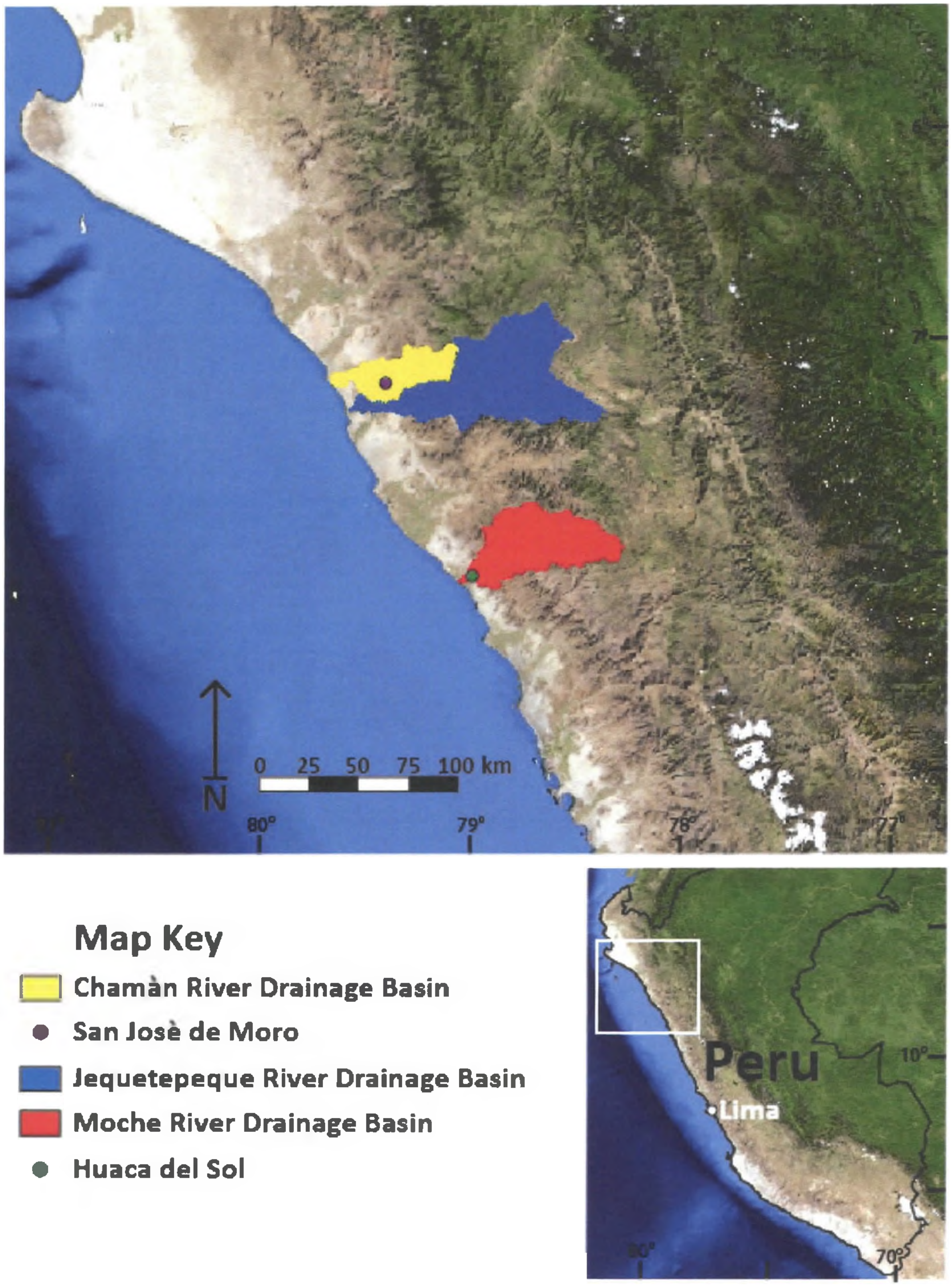

Figure 1.1. Locations of San Josė de Moro, Huaca del Sol and drainage basins discussed in the text.

	Chamán	Jequetepeque	Moche
Length (km)	80	161	102
Drainage Area (km^2)	1124	3961	2708
Highest Elevation (masl)	3521	4201	4200

Table 1.1. Estimated dimensions of the drainage basins discussed in the text. Data for the Moche basin from MINEM (1997). Data for Chamán and Jequetepeque Basins estimated using geographic information system software (ArcGIS) analysis of ASTER Global Digital Elevation Model, version two (product of METI and NASA, distributed by the Land Processes Active Archive Center, located at USGS/EROS, Sioux Falls, South Dakota).

during normal conditions. The river's drainage basin is relatively small, and it does not reach a high enough elevation to receive adequate seasonal rainfall to cause flooding during normal non-El Niño years (Table 1.1). During El Niño years, however, the Chamán River can experience significant flooding. In fact, for this reason it is also referred to as the Rio Loco de Chamán (the Crazy River of Chamán), or simply, the Rio Loco. Based on this phenomenon, it is presumed that the Chamán floodplain at San José de Moro is composed primarily of fluvial sediments deposited during El Niño flood events. San José de Moro is thus an ideal place to investigate flooding caused by El Niño.

Huaca del Sol is located southeast of the Moche River and just outside the city of Trujillo, La Libertad. Although small compared to the Jequetepeque Valley as a whole, the Moche River is much larger than the Chamán River and extends further and higher into the Andes Mountains (Figure 1.1 and Table 1.1). For this reason, the Moche River experiences higher annual flows and floods from seasonal high precipitation events in addition to El Niño rainfall. The fluvial sequence at Huaca del Sol is therefore interpreted to consist largely of flood deposits from both seasonal and El Niño sources. Strong El Niño events, however, can produce much more rainfall than the average seasonal variation. The recording station at Quiruvilca, for example, located near the source of the Moche River at about 4000 masl, has received as much as 1400 mm in non-El Niño conditions. During El Niño it has received up to 2740 mm (MINEM 1997), an increase of over 100%.

Depositional Influences

The Chamán and Moche Rivers are both braided streams. Braided streams generally form in areas with a relatively steep slope, a large amount of bedload-sized particles available for transport and where banks are easily eroded (Collinson 1986a; Waters 1992). The topographic variability of western Peru provides steep slopes for rivers flowing out of the Andes, and the arid nature of the region means there is limited vegetation, increasing the ability for loose sediment to become entrained by fluvial processes. The abundance of sediment causes channels to become choked with their own accumulated alluvium, creating gravel and sand bars. Braided streams are characterized by multiple channels that diverge and converge around these bars (Miall 1977; Waters 1992; Boggs 2012). Vegetation stabilization is also an important factor in determination of whether a stream will be meandering or braided – unvegitated banks are more susceptible to rapid migration and the formation of braided systems (e.g., Hupp and Osterkamp). During periods of low flow, there is little erosion or movement of sediment and the river is essentially stable. During high flow conditions large amounts of erosion and sediment transport take place resulting in the shifting, migration, formation and destruction of channels and bars (Boggs 2012).

Braided stream deposits are generally characterized by channel structures filled with cross-bedded and flat-bedded sands.[2] In many types of fluvial deposits, entrained particles settle out when the flow drops below a critical velocity, which is higher for larger particles. Particles, therefore, generally settle in order of size from more coarse to more fine. As a result, fluvial deposits commonly display a fining upwards sequence, with coarser sediments at the bottom and finer sediments at the top of each sedimentary unit (Boggs 2012).

When water spills over the bank onto the floodplain the load is generally dominated by suspended particles, resulting in finer-grained deposition than is seen in the channel. Floodplain deposits also tend to become finer with greater distance from the channel, and are broad and horizontally layered. Only very large floods deposit more than a few centimeters of sediment (Collinson 1986a).

The locations of San José de Moro and Huaca del Sol along the banks of rivers suggest that fluvial processes are the primary source of sediment deposition observed at each site. Aeolian processes, however, also have the potential to affect either site. In an arid environment, such as coastal Peru, limited vegetation and relatively little moisture increase the ability of wind to entrain and transport sediments. Wind erosion and transport of unvegetated flood sediments can produce deposits of medium to fine-grained sand characterized by large-scale cross-bedding (Bagnold 1941; Collinson 1986b).

[2] Braided stream deposits are also generally described as consisting almost exclusively of gravel and sand. As will be shown in Chapter 3, channelized deposits at San José de Moro contain a significant amount of silt/clay. Although many, perhaps most, braided streams do consist almost exclusively of sand and gravel, Bridge (2003) and Boggs (2012) point out that many braided rivers do in fact contain finer grained sediments, contrary to the orthodox characterizations.

El Niño

The term El Niño refers to the warming of ocean water that occurs off the Pacific coast of South America. It typically occurs every three to seven years, beginning in December and lasting for several months. There is a large degree of variability in both intensity and duration of these events. El Niños are associated with an inversion in the arrangement of surface air pressure over the Pacific Ocean. Generally, average air pressure at sea level over the warm waters of the western Pacific is lower than that of the colder southeastern Pacific. This creates what is known as the Walker Cell, where air rises over the western Pacific, descends in the southeastern Pacific and moves from east to west over the sea-surface as the easterly trade winds. During El Niño events, however, surface air pressure increases in the west and decreases in the east, weakening the trade winds. In the west, sea level drops and the ocean thermocline becomes shallower. In the east, sea level rises and the thermocline becomes deeper. This suppresses the upwelling of the Humboldt Current along the coast of South America, and results in warmer sea-surface temperatures. The suppression of upwelling and change in water temperature causes a decrease in marine productivity, and greatly affects the yield of fisheries that are important as a human food source and a basis for the local coastal ecosystem. The warmer sea-surface temperatures also result in increased precipitation along the South American coast and throughout the eastern Pacific (Philander 1985; Maasch 2008).

Although there is still much to be learned, a general chronological sequence of El Niño has been established through a variety of environmental proxies (discussed in detail in Sandweiss et al. 2007). Evidence suggests that El Niño was active during the initial human occupation of Peru at roughly 14,000 cal yr BP (e.g., Keefer et al. 1998, 2003;

Rodbell et al. 1999; Rein et al. 2005). Quebrada Tacahuay, one of the earliest sites in coastal Peru, has produced evidence of El Niño-induced debris flows directly above and below an occupational surface dated between ca. 12,700 and 12,500 cal yr BP (Keefer et al. 1998) (see Figure 1.2 for the location of archaeological sites mentioned in the text). The intensity and frequency of El Niño remains uncertain between the first human occupation and ca. 9,000 cal yr BP. After ca. 9,000 until ca. 5,800 cal yr BP, there appears to be a hiatus in El Niño activity; it was either completely absent or occurrences were extremely rare (Rollins et al. 1986; Sandweiss 2003; Sandweiss et al. 1996, 2007). Carré et al. (2014) suggest that this may represent a temporary shift in the effects of El Niño from the eastern Pacific and the coast of Peru to the central Pacific. Activity in coastal Peru appears to have resumed ca. 5,800 cal yr BP, although the frequency was lower than today (Rollins et al. 1986; Sandweiss et al. 1997, 2001, 2007). At 3,000 cal yr BP El Niño increased in frequency, essentially reaching modern levels (Sandweiss et al. 2001, 2007). While many details are still in question, these major shifts provide a basic framework upon which we can continue to build our knowledge about Peru's climatological past and speculate on the impacts of El Niño on prehistoric humans.

There are multiple lines of evidence useful in reconstructing El Niño prehistory. Below is a summary of some the important studies that have been undertaken to investigate this topic. A more detailed summary discussing most of these studies can be found in Sandweiss et al. (2007).

Figure 1.2. Locations of archaeological sites mentioned in the text. 1. Siches; 2. San José de Moro; 3. Puemape; 4. Huaca del Sol; 5. Cerro Arena; 6. Ostra Complex; 7. Quebrada Tacahuay; 8. Quebrada de los Burros.

It has been recognized that north of approximately 10°S latitude molluscan and fish assemblages in both archaeological and paleontological contexts undergo a shift from warm water to cold water species at 5,800 cal yr BP (Rollins et al. 1986; Reitz and Sandweiss 2001; Sandweiss et al. 1996, 2001, 2007). Areas south of 10°S latitude prior to 5,800 cal yr BP, and throughout coastal Peru after this date are characterized by cold water marine assemblages. The pre-5,800 cal yr BP presence of warm water species is interpreted to indicate variations in the strength or path of the Humboldt Current. As El Niño is characterized by a warming of sea-surface temperatures on the Peruvian coast, the permanent presence of warm water has strong significance regarding El Niño behavior. The already warm sea-surface conditions are not likely to see El Niño-like interannual variation in temperature, thus suggesting that El Niño did not exist in this area during this period.

After ca. 5,800 cal yr BP molluscan assemblages begin to consist primarily of *Choromytilus chorus* and *Mesodesma donacium.* These cold water species are both extremely sensitive to warm water, and die off during El Niño events. The abundance of these species north of Lima between 5,800 and 3,000 cal yr BP suggest largely colder water, which precludes an El Niño frequency like that of today. If El Niño existed during this time period it must have been at a lower frequency. Both species disappear in the north and central coast of Peru at ca. 3,000 cal yr BP. This is interpreted to be a result of increased sea-surface temperatures tied to increased El Niño frequency at this time, which would have created conditions in which *Choromytilus chorus* and *Mesodesma donacium* were unable to survive (Sandweiss et al. 2001, 2007).

Further supporting evidence of changes in ocean temperature is provided by geochemical analysis at two sites: the Ostra complex and Siches (Andrus et al. 2002, 2003, 2005; Sandweiss et al. 2007). Delta ^{18}O values from calcium carbonate in the growth increments in fish otoliths and mollusk shells at both locations indicate that between ca. 6,800 and 5,800 cal yr BP the average sea-surface temperature was approximately 3-4°C warmer than today. The two sites studied, however, provided differing results in regards to seasonality. At the site of Siches, seasonal changes in sea-surface temperature were of the same magnitude as those of today, only offset by 3-4°C. Seasonal data from the other site, the Ostra Base Camp, indicate that winter sea-surface temperatures were about the same as today, but that summer temperatures were significantly warmer. The meaning of the seasonal variation discrepancy between Siches and Ostra is not understood, but delta ^{18}O from both sites clearly indicate that prior to ca. 5,800 cal yr BP the average sea-surface temperature was higher than today (Andrus et al. 2002, 2003, 2005; Sandweiss et al. 2007).

The normally dry conditions west of the Andes mean that the impact of rainfall brought by El Niño events has unique consequences, many of which are very visible and distinguishable. Landslides and floods can cause significant destruction, but they also leave behind distinct signs that can be used to interpret El Niño's past. Sedimentological research is thus an invaluable tool for developing chronologies and understanding processes of this climatic phenomenon.

At the site of Quebrada Tacahuay in the southern coastal plain, Keefer et al. (1998, 2003) discovered deposits they interpret as debris flows and sheet or channelized flows caused by El Niño events. Radiocarbon and relative dating allowed for some general chronological reconstruction. The site's earliest occupation level is dated to approximately 12,700 to 12,500 cal yr BP, and overlies debris flow and flood deposits that are similar to later El Niño-caused deposits. While the deposits are not clearly dated themselves, they indicate a strong likelihood that El Niño events were present during the Late Pleistocene and Early Holocene. Four large debris flow deposits and a large sheetflow deposit dating to between approximately 12,500 and 8,900 cal yr BP are located stratigraphically above the lower occupation level. This averages out to one large-scale sedimentary event every 700 to 800 years. Between approximately 8,900 to 8,700 cal yr BP and 5,300 cal yr BP, only two thin flood deposits and no debris flow deposits are present. These flood deposits were confined to a small channel and only exposed in one profile, and suggest much smaller scale events. At ca. 5,300 cal yr BP a large debris flow covered the site. The incision of the current main channel cut off sediment supply, so no later events could be distinguished. Although the start date is ca. 100-200 year later than that proposed by Sandweiss et al. (2007), the sedimentary sequence at Quebrada Tacahuay supports the idea of a hiatus, or limited frequency manifestation, of El Niño before ca. 5,800 cal yr BP.

Like Quebrada Tacahuay, a series of debris flows is also present at Quebrada de los Burros. It also has a large hiatus, in this case dated between ca. 9,600 and 3,400 cal yr BP, which includes the period of El Niño paucity suggested by Sandweiss et al. (2007). During this time period the site's sedimentary record consists of organic layers indicative of increased moisture in the region, which is believed to be inconsistent with conditions that would be present if El Niño were prevalent (Fontugne et al. 1999).

Wells (1987, 1990) describes a sequence of overbank flood deposits from the Casma River in northern Peru. Four of the 32 radiocarbon dates were reversed, raising concern regarding the choice of materials used, the potential for mixing of material or incorporation of older detrital material. This illustrates the potential problems when dating erosive events such as floods and landslides using flood transported debris. The biggest success of Wells' work was identifying likely candidates for floods known from the historic record, which is beyond the scope of this thesis. In her stratigraphic sequence 18 flood events were recognized, 13 of which were dated to the last 3,200 years. Although the flood events pre-dating 3,200 years are not dated, Wells concludes that the minimum frequency during the past 7,000 years is one El Niño event every 1,000 years (Wells 1990).

The extremely dry desert environment of coastal Peru precludes the existence of lakes in the region. A lake core from the Ecuadorian Andes, however, provides some potentially useful information. In this core from Laguna Pallcacocha, Rodbell et al. (1999) and Moy et al. (2002) note the presence of distinct inorganic laminae in a sequence otherwise dominated by organic deposition. It is presumed that large rainstorms washed sediment into the lake to form these inorganic layers. Correlation of the most recent part of their record with historically known occurrences of El Niño suggests that the inorganic sedimentation is a result of El Niño events. While there is regular rainfall in this region from non-El Niño sources, strong El Niño events cause precipitation well beyond background levels, and leads to a significant increase in stream discharge and sediment load into the lake. The authors use this record to estimate El Niño frequency. They determine that between ca. 15,000 and 7,000 cal yr BP El Niños were weaker than present day and occurred at a periodicity of 15 years or greater. Between ca. 7,000 and 5,000 cal yr BP events occurred at 10 to 20 and 2 to 8.5 years apart. After ca. 5,000 cal yr BP, the 2 to 8.5 year periodicity becomes dominant, and this frequency continues to present day (Rodbell et al. 1999; Moy et al. 2002).

This 15,000 year trend of gradually increasing frequency of El Niño events does not fit directly with the chronological framework previously discussed. However, there is closer agreement if the chronology is offset by 1,000 to 2,000 years. This suggests a possible latitudinal gradient where change occurred earlier in lower latitudes. The degree of compatibility of records from this region with those of coastal Peru are unknown.

Off the coast of Peru, Rein et al. (2004, 2005) were able to recover a high-resolution marine sediment record stretching back 20,000 years. Using ratios of photosynthetic pigments to lithic material, this study was able to produce a chronology of El Niño events based on the assumption that increased lithic material represents substantially increased levels of terrestrial discharge washing sediment into the ocean—almost certainly due to El Niño rainfall—while increased photosynthetic pigment represents increased ocean productivity characteristic of cold water present when El Niño is not in effect. Based on this reconstruction, they concluded that El Niño increased in strength at ca.17,000 cal yr BP, underwent a weak period between ca. 8,000-5,600 cal yr BP and reached peak strength after ca. 3,000 cal yr BP (Rein et al. 2005). This pattern correlates closely to the proposed chronological framework (Sandweiss et al. 2007). Rein et al.'s study does not discuss potential large-scale shifts in sea-surface temperature, such as those indicated by the aforementioned biogeography and delta ^{18}O studies (Rollins et al. 1986; Sandweiss et al. 1996, 2001, 2007; Andrus et al. 2002, 2003, 2005), and how they may have affected photosynthetic pigment values.

Sandweiss et al. (2007; also see Sandweiss and Quilter 2012) point out two interesting correlations between the chronology of El Niño variability and major cultural changes in coastal Peru (Table 1.2). The time when El Niño returns from its suspected hiatus ca. 5,800 cal yr BP, also marks the beginning of the Late Preceramic Period, which is characterized by the development of monumental architecture, eventually culminating in large complex centers. Such structures and complexes became common in multiple areas, and had cultural traditions that lasted through the Initial Period. Although still the subject of much debate, there is some evidence that there was significant social stratification in some of these societies. At ca. 3,000 cal yr BP the construction of monumental architecture ceases, at roughly the same time El Niño increases, and does not return for several hundred years (Sandweiss et al. 2007).

cal yr BP	**El Niño**	**Culture**
> ca. 9,000	El Niño present, frequency unknown; high risk	Fisher-hunter-gatherers living seasonally in small settlements; low complexity
ca. 9,000-5,800	El Niño absent, or present at very low frequency; low risk	Fisher-hunter-gatherer lifestyle continues with the addition of domesticated plants; Some larger settlements may have been permanent; medium complexity
ca. 5,800-3,000	El Niño present, frequency lower than the modern frequency; medium risk	Gradual beginning and eventual florescence of monumental architecture; high complexity
< ca. 3,000	El Niño increases in frequency to its modern range in variability; high risk	Monumental architecture ceases for a few hundred years; very high complexity

Table 1.2. El Niño and cultural chronology for coastal Peru. Adapted from Sandweiss et al. (2007) and Sandweiss and Quilter (2012).

While these observations are nothing more than temporal correlations, it is very possible that these coeval shifts in complexity, lifestyle and the risk people would have experienced associated with variable El Niño frequency and strength are all closely related. As we begin to link individual pieces of evidence from site-specific contexts with larger patterns that have been correlated between environmental and cultural changes, a much more detailed and illuminating picture will begin to immerge.

Cultural Context

San José de Moro and Huaca del Sol are two important archaeological sites of the Moche Culture that existed in northern coastal Peru between ca. 1,750 and 1,100 cal yr BP (Castillo and Uceda 2008). The stratigraphic sequences we investigated were located below the earliest known Moche occupations at both sites. Radiometric dating of the stratigraphy is incomplete at the time of writing, so deposits cannot yet be temporally correlated with the prehistoric cultures of the region. The cultural record for the time between the 5,800 cal yr BP onset of El Niño and the Moche occupations at San José de Moro and Huaca del Sol is not well known in the region, but includes some very important cultural changes. This span of time and the development of the Moche culture are briefly summarized below.

Coastal Peru underwent a shift 5,800 years ago from the Middle to the Late Preceramic period. Prior to this, during the Middle Preceramic, many mobile hunter-gatherer groups were settling down. Sedentary or semi-sedentary village sites were becoming larger and more common, groups of people were undertaking more public works projects, and domesticated plants were increasing in importance. The Late Preceramic period represents a great intensification of these trends. After this point, people began constructing large-scale monumental architecture along the coast between Lima and the Lambayeque Valley (e.g., Hass et al. 2004; Sandweiss et al. 2007, 2009, 2010). Extensive long-distance exchange, farming, social complexity and use of cotton textiles all also appear at this time. Subsistence was based primarily on a combination of marine resources and both domesticated and wild plants (Quilter 1991). The Late Preceramic Period lasted until ca. 3600 cal yr BP.

Beginning ca. 3,600 cal yr BP, the culture history of coastal Peru exhibits some significant changes that mark the start of the Initial Period, which would last until approximately 2,900 cal yr BP. Ceramic technology was adopted, agriculture continued to grow in importance, the size of monumental structures increased, and the range of monumental architecture expanded both north and south (Moseley 2001; Sandweiss et al. 2007). The Cupisnique culture developed between the Lambayeque and the Víru valleys (Burger 1992; Salazar-Burger and Burger 1996; Nesbitt 2012). The origin of the Cupisnique culture is highly debated; while some people feel it is primarily the product of diffusion of the Chavín culture, others believe it developed independently and may have even inspired some Chavín innovations (Shimada 1994; Elera 1993, 1998). As with many archaeological cultures, Cupisnique was initially defined by its ceramic tradition. Cupisnique ceramics are characterized by grey to black reduced monochrome finish and incised-line and sculptural representations of people, animals and plants (Shimada 1994). The iconographic styles associated with Cupisnique ceramics have since also been found to adorn architecture and rock art. Cupisnique monumental architecture generally consists of rectangular terraced platforms constructed of stone and conical adobes. As in the Late Preceramic Period, Cupisnique subsistence combined coastal and terrestrial resources. Sites have produced a large number of domesticated plants, including cotton, gourds, squash, acacia, chili peppers, avocado, lucuma, beans, maize and peanuts, as well as a large number of marine animals and deer and llama (Pozorski 1983; Elera 1998; Nesbitt 2012).

Cupisnique culture continues into and throughout the Early Horizon, which stretches from ca. 2,900 to 2,400 cal yr BP. The late Initial Period and the Early Horizon are characterized by an abandonment of the construction of monumental architecture at roughly the same time as El Niño increased frequency (Sandweiss et al. 2001, 2007). Although this period is poorly understood in the north coast, it appears that in several valleys throughout Cupisnique "territory" this halt in construction seems to have happened slightly later in time than it does further south (Nesbitt 2012). Despite this decrease in new monumental architecture, Cupisnique sees the introduction of metallurgy, the appearance of more exotic items on sites, a further increase in the reliance on agriculture and greater social stratification in funerary contexts during the Early Horizon (Elera 1993, 1998).

The Early Horizon begins at around 2,400 cal yr BP. Two new groups appear on the North Coast at this time: the Salinar and the Gallinazo (also referred to as the Virú). Both, like the Cupisnique, are primarily defined by their ceramics styles. Their relationship to Cupisnique is unclear, but both are considered by many researchers to have developed directly from the earlier tradition. Early Horizon architecture increasingly utilized stone as a building material, including for compounds, stone-faced platform mounds, and stone-lined tombs. Ground stone blades are another diagnostic technology of the period. Throughout the north coast, canals become more common and there is a further increase in the utilization of agriculture (Shimada 1994).

Salinar is often seen as a transitional phase between Cupisnique and Moche. Indeed, Puemape, one of the largest, earliest and most important known Salinar sites, was originally a Cupisnique site that was reoccupied by Salinar sometime after its abandonment (Shimada 1994; Elera 1998; Warner 2010). Cerro Arena, however, is a large, nucleated mostly residential site of Salinar construction which contains evidence for economic specialization and social stratification to a higher degree than is present in the earlier Cupisnique sites, indicating that the Salinar were likely responsible for some of the important social developments that would be adopted by the Moche (Brennan 1982).

Gallinazo style ceramics are notable for their relative uniformity over space and time. They have been variously interpreted as representing a multi-valley state level society with an urban capital (Fogel 1993) and the generally utilitarian wares of commoners that are specifically not affiliated with any specific larger state or religious formations (Castillo 2009). The latter view has some credence based on the persistence of the style on the north coast during Moche times, and the integration of the ceramics at Moche sites, including San José de Moro and the urban complex associated with Huaca del Sol (Del Carpio 2009; Uceda et al. 2009).

The Moche culture, also known as the Mochica, came into existence in the north coast of Peru approximately 1,750 cal yr BP near the start of the Early Intermediate Period. The Moche are well known for their realistic portrait vessels as well as vessels with intricate line paintings showing vividly detailed religious or mythological subjects, among other themes. Many of the subjects shown on fine line vessels are repeated in painted murals that appear in architectural contexts. The Moche also have distinctive styles of metalwork, textiles and various objects made of wood, gourds, feathers and other materials (Quilter 2002). Like the coastal societies that came before them, Moche subsistence took advantage of both marine and terrestrial resources. Agricultural intensification, however, reached a new level. Extensive canal systems were built to support more crops on fertile but arid land. All major domesticated plants and animals that reached coastal Peru before the arrival of Europeans were utilized by this time (Quilter 2002).

The exact nature of Moche culture is a matter of some controversy. It is uncertain if Moche represents a single great state, a series of smaller polities, an ethnic group, or something else. One of the more convincing arguments, put forth by Quilter (2010), is that Moche cultural cohesiveness recognized thus far in archaeological and iconographic studies points to the Moche style as primarily representing a religious cult. For the most part it is today generally considered untenable that Moche represents a single state due to the variations its archaeological signature takes on in different areas (Quilter 2002, 2010; Castillo and Uceda 2008).

San José de Moro is a Moche ceremonial center and cemetery that was established approximately 1,600 cal yr BP. It is well known for its elite burials, especially those of the Priestesses of San José de Moro. Before they were discovered here, priestesses were known through iconographic representation as an integral part of the sacrifice ceremony represented on Moche fineline vessels, but it was unknown whether or not these images represented real people. Numerous large ceramic jars and extensive work areas suggest that large amounts of chicha, a type of beer made from maize, were produced and consumed on site (Castillo et al. 2008).

Huaca del Sol is a monumental adobe structure, perhaps the largest in the New World. It is part of an immense archaeological complex that includes a second great monumental structure called Huaca de la Luna, located less than half a kilometer to the southeast. Between the two is the remains of an extensive urban center. This colossal complex is often considered to be the capital of the Southern Moche sphere (Castillo and Uceda 2008) although, as Quilter (2010) points out, there is no conclusive evidence for this supposition. The dates of the earliest occupation of the complex and of the initial construction of Huaca del Sol are both unknown. According to Uceda (2010) Huaca de la Luna was of much greater importance and focus than Huaca del Sol from its foundation until approximately 1,300 years ago. During this time, Huaca de la Luna was the subject of many new constructions and alterations. There is extensive evidence of ritual ceremony taking place on the huaca[3] and of the production of ritual items in the urban center. At around 1,300 cal yr BP large-scale construction began on Huaca del Sol, which is seen as less of a ritual center, and more of an administration center than Huaca de la Luna. At the same time production in the urban complex seems to have shifted towards more household goods and less ritual artifacts. These trends are interpreted as a relative secularization of the Huaca del Sol and Huaca de la Luna archaeological complex. This more secular orientation lasted until the end of the Moche occupation around 1,150 cal yr BP (Castillo and Uceda 2008; Uceda 2010). Our record of flood

[3] In the Quechua language of Andean South America the word "huaca" refers to a variety of sacred objects, but for the purposes of this thesis it will be used to refer to large ceremonial structures.

deposits at San José de Moro and Huaca del Sol stops during the middle of the Moche culture, so I do not review later cultural developments in this region.

CHAPTER 2

METHODS

Field Methods

Fieldwork took place in July of 2013 with the primary goal of describing and sampling alluvial sequences with potential strong El Niño influences. We investigated three stratigraphic profiles: two at San José de Moro and one at Huaca del Sol.

The two San José de Moro profiles were located in an excavation block, Area 35, of El Proyecto Arqueológico San José de Moro (PASJM), under the direction of Professor Luis Jaime Castillo Butters of Peru's Pontifical Catholic University (Figure 2.1). The author designated the profiles as Unit 1 and Unit 2. San José de Moro Unit 1 was on the northeast wall of a 4 x 4 m unit excavated by PASJM. At this location, excavation began below the lowest surface previously reached by excavation in Area 35, which was thought to be the base of cultural material and the beginning of culturally sterile layers. Excavations revealed an unexpected cultural feature extending into Unit 1 from the northwest. For this reason, the western corner of the unit was not excavated. With the exception of this corner, the unit was excavated to a depth of approximately 2.75 m below the floor of Area 35. The floor of Area 35 was approximately 3.60 m below the original pre-excavation ground surface. It is important to note that this surface is located at the edge of a huaca and may be an anthropogenic surface (Castillo 2008; Cusicanqui and Barrazueta 2008). The bottom of our unit was thus approximately 6.35 m below the level of the ground surface prior to excavation. PASJM completed a survey to

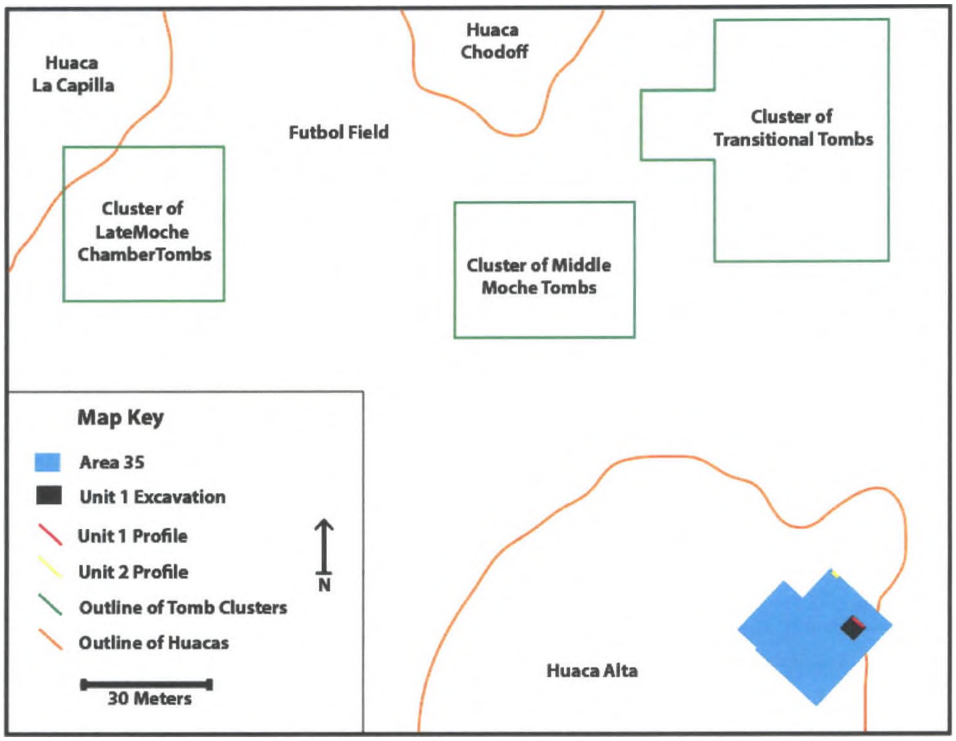

Figure 2.1. Map of approximate profile locations within San José de Moro (adapted from Castillo 2008). Southeast corner of map located at approximately 7°10'57"S, 79°26'13"W.

Figure 2.2. Removing the column sample in Unit 1 at San José de Moro.

determine the elevation of the unit relative to the Chamán River, but the data are currently unavailable.

The northeast wall of Unit 1 was chosen for detailed analysis because it provided the clearest view of the stratigraphy and contained the most well-defined channel features (Figures 3.1 and 3.4). The stratigraphic profile exposed in this wall was carefully drawn, described and photographed using standard methods. A column sample was taken from the profile at 120 to 130 cm from the northern corner of the unit from the top of the unit to a depth of 240.5 cm. The samples were 10 cm wide and extended 5 cm into the wall (Figure 2.2). Visible natural strata were separated and larger strata were collected in segments approximately 5 cm in depth (the exact depth of the segmentation depending on the depth of the entire stratum).

A second unit, San José de Moro Unit 2, was investigated in order to shed light on potential agricultural furrows recognized in several profiles in this portion of the site (described in further detail in Chapter 3). The profile was located along the wall in the northern corner of Area 35 where these features appeared the clearest (Figure 2.1). A 1.5 m wide by 1 m high section of the profile, just below the lowest level of dark artifact-bearing fill, was drawn, described and photographed. A 5 cm wide column sample was taken through the profile, extending 10 cm into the wall. The sample was 58 cm in height. As with Unit 1, visible natural strata were separated and larger strata were collected in segments approximately 5 cm in depth.

At Huaca del Sol the excavation team led by Professor Santiago Uceda Castillo of the National University of Trujillo excavated a pit to expose a 1 m wide profile to a depth of 4.5 m below the base of the Huaca del Sol adobe structure (Figures 2.3 and 4.1). The excavation was located below the small surviving portion of the base of the west wall just by the southwest corner of the huaca. As with the two profiles at San José de Moro, the profile was drawn, described and photographed. A 10 cm wide column sample was taken from the profile, extending 5 cm into the wall and 282.5 cm in height. Visible natural strata were separated and larger strata were collected in segments approximately 5 cm in depth.

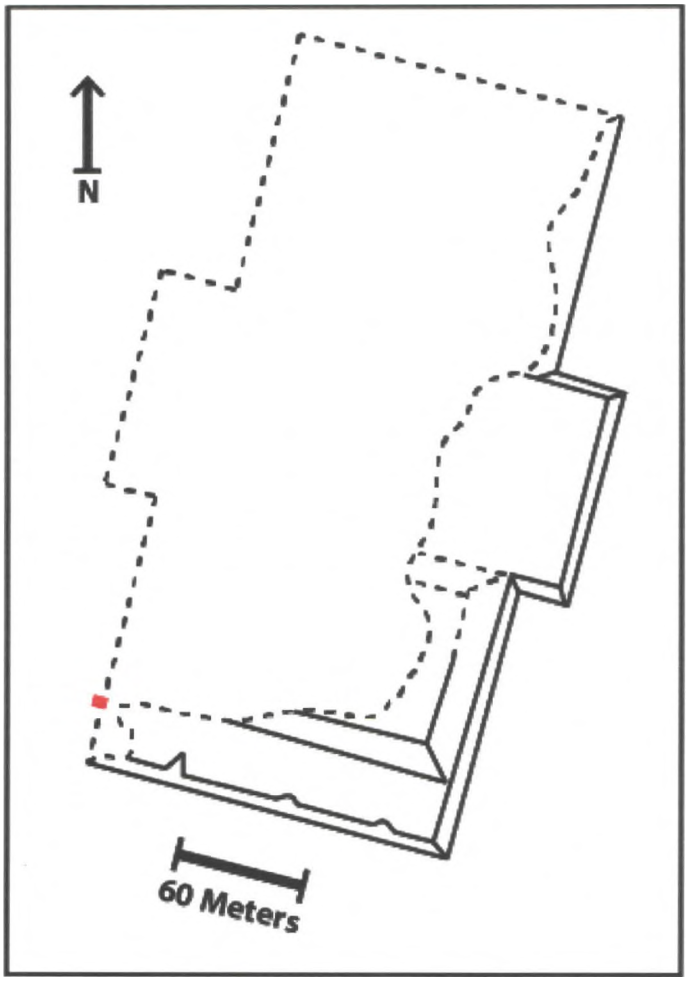

Figure 2.3. Huaca del Sol plan (adapted from Hastings and Moseley 1975). Red square indicates the location of profile location (not to scale with rest of drawing). Southeast corner of map located at approximately 8°7'59"S, 78°59'39"W.

Samples were collected from all three profiles for optically stimulated luminescence dating. These were collected by hammering specially designed 1 5/8 inch (approximately 4.1 cm) diameter metal tubes into the profile wall. When possible a dark colored cloth was held over the tube and profile while sampling to help minimize the chance of contamination by light exposure. Samples were sent to Professor James Feathers of the University of Washington for analysis. Analysis of the samples is incomplete at the time of writing. Preliminary results from Huaca del Sol are reported in Chapter 4.

Laboratory Methods

All samples collected from San José de Moro and Huaca del Sol were brought to the University of Maine for textural analysis to further illuminate depositional processes. After each sample was weighed, a subsample was removed using a laboratory sample splitter. The subsample was weighed, and then wet screened through 2 mm and 0.063 mm mesh sieves to separate gravel (greater than 2 mm), sand (between 2 and 0.063 mm), and silt/clay (less than 0.063 mm) fractions (based on the Wentworth grain size classification, Boggs 2012). Gravel and sand fractions were dried and weighed. Due to the large amount of water needed to wash out silt/clay fractions it was impractical to collect the entire fraction; a representative sample of the fraction was collected suspended in water and the rest was discarded. Samples high in silt/clay content were put in a solution of Calgon and water to aid in disaggregation.

Sand fractions were further analyzed using a settling tube to determine particle-size distribution. The Rapid Sediment Analyzer settling tube (Figure 2.4) uses the relative settling velocities of different particle sizes to measure their distribution within a sample. Sediment, with approximately 10 mL of Calgon solution to aid in the disaggregation of grains, was released at the top of a 2 meter tube filled with water. Sediments accumulated on a pan located at the bottom of the tube, suspended from an electronic balance at the top of the tube, which recorded the change in mass over regular time intervals. A computer then calculated the weight of each interval in phi size.

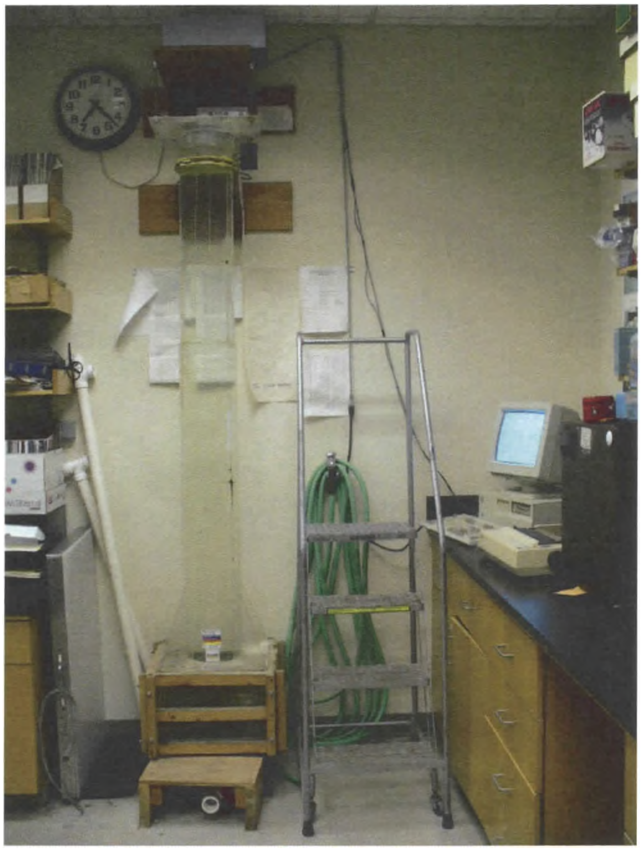

Figure 2.4. Rapid Sediment Analyzer settling tube at the University of Maine.

The terminology used to classify sediments is based on Folk (1954, 1974). Within this thesis, for the sake of consistency with Folk's system, the terms "mud" and "muddy" are used in classifications of sediment types but the term "silt/clay" is used to refer to the constituents of the sediments that are smaller than sand sized particles (less than 0.063 mm). The terms "mud" and "silt/clay" are equivalent in meaning. Folk's classification system is based on the ratios of grain size descriptors "gravel", "sand" and "mud" (silt/clay) found in sediment as illustrated in Figure 2.5.

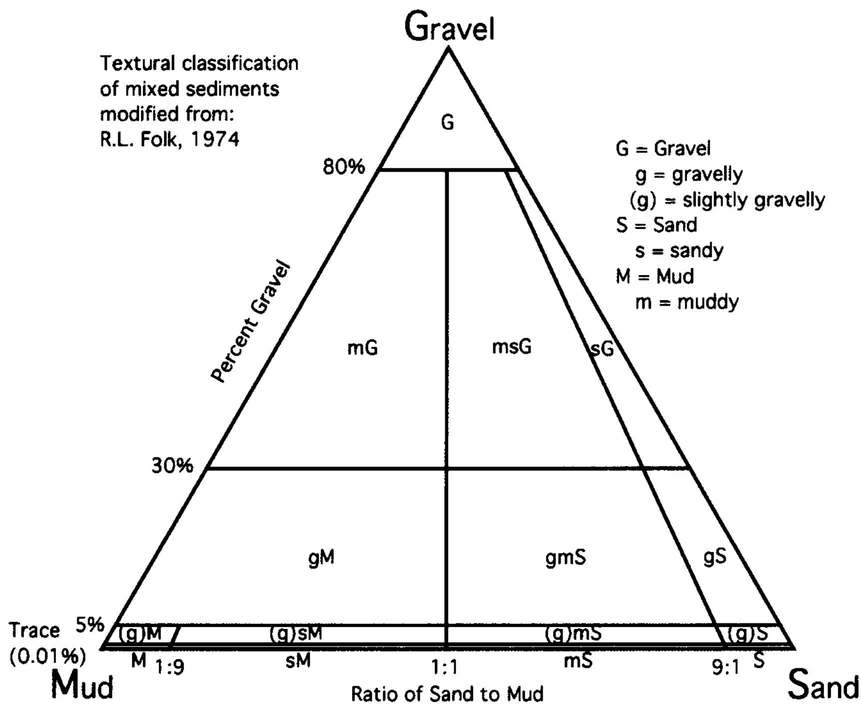

Figure 2.5. The Folk Textural Classification of Sediments used in analysis (Folk 1954, 1974, diagram from Belknap n.d.).

In addition to textural analysis, three samples from San José de Moro were sent to Dr. Linda Perry for analysis of macro and micro-botanical remains. Marcobotanicals were examined under a compound, dissecting microscope. For microbotanical analysis baking soda was used to disperse sediment and starch grains were floated out using a heavy liquid separation. Starch grains were examined under a Zeiss Pol compound, light microscope. There was no analysis for spores, pollen or phytoliths (Linda Perry, personal communication 2013).

CHAPTER 3

RESULTS: SAN JOSÉ DE MORO

The two units investigated at San José de Moro yielded fluvial sequences consisting of muddy sands and sandy muds. The exposed profile and 240.5 cm long column sample taken from Unit 1 provide an in-depth picture of the sedimentary processes at the site prior to the well-studied Moche occupation. The profile analyzed in Unit 2 offers a clear view of the potential agricultural furrows recognized at the site, while the 58 cm column sample collected provides more information on the nature and identity of these features. This chapter will presents in detail the results of the investigations of Units 1 and 2 at San José de Moro.

Unit 1

Unit 1 at San José de Moro consisted of an approximately 2.7 m thick sequence of fluvial deposits made up primarily of muddy sands and sandy muds with widely varying ratios of sand to silt/clay (Figures 3.1, 3.4 and 3.5). The upper portion consists of an approximately 1.4 m of cross-bedded channelized deposits. This sequence overlies approximately 1.2 m of broad, horizontally layered floodplain deposits. Most strata, but not all, contained a small amount of gravel-sized material. Gravel fractions ranged from 0% to 8.29%, sand fraction ranged from 11.92% to 92.33%, and silt/clay fractions ranged from 7.67% to 86.81%. Sand fractions all consisted primarily of fine and/or very fine sand, most of which was well or moderately well sorted. Medium sand fractions ranged from 0.0% to 16.3%, fine sand fractions ranged from 25.4% to 79.6% and very fine sand fractions ranged from 12.9% to 65.0%. Coarse and very coarse sand combined made up less than 10% in all but one sample analyzed, and less than 4% in all but three. A summary of the results of textural analysis is presented in Figure 3.5 and the full results are listed in Appendix A.

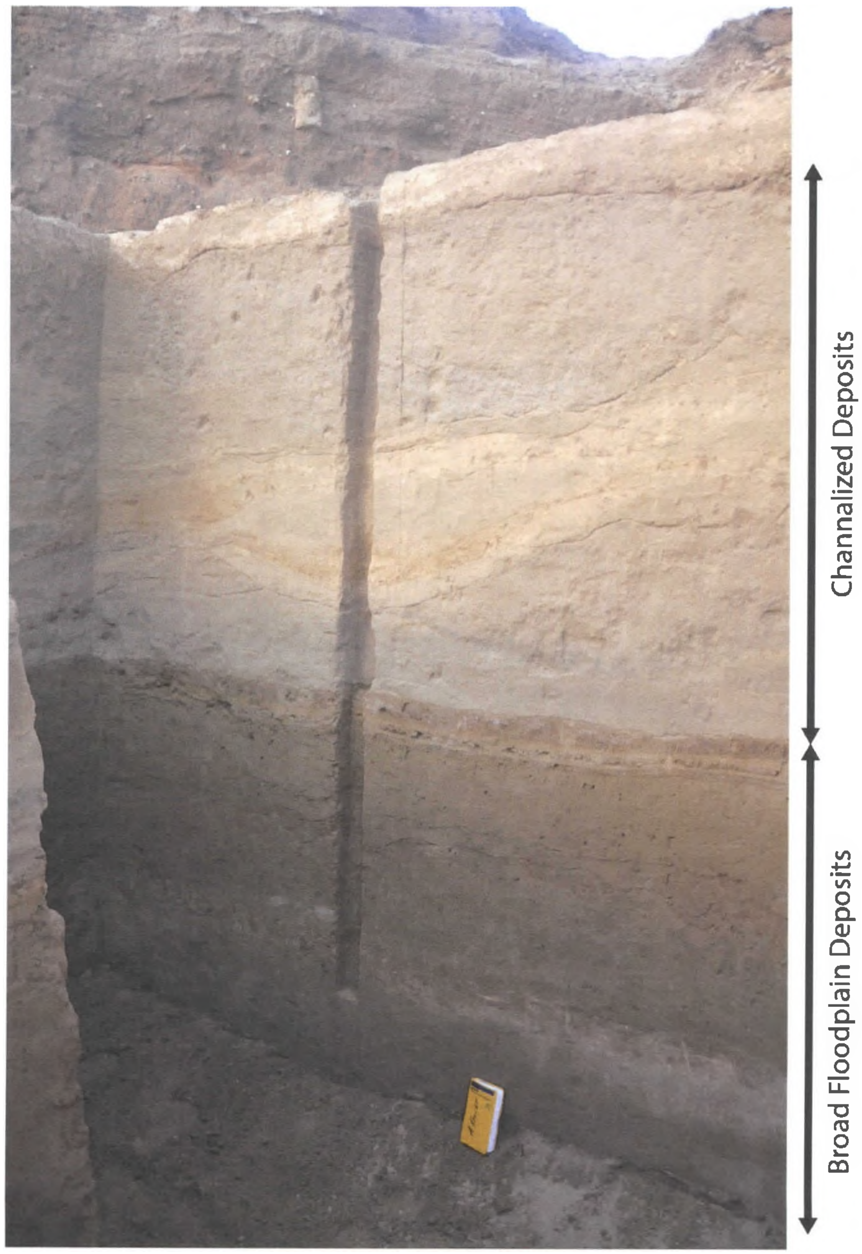

Figure 3.1. Unit 1 profile at San José de Moro.

Most samples included clumps of loosely aggregated sediment ranging in size from approximately 3 mm to 32 mm. These loosely aggregated clumps disaggregated easily when wet screened. Their presence in each sample is noted in Appendix A. In most samples there are also tightly aggregated clusters of finer sediments approximately 8 mm or smaller. Unlike the aforementioned loose aggregations of sediment, many of these did not break apart during wet screening. In some cases these tightly aggregated clusters have a hollow cylindrical form. Sometimes this hollow cylinder protruded from a larger body of aggregate. Due to their shape we believe these to be root casts. Analysis using a Scanning Electron Microscope (SEM) concluded that the material cementing these aggregates together consists primarily of calcium, oxygen and some carbon. This composition was interpreted to be calcium carbonate, a chemical compound associated with the roots of a variety of plant species. Additionally, root cast material effervesced when treated with dilute (10%) HCL, a standard field indicator of calcium carbonate composition. Gravel fractions stratigraphically below sample 1-2-1 consist almost exclusively of these root casts. As the aggregations are believed to have formed post-depositionally, there was likely little to no true gravel-sized particles in these levels at the time of deposition.

Analysis of individual sediment grains was largely focused on the root casts. However, SEM analysis of selected sediment samples identified mica (probably muscovite) as well as charcoal in sample 1-2-25, the basal sample from the column. Visual analysis of samples identified ubiquitous amounts of dark-colored material, which may represent heavy minerals or may be organic in nature.

The very top of the Unit 1 profile, stratum I (samples 1-1-1 through 1-1-3), consists of sandy mud. Silt/clay fractions ranged from 51.44% to 72.10% and sand fractions ranged from 27.33% to 48.56%. The ratio of silt/clay to sand increases with height between the three samples from stratum I, showing a fining upward sequence. The sand fractions of these samples consist primarily of fine and very fine sand; fine sand makes up 44.25% to 58.78% of the sand fraction and very fine sand makes up 40.54% to 50.00%.

The contact between strata I and IIa is broadly undulating. The undulations of this contact were more pronounced outside of the profile in the other three walls of the Unit 1 excavation block. Detailed textural analyses were not carried out on these profiles. Where they are present, these undulations are relatively uniform in size and shape. This pattern is unlikely to occur naturally, and we believe these undulations may represent agricultural furrows. Unit 2 was placed at a nearby location, approximately 8 m northwest of Unit 1, where these undulations were even more pronounced. For a more in-depth investigation of this feature, see the results discussed below. Other than the presence of the possible furrows, the stratigraphic sequence of the levels above and below the furrows is not consistent at the two locations despite their similar elevation.

Below the potential furrow, from strata IIa to XIV (samples 1-1-4 through 1-1-29), several of the strata show sloping contact surfaces and concave upward surfaces, which appear to be fluvial channel deposits. Stratum VIIIe in particular has a very well defined channel shape. Texture is widely variable, and shifts abruptly at several strata contacts. Several of the strata in this segment of the profile contain horizontal or cross-bedding (Figure 3.2).

Figure 3.2. Cross-bedding in stratum IIc.

Stratum II (a and b, samples 1-1-4 through 1-1-15) consists of sand and muddy sand. Sand fractions range from 72.73% to 90.24%. Silt/clay fractions range from 9.76% to 27.27%. No gravel was present in any sample. With the exception of 1-1-15, stratum II has a general fining upward pattern based on the ratio of silt/clay to sand. The sand fraction consists primarily of fine sand and also shows a general fining upward sequence. Medium sand makes up 0.08% to 13.54%, fine sand makes up 54.13% to 79.61% and very fine sand makes up 12.93% to 44.67% of the sand fraction.

Below stratum II the stratigraphic complexity increases. The profile contains a large number of lenses of varying lengths and thicknesses. This complexity was visible in the textural analysis, which sharply fluctuates between coarser and finer sediments.

Strata III and IV are both lenses that were not intersected by the column (Figure 3.4). Strata V and VI (samples 1-1-16 and 1-1-17, respectively) consist of muddy sand, with more silt/clay content than strata II. Stratum V contains 67.17% sand and 32.23% silt/clay. Stratum VI contains 56.77% sand and 42.87% gravel. Strata VII (sample 1-1-18) and VIIIa (sample 1-1-19) are both sandy muds and constitute a further drop in grain size. Stratum VII consists of 18.91% sand and 79.03% silt/clay and stratum VIIIa consists of 16.34% sand and 83.27% silt/clay.

Stratum VIIIf (samples 1-1-20 through 1-1-22) is coarser than immediately surrounding strata. Sand content ranges from 37.79% to 52.06% and silt/clay content ranges from 47.76% to 61.69%. This stratum also comprises the uppermost fill of a relatively large and well-defined channel made up of strata VIIIc, VIIId and VIIIe. Strata VIIIc (samples 1-1-23 and 1-1-24) and VIIId (sample 1-1-25) represent another drop in grain size, with sand to silt/clay ratios similar to strata VII and VIIIa. Sand contents range from 11.92% to 14.90% and silt/clay fractions range from 82.08% to 86.81%. Stratum VIIIe (sample 1-1-26) constitutes a sharp increase in grain size. It is a muddy sand with 57.81% sand and 42.04% silt/clay. It is the lowermost portion of the channel.

The channel cuts strata X, XI, XIIa and XIII. As our column sample was collected straight down the center of the channel only stratum XIII, located directly below the channel, was sampled. Strata X and XI are located at overlapping depths with stratum XIIa, but are separated by the channel cut. It is possible that either strata X or XI represents a continuation of stratum XIIa but there are noticeable differences between the three strata. Stratum XI consists of gravelly sand, and gravel was not noted in either strata X or XIIa. Stratum X consists of fine to very fine sand while stratum XIIIa consists of fine sand. Both stratum X and XIIIa contain similar horizontal bedding, although the bedding in stratum XIIIa appears to be slightly thinner.

Strata XIII (samples 1-1-27 and 1-1-28) and XIV (sample 1-1-29) consist of relatively coarse sediment with 81.74% to 92.33% sand and 7.67% to 18.26% silt/clay. Sample 1-1-28 is the sample from Unit 1 with the highest sand content (92.33%).

Below strata XIII and XIV, and in great contrast to these strata, is a series of very-fine-grained layers with greater clay content. These strata, shown in Figure 3.3, are relatively flat, thin, horizontal layers that extend the entire length of the profile with a few short breaks filled with fine sand/silt in stratum XVIIa. These breaks may constitute mud cracks or bioturbation from roots, rodents or insects. The thin clay layers alternate with layers of fine to very fine sand (Figure 3.4). Unfortunately, the thinness of these layers, the presence of two of the aforementioned breaks within the area we sampled and the fact that the surrounding sand tended to stick to the clay at their contact, made it extremely difficult to collect these layers without some contamination from surrounding layers. For this reason textural analysis result may not reflect the true nature of the strata, with layers appearing as more sand rich than they are. The two lowermost clay layers, strata XIX and XXI were particularly thin and only separated by an extremely thin sand layer that ranged from 0.1 to 1 cm in thickness, and were collected together in a single sample, sample 1-2-6. This sample is therefore not representative of any single stratum. Despite these issues, textural analysis of these strata shows a significant drop in grain size.

Figure 3.3. Strata XIV through XXIIIa: Alternating layers of silt/clay and sand.

Stratum XVa (sample 1-2-1), the uppermost clay layer, contains 84.64% silt/clay and 15.07% sand. Stratum XVIIa (sample 1-2-3), the second clay layer, contains 75.26% silt/clay and 24.07% sand. Both of these layers contain hard, compact clumps of aggregated sediment up to approximately 23 mm in size which did not easily disaggregate while wet screening; these clumps are presumably caused by the high clay content of these strata. Strata XVI, XVIIb (the sediment filling in the gaps in stratum XVIIa) and XVIII (samples 1-2-2, 1-2-4 and 1-2-5 respectively) represent the coarser material separating strata XVa, XVIIa and XIX. They contain between 41.19% and 70.32% silt/clay and their sand fractions range from 29.41% to 57.23%. As previously mentioned, the two lowermost clay levels, strata XIX and XXI, were collected together with the layer that separated them, stratum XX. This combined sample, sample 1-2-6, contained 66.30% silt/clay and 30.70% sand.

The clay layers below strata XIII and XIV mark the point in profile at which strata in general become flatter and broader, with no clearly defined channelization. From here until the bottom of the profile the grain size does not reach the same degree of coarseness as strata IIa, IIc, XIII and XIV, which together make up over half of the upper segment. This bottom segment of the profile is also generally finer towards the top and coarser towards the bottom. From samples 1-2-1 to 1-2-11, which includes strata XVa, XVI, XVII, XXIII, all but one sample consist of sandy mud with less than 50% sand; all but two samples (samples 1-2-5 and 1-1-6) have less than 40% sand. Below sample 1-2-11 only two samples contain less than 50% sand and below sample 1-2-14 no samples contain less than 50% sand.

Also starting below strata XIII and XIV, rootcasts occur with a greater frequency and density. All of the gravel fractions present in samples in the lower segment of the profile consist almost entirely of rootcasts, and all samples that contain a gravel fraction contain rootcasts.

Stratum XXIIIa (samples 1-2-7 through 1-2-11) is sandy mud containing between 59.78% and 71.78% silt/clay and between 29.66% and 39.42% sand. Stratum XXIIIc (sample 1-2-12) is a muddy sand consisting of 40.80% silt/clay and 59.20% sand. Stratum XXIVa (samples 1-2-13 and 1-2-15 through 1-2-21) consists mostly of muddy sand with samples containing between 49.95% and 71.53% sand and 27.95% to 48.96% silt/clay. Sample 1-2-21 contains 8.26% gravel most of which is made up of rootcasts. The sample has the highest gravel content in San José de Moro Unit 1, and the highest density of rootcasts. Stratum XXVa is a muddy sand that was collected in two samples. Sample 1-2-22 consists of 55.18% sand and 44.59% silt/clay. Sample 1-2-23 is made up of 51.22% sand and 48.70% silt/clay. Stratum XXVd was the lowermost stratum from which samples were collected. The sample column only penetrates the top of the stratum, and only two samples were taken though the stratum extends deeper. Sample 1-2-24 contains 64.99% sand and 34.56% silt/clay. Sample 1-2-25 contains 68.01% sand and 31.99% silt/clay.

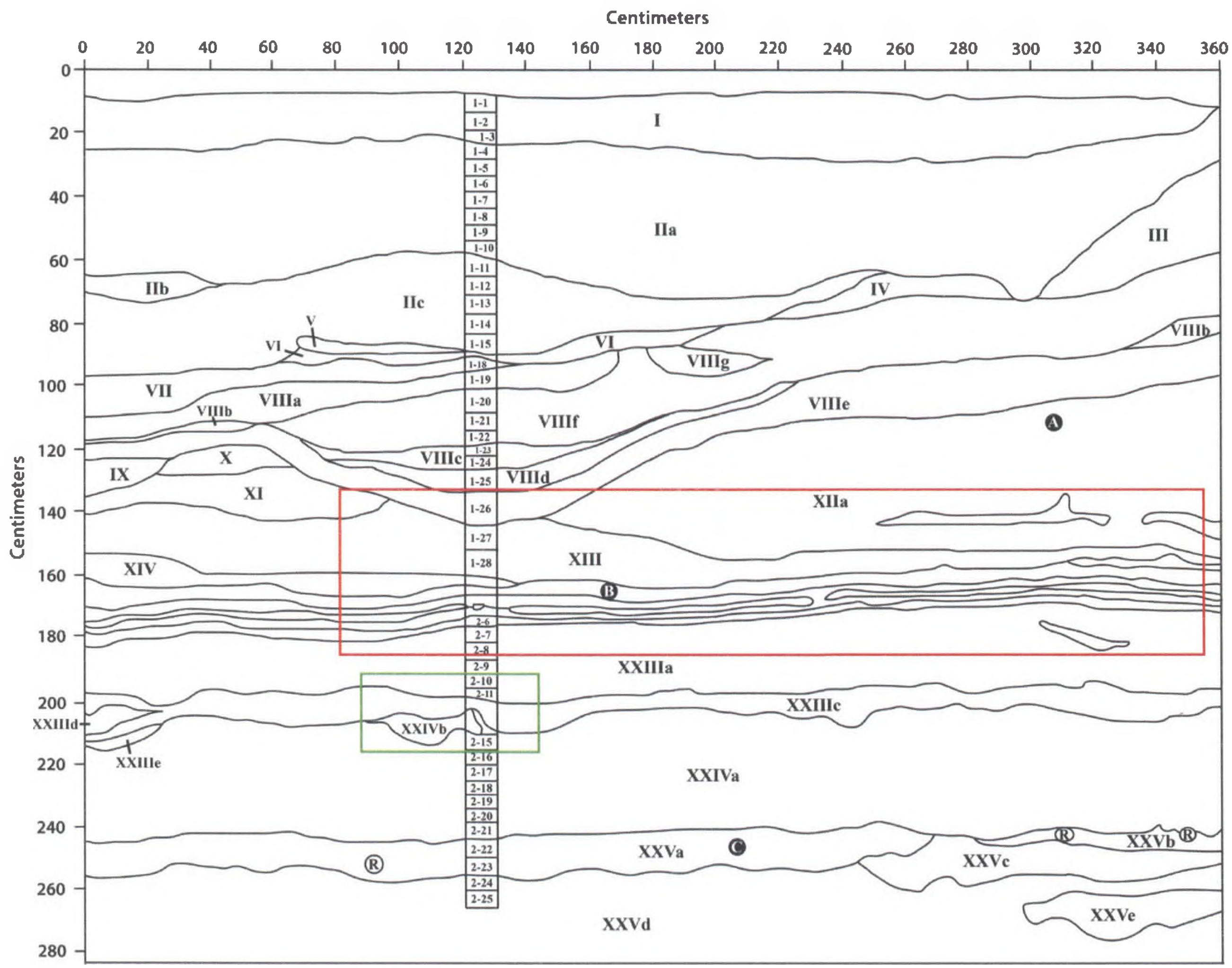

Figure 3.4. Profile drawing of Unit 1 at San José de Moro.

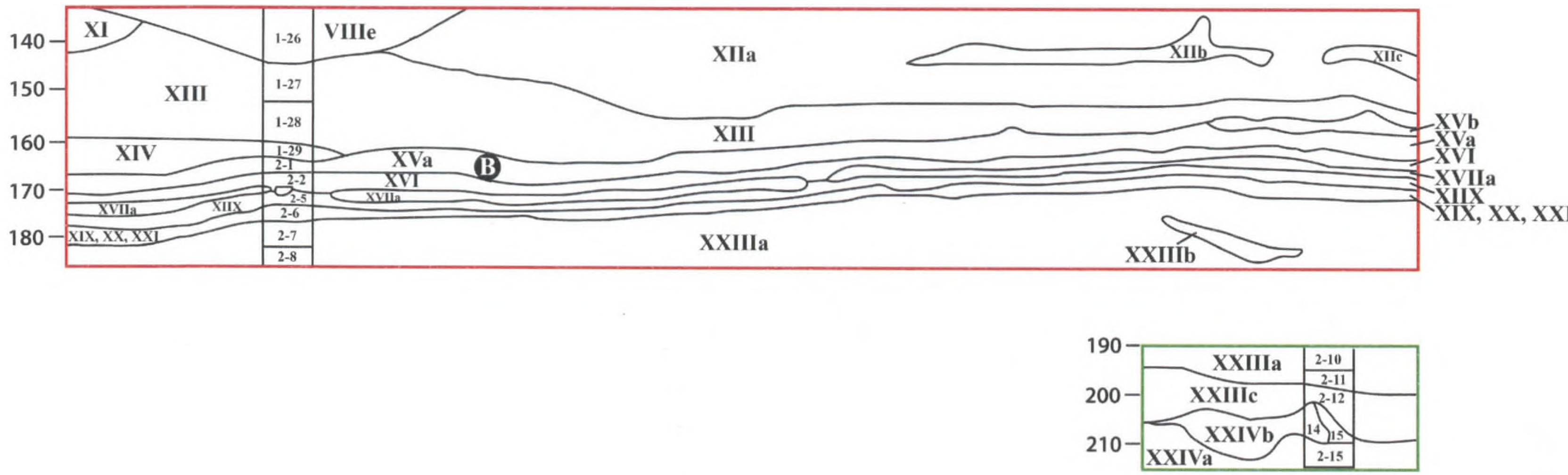

Key	
R	Rodent Borrow
A	OSL Sample 1-4-1
B	OSL Sample 1-4-2
C	OSL Sample 1-4-3
Roman numerals represent stratigraphic designations	
Arabic numerals represent the last two numbers in our three number sample naming system (example: "2-10" represents sample 1-2-10)	

Figure 3.4. Continued. Excerpts from profile drawing and key. Colored boxes on profile drawing show location of excerpts with outline of corresponding color.

Stratum	Description
I	Sandy clayey silt; 2.5Y 5/4; White mottling: Sporadic fine horizontal bedding.
IIa	Medium to fine sand at bottom fining upward to fine to very fine sand; 2.5Y 5/3; Concretions throughout; Slightly undulating fine horizontal bedding ~1mm thick; undulations in the top of this unit thought to represent agricultural furrows.
IIb	Medium to fine sand; 2.5Y 5/4; Unclear boundary with IIa; Concretions throughout; Slightly undulating fine horizontal bedding ~1mm thick; Slightly more compact than surrounding strata.
IIc	Medium to fine sand; 2.5Y 5/3; Unclear boundary with IIa; Pronounced bedding ~1mm thick, undulating at some points and crossing at others.
III	Sandy silt; 2.5Y 5/3; Faint, very fine horizontal bedding.
IV	Fine sand; 2.5Y 5/3.
V	Silt/clay; 2.5Y 6/4; thin layer; massive/uniform.
VI	Fine to very fine sand; 2.5Y 5/3; uniform/massive.
VII	Very fine sand/silt/clay; 2.5Y 5/4; Very faint fine horizontal bedding ~1mm thick.
VIIIa	Silt/clay; 2.5Y 5/4; Horizontal bedding less than 1mm thick.
VIIIb	Silt/clay; 2.5Y 5/4; Faint horizontal bedding; Slightly harder and darker than surrounding sediment.
VIIIc	Silt/clay; 2.5Y 6/4; Massive; very small rust colored mottles; White (calcium carbonate?) concretions.
VIIId	Silt/clay; 2.5Y 5/4; Massive; Occasional gravel.
VIIIe	Silt/clay/fine sand; 2.5Y 5/4; Occasional white concretions; Occasional gravel; faint bedding less than 1mm thick, some horizontal, some inclined.
VIIIf	Very fine silty clay; 2.5Y 6/4; Faint bedding slightly inclined; Very occasional concretions and gravel throughout.
VIIIg	Very fine silty clay; 2.5Y 6/4; Faint bedding, slightly inclined; Very occasional concretions and gravel throughout.
VIIIh	Silt/clay; 2.5Y 6/3; Horizontal bedding less than 1mm thick.
IX	Fine to very fine sand; 2.5Y 5/3; Pronounced crossing horizontal and inclined bedding ~1mm thick.
X	Fine to very fine sand; 2.5Y 6/3; fine bedding ~1mm thick, slightly inclined.
XI	Gravelly sand; 2.5Y 6/3; cross-bedded fine sand layers ~1mm thick.
XIIa	Fine sand; 2.5Y 6/3; Very vine horizontal bedding less than 1 mm thick.
XIIb	Fine to very fine silty sand; 2.5Y 6/3.
XIIc	Fine to very fine silty sand; 2.5Y 6/3.
XIII	Fine to very fine sand; 2.5Y 6/3; very pronounced bedding ~1 mm thick, horizontal or slightly inclined.
XIV	Very fine sand; 2.5Y 5/3; Massive/uniform.
XVa	Clay; 2.5Y 5/3; Thin horizontal layer, ranges from approximately 3-8 cm thick; Contains small reddish/rust colored specks; Upper and lower contacts are irregularly shaped in places; Contains calcium carbonate nodules.

Table 3.1. Field descriptions of strata of Unit 1 at San José de Moro.

XVb	Fine to very fine sand; 2.5Y 6/3; Thin horizontal layer, ranges from approximately 0.5-3 cm thick.
XVI	Very fine sand; 2.5Y 5/4; Thin horizontal layer, ranges from approximately 2-4 cm thick; Contains occasional small reddish/rust colored spots up to approximately 3 mm in diameter.
XVII	Clay; 2.5Y 5/4; Thin horizontal layer, ranges from approximately 10-13 cm thick; gaps and cracks in layer, ranging from <1-12 cm wide; Occasional slight impressions of rootlets.
XVIII	Fine to very fine sand; 2.5Y 5/4; Thin horizontal layer, ranges from approximately 1-2.5 cm thick; Occasional sediment concretions up to 2 mm.
XIX	Clay; 2.5Y 5/3; Thin horizontal layer, approximately 1 cm thick; Contains small reddish/rust and black colored specks.
XX	Fine to very fine sand; 2.5Y 5/4; Thin horizontal layer, ranges from approximately 1-10 mm thick
XXI	Clay; 2.5Y 5/4; Very thin horizontal layer, approximately 1 mm thick; Contains small reddish/rust colored specks
XXIIa	Coarse to fine sand; Multicolored; Small pocket (less than 8x3 cm) of mostly coarse material directly beneath Stratum XXI.
XXIIb	Coarse to fine sand; Multicolored; Small pocket (less than 8x3 cm) of mostly coarse material directly beneath Stratum XXI.
XXIIc	Coarse to fine sand; Multicolored; Small pocket (less than 8x3 cm) of mostly coarse material directly beneath Stratum XXI.
XXIIIa	Very fine muddy sand; 2.5Y 6/4; Appears to fine upwards; Occasional red and black mottling; Exact boundary with XXIVa is unclear.
XXIIIb	Same as XXIIIa but slightly darker; 2.5Y 4/4; Possible bioturbation.
XXIVa	Fine to very fine sand; 2.5Y 5/4; Massive or possibly fining upwards; Very occasional coarse sand sized particles; Exact boundaries with surrounding strata unclear.
XXIVb	Fine to very fine sand; 2.5Y 5/4; Massive or possibly fining upwards slightly; Well sorted; Very slight off-white and red/orange mottling; Exact boundaries with surrounding strata unclear.
XXIVc	Fine to very fine sand; 2.5Y 6/4; Very occasional coarse sand sized particles.
XXIVd	Fine to very fine sand; 2.5Y 5/4; Occasional black specks up to 1 mm.
XXIVe	Fine to medium sand; 2.5Y 6/4; Thin lens approximately 4x25 cm.
XXVa	Fine sand; 2.5y 5/4; Occasional pockets of slightly coarser sand; Vertical root or insect channels; Possible rodent holes up 4-5 cm in diameter; Small specks of calcium carbonate; unclear boundaries with surrounding strata.
XXVb	Same as XXVa; Possibly same stratum separated by XXVc.
XXVc	Silty fine sand; 2.5y 6/4; White colored mottles; unclear boundaries with surrounding strata.
XXVd	Silty fine sand; 2.5y 5/4; Uniform/massive; unclear boundaries with surrounding strata.
XXVe	Silty fine sand; 2.5y 7/4; unclear boundaries with surrounding strata.

Table 3.1. Continued.

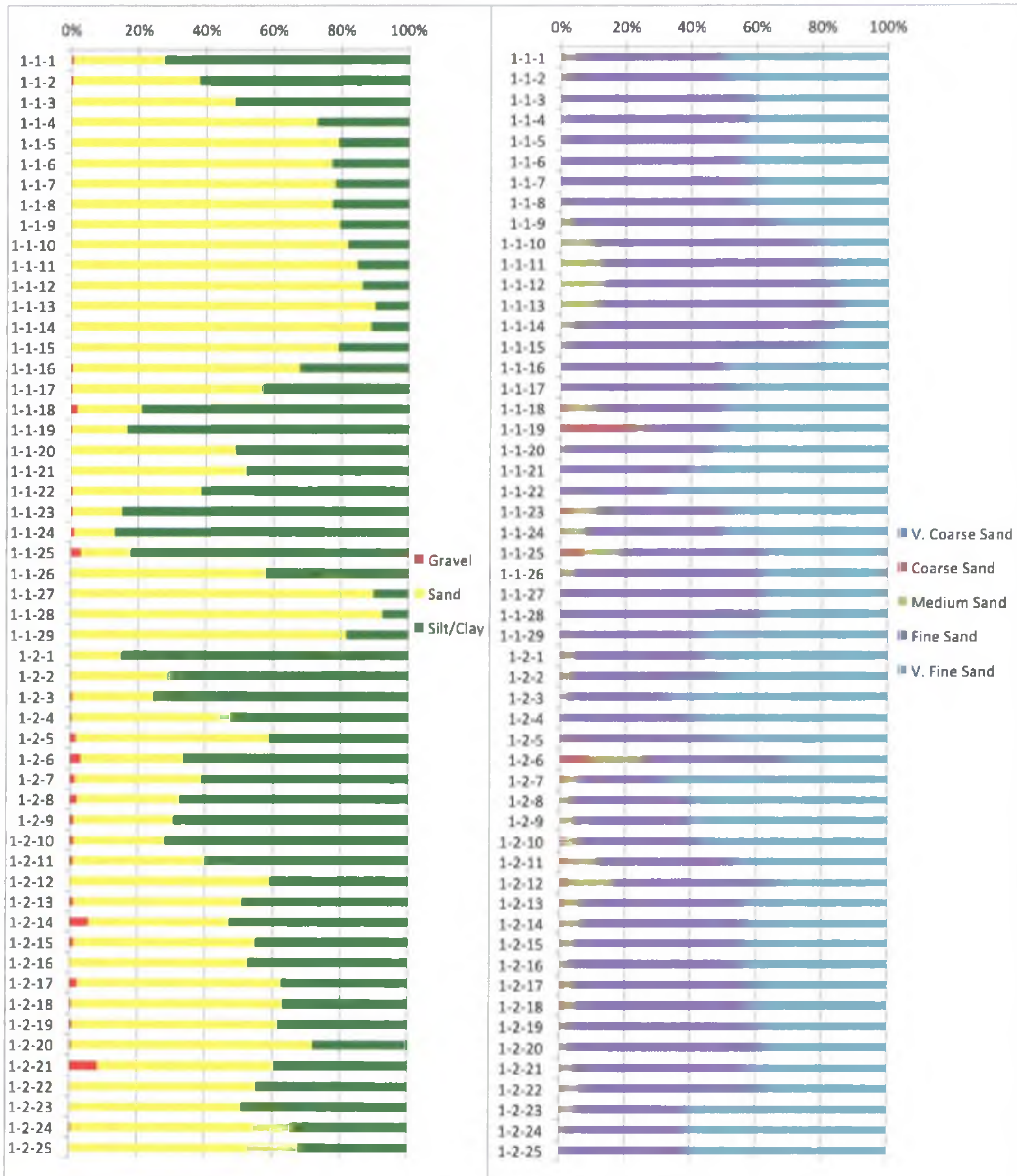

Figure 3.5. Results of textural analysis of Unit 1 at San José de Moro. On the left is percent gravel, sand and silt/clay of the entire sample. On the right is the grain size distribution of the sand fraction.

Unit 2

Unit 2 at San José de Moro is located on the northern end of the northeast wall of the San José de Moro Archaeological Project's Block 35. The location was chosen as the most accessible and clear example of a specific stratum, first noticed in the Unit 1 excavation, that has regular undulations in its upper contact (Figure 3.6). The undulations appear too regular to be natural and it is postulated that they represent agricultural furrows. A column sample was taken passing through the concave dip in one of the furrows to explore this possibility. Textural analysis was performed and two samples (2-1-3 and 2-1-5) were sent for botanical analysis.

The column sample from Unit 2 contains high silt/clay contents, ranging from 64.40% to 93.94%. Sediments include clumps of loosely aggregated particles ranging in size from approximately 3 mm to 13 mm. These loosely aggregated clumps disaggregated easily when wet screened, but all samples except 2-1-7 required a relatively significant amount of time under running water to sufficiently separate sediment.

The textural analyses of the sand fraction of over half of the samples (2-1-1, 2-1-3, 2-1-4, 2-1-5, and 2-1-6) showed a greater than 5% error. This is most likely a result of the small amount of sand analyzed in the settling tube once the silt/clay fraction was removed; in all cases, the sand fraction analyzed was less than the 10 g suggested for the most accurate results from the settling tube. Samples with a high percent error were not re-analyzed due to the small amount of sand present and a desire to preserve the remaining sediment for botanical analysis.

All samples contain gravel-sized material, ranging from 0.15% to 5.67%. Gravel in every sample includes what appears to be tightly aggregated clusters of finer sediments approximately 5mm or smaller. Unlike the aforementioned loose aggregations of sediment, these did not break apart during wet screening. Three samples (2-1-1, 2-1-3 and 2-1-4) from strata IV and V have aggregates with clear holes or a cylindrical form representing the same rootcast structures found in Unit 1. Three samples (2-1-5, 2-1-6 and 2-1-9) have aggregates with similar features that may also represent root casts, but do not have a clearly recognizable form. The remaining three samples (2-1-2, 2-1-7 and 2-1-8) do not appear to contain any rootcast-like structures. The presence of gravel-sized rootcasts does not appear to correspond with recognized stratigraphic boundaries. It is likely that some of the sand fraction is also made up of smaller fragments of aggregated clusters. For this reason it appears that the texture of the Unit 2 profile may have consisted of an even higher percentage of finer sediments before the action of post-depositional processes. Sample 2-1-5 also contains gravel-sized concretions of sediment held together by a dark rust-colored material.

The sand fractions of all samples include a gold-colored mineral with a submetallic luster that appears very thin in one dimension; SEM analysis identified this material as mica. Several of the samples have small amounts of dark colored material that may be organic in nature. Sample 2-1-3 contained some distinguishable organic material in the form of a small rootlet.

In the field, we interpreted the top of sample 2-1-3 to correspond to the top of a layer of furrow-fill sediment (the top of stratum V). This level contains the only clearly

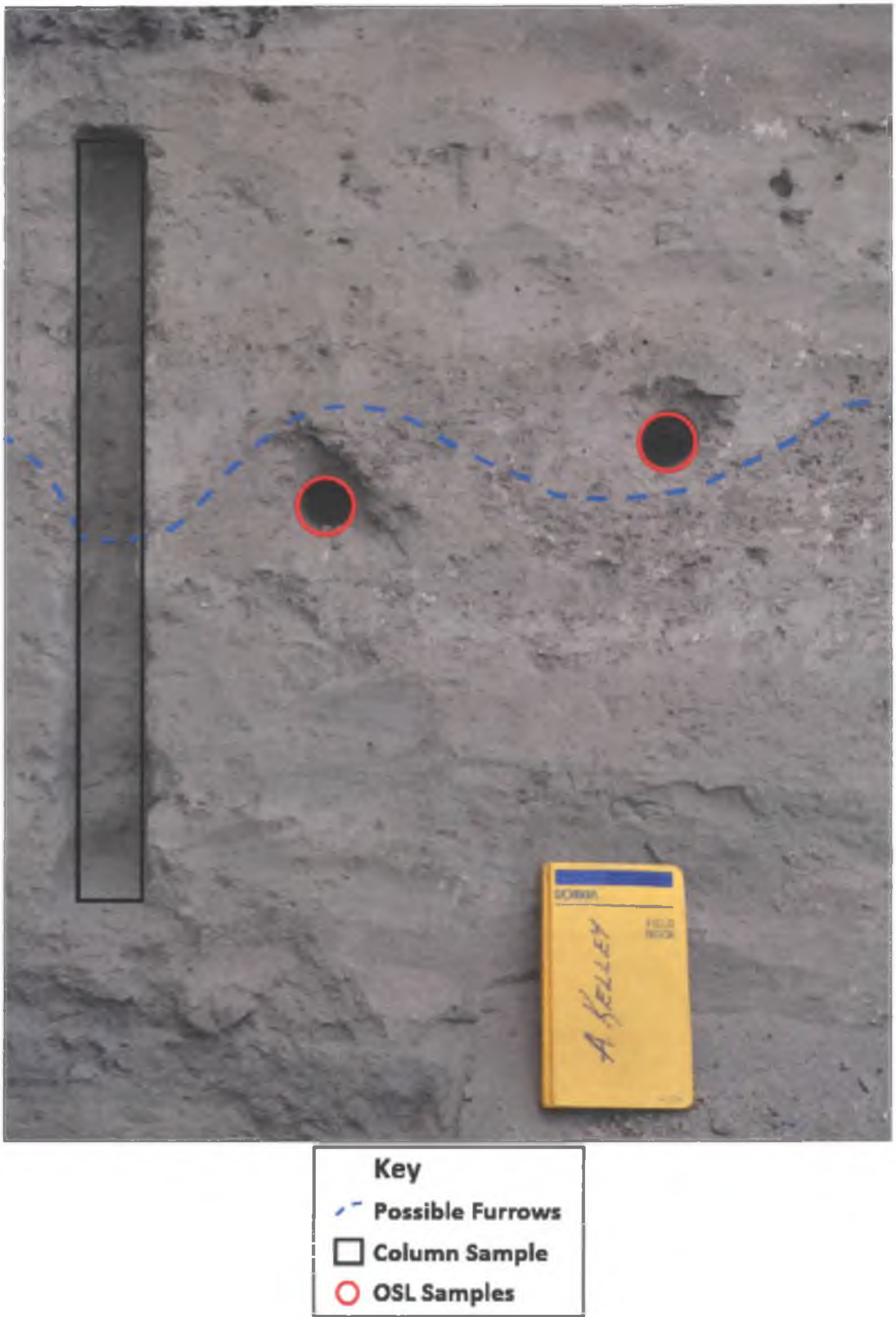

Figure 3.6. Unit 2 profile at San José de Moro.

distinguishable organic material and, along with sample 2-1-2, has unidentified powdery off-white colored material. Sample 2-1-3 also has a high sand fraction relative to immediately surrounding layers. These characteristics distinguish sample 2-1-3 from those above or below in the stratigraphic sequence. It is possible that this layer represents a surface that was stable for some period of time. This would allow surface drainage and aeolian processes to winnow the finer sediments, increasing the percentage of sand content of the horizon.

The relatively well-sorted, fine-grained nature of these deposits supports the interpretation that these sediments were deposited by a low-energy fluvial source, such as overbank flooding. Stratum Ia contains visible artifacts and represents culturally disturbed material or fill. It represents what was thought to represent the lowermost human occupation of the site before the discovery of the agricultural furrows (Luis Jaime Castillo, personal communication 2013). Strata Va, VI, VIa, VIb and VII together make up the agricultural furrows, while stratum V represents the sediment that eventually filled in the furrows.

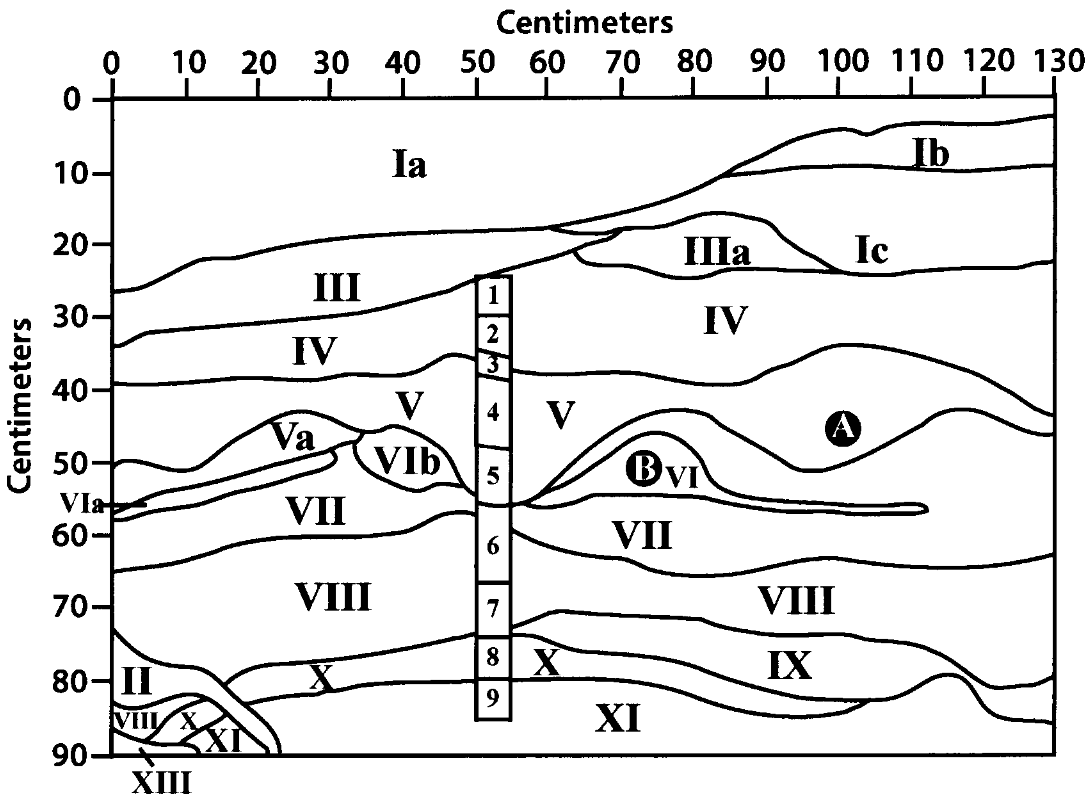

Key	
A	OSL Sample 2-3-1
B	OSL Sample 2-3-2
Roman numerals represent stratigraphic designations	
Arabic numerals represent the last number in our three number sample naming system (example: "6" represents sample 2-1-6)	

Figure 3.7. Profile Drawing at San José de Moro Unit 2.

Stratum	Description
Ia	Sandy clayey silt; 2.5Y 4/3; Contains charcoal, unfired clay lumps, rocks, and ceramics.
Ib	Sandy clayey silt; 2.5Y 5/3.
Ic	Sandy clayey silt; 2.5Y 5/4.
II	Silty sand; 2.5Y 6/2; Contains charcoal; Fill in crack caused by slumping in nearby grave.
III	Clayey silt; 10YR 6/3; Orange mottling.
IIIa	Clayey silt; 2.5Y 5/6; Orange mottling; White concretions.
IV	Clayey silt; 2.5Y 5/4.
V	Clayey silt or silt clay; 2.5Y 5/4; Occasional slight orange mottling.
Va	Clayey silt or silt clay; 2.5Y 5/4; Occasional slight orange mottling; Appears slightly darker than stratum V.
VI	Very fine sand; 2.5Y 5/3; Orange stains.
VIa	Very fine sand; 2.5Y 5/3; Orange stains.
VIb	Very fine sand; 2.5Y 5/3; Orange stains.
VII	Clayey silt; 2.5Y 5/4; White concretions.
VIII	Very fine silty sand; 2.5Y 5/4; Brown and orange stains; Possible bedding (parallel horizontal reddish orange undulating lines).
IX	Very fine silty sand; 2.5Y 5/3; Brown and orange stains; Possible bedding (parallel horizontal reddish orange undulating lines).
X	Silty clay; 2.5Y 5/4; White concretions.
XI	Silty clay; 2.5Y 5/4; Faint horizontal bedding with occasional undulations.
XII	Sandy silt; 2.5Y 5/3; Contains possible charcoal.

Table 3.2. Field descriptions of strata of Unit 2 at San José de Moro.

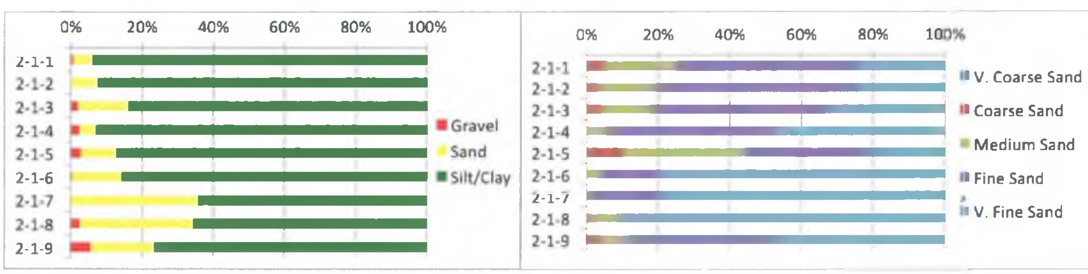

Figure 3.8. Results of textural analysis of Unit 2 at San José de Moro. On the left is percent gravel, sand and silt/clay of the entire sample. On the right is the grain size distribution of the sand fraction.

Botanical Analysis

We selected samples 2-1-3 and 2-1-5 from San José de Moro Unit 2 as key candidates for botanical analysis in order to investigate the hypothesis of agricultural furrows. Both samples are located in the fill (stratum V) within one of the furrow depressions. Sample 2-1-3 is located at the top of the furrow fill at the transition between strata IV and V. Sample 2-1-5 is located at the very bottom of stratum V, at the base of the furrow trough. We also chose to analyze sample 1-1-25 from San José de Moro Unit 1 stratum VIIId for use as a control. This sample came from approximately one meter below the elevation of the furrows present in Unit 1; it was chosen because it has a similar texture to samples 2-1-3 and 2-1-5.

As previously mentioned, during textural analysis sample 2-1-3 yielded a single rootlet fragment, observed in the process of wet screening of the subsample. No other rootlet fragments were discovered during botanical analysis. This is particularly unfortunate because the rootlet may have provided insight regarding the plant responsible for forming the rootcasts present at San José de Moro. Macrobotanical remains found during analysis consisted of charcoal. Microbotanical analysis found the sample to contain one starch grain consistent in morphology with starch from maize, five torn or mechanically damaged unidentified starch grains and one gelatinized mass of unidentified starch. The torn starches could have been damaged by either natural or human processes. The gelatinized mass of starch may represent a single large grain or several smaller ones, and is typical of plant foods heated in water (Linda Perry, personal communication 2013).

Sample 2-1-5 contained two unidentified starch grains and a pair of grass starches consistent in morphology with starch from maize. One of the unidentified starch grains had damage consistent with heating in the absence of water and appears to have a lenticular shape typical of both chiles and Pooid grasses. The possible maize starches are not completely gelatinized, but show evidence of damage from heating in the form of distortion in the birefringent properties of both grains (Linda Perry, personal communication 2013).

As naturally caused fires are not known to occur in northern coastal Peru, the charcoal in sample 2-1-3 probably represents human burning activity. The heat damage to several of the starch grains from both samples 2-1-3 and 2-1-5 could potentially represent the cooking of plant materials. The torn/mechanically damaged starch grains may have been damaged by natural causes, such as through alluvial transport, or by human processing activities (Linda Perry, personal communication 2013). The botanical evidence from these samples therefore represents possible human activity and is consistent with our interpretation of the feature as agricultural furrows. Further botanical analysis of this feature would be very valuable in verifying the agricultural nature of the landscape and identifying which plants prehistoric humans grew there.

Our control sample, sample 1-1-25, also contained botanical remains likely indicative of a human presence in the area. Charcoal was identified in the macrobotanical analysis. Microbotanical analysis revealed a cluster of starch grains and two single starch grains, all consistent in morphology with starch grains from maize. These grains are different in morphology from the potential maize starch grains found in samples 2-1-3 and 2-1-5 (Linda Perry, personal communication 2013). As sample 1-1-25 comes from a fluvial channel deposit, botanical remains likely originated upriver from San José de Moro rather than at the site itself. Nevertheless, these materials imply a potential human presence in the area prior to the earliest known Moche occupation of the area, and suggests the possibility of maize agriculture.

Sample	Cf. Maize	Unidentified, Unaltered	Parched	Gelatinized	Torn/ Damaged	Total
SJM 2-1-3	3 (1 clump)					**3**
SJM 2-1-5	1	1		1	5	**8**
SJM 1-1-25	1 (pair)	1	1			**3**
Total	**5**	**2**	**1**	**1**	**5**	**14**

Table 3.3. Summary of starch grains recovered during microbotanical analysis. Based on results reported by Linda Perry (personal communication 2013).

CHAPTER 4

RESULTS: HUACA DEL SOL

The unit investigated at Huaca del Sol (Figure 4.1) consisted primarily of a thick 3.6 m sequence of fluvial deposits similar to those found at San José de Moro, with some influence from aeolian and anthropogenic sources (Figure 4.2). It is composed of sediments ranging in texture from gravelly muddy medium sand (47.87% sand, 40.11% silt/clay and 12.02% gravel) to fine sand (97.15% sand, 2.85% silt/clay and 0.00% gravel) to mud (97.00% silt/clay, 3.00% sand and 0.00% gravel).

Figure 4.1. The adobe structure of Huaca del Sol at the top of the investigated section (partially visible in bottom left of photo).

Figure 4.2. Profile at Huaca del Sol. Level line corresponds

to 110 cm depth in drawing (Figure 4.5).

The exposed section at Huaca del Sol was located directly at the base of the adobe structure, with the uppermost limit of our profile composed of the western wall of the structure (Figure 4.1). This section is the oldest part of the Huaca del Sol structure according to site archaeologist Santiago Uceda, director of current excavations at Huaca del Sol (personal communication 2013). A dark midden containing charcoal, bone, shell, small ceramic fragments, and what appeared to be rodent feces was located approximately 47 centimeters above the lowest level of adobe bricks, just above and slightly to the north of our profile. A level of compact silt/clay, approximately one meter thick is directly below the lowest adobes, and is identified by Santiago Uceda as agricultural soil (personal communication 2013).

Our detailed investigation of the profile began directly below the layer of agricultural soil. A summary of the results of textural analysis is presented in Figure 4.6 and the full results are listed in Appendix B. The sand fractions of all samples include a gold-colored mineral with a submetallic luster that appears very thin in one dimension; this material was identified as mica during SEM analysis.

The uppermost stratum, stratum I, was massive, very well sorted and composed of fine sand. The top of the column sample was located at the base of this stratum. Textural analysis (sample 1-1-1) revealed the base to consist of 97.15% sand and 2.85% silt/clay. This is the highest percentage of sand found in any of the samples collected. The sand fraction consists of 24.90% medium sand, 68.35% fine sand, 5.85% very fine sand and less than 1.00% coarse and very coarse sand. The well-sorted massive fine sand nature of this stratum likely indicates that this is an aeolian deposit (see discussion of aeolian processes and grain size in chapter 2).

Below stratum I all deposits appear to be primarily fluvial in nature: most are well-sorted muddy sand or sandy muds and several deposits display fining upward sequences (see discussion of fluvial processes in Chapter 1). Textural analysis revealed gravel fractions ranging from 0.00% to 12.02%, sand fractions from 3.00% to 90.80, and silt/clay fractions from 8.25% to 97.00%. From strata II through IX (samples 1-1-2 through 1-2-35) most levels consist of muddy sand. Sediment in most samples below stratum I include clumps of loosely aggregated sediment ranging in size from approximately 3 mm to 58 mm; most are less than 20 mm. These clumps are distinct from the aforementioned dark rust-colored hard concretions. These loosely aggregated clumps generally disaggregated easily when wet screened. Their presence in each sample is noted in Appendix B.

Stratum II (samples 1-1-2 through 1-1-10) consists of massive, well sorted muddy sand. Samples 1-1-2 through 1-1-9 range from 71.85% to 78.41% sand. All sand fractions are greater than 72% fine sand. None of these samples have more than 0.30% gravel, so the remaining fraction consists of 28.15% or less silt/clay. Sample 1-1-10 is slightly finer with 64.00% sand, 68.34% of which is fine sand, verses 36.00% silt/clay. Stratum II may represent a single flood event, but only the bottom three samples showed a fining upward sequence.

Below stratum II there is a thin interval of finer samples. In strata III (sample1-1-11), IV (samples 1-1-12 and 1-1-13) and the top of V (sample 1-1-14), texture ranges from 46.79% to 60.97% sand and 38.63% to 53.10% silt/clay. The sand fraction of sample 1-1-11 is well sorted and contains less fine sand and more very fine sand than overlying layers (60.63% fine sand and 33.98% very fine sand). In samples 1-1-12 and

1-1-13 the sand fractions are only moderately well sorted, and are thus less well sorted than all levels above and those directly below.

Below sample 1-1-14 the coarseness again increases. Samples 1-1-15 through 1-1-20, which were taken from the bottom of stratum V through the bottom of stratum VII (stratum VI was a lens that did not cross the column and thus was not sampled), represent an increase in percent sand, as compared to levels immediately above, ranging from 68.76% to 80.54%. This distinct spike in sand content may represent a single flood event. While samples 1-1-15 and 1-1-16 (stratum V) are well sorted, samples 1-1-17 through 1-1-20 are much less so. Their sand fractions are moderately sorted, and the overall samples contain a significant gravel fraction ranging from 2.03% to 4.75%, with gravel particles as large as three centimeters.

Stratum VIII (samples 1-1-21 through 1-1-30) consists of a decrease in coarseness followed by an increase in coarseness. Sample 1-1-21 consists of 58.64% moderately well sorted fine sand, and 40.57% silt/clay. The sand content decreases to a nadir of 35.19% in sample 1-1-25, verses 64.81% silt/clay. Coarseness then increases to reach 63.33% moderately well sorted sand with 36.67% silt/clay in sample 1-1-30. These two distinct segments, distinguished by increasing versus decreasing coarseness, may represent more than one event that were unable to be distinguished into different strata during field analysis.

In the bottom half of stratum VIII two stones up to approximately 5 centimeters in diameter were visible in the exposed section. These were too large to have been transported by the same fluvial processes that deposited the surrounding sandy mud to muddy sand matrix, and were angular so they clearly did not travel far by fluvial processes (Figure 4.3). They did not appear to be debris flows on the basis of structures and grain-size trends, and no other possible natural process that may have been responsible for moving these stones was apparent (e.g., attachment to tree roots or association with rodent burrows). We therefore conclude that they must be manuports. Both had irregular fracture surfaces and slight reddening, indicating that they are fire-altered rock. These artifacts are a clear indication of human use of the site.

Figure 4.3. One of the probable manuports/fire altered rocks discovered in stratum VIII.

Orange, red, black, light tan and/or gray colored staining or mottling appears in stratum VIII and maintains its presence in some form in all levels below (details for each stratum in table 4.1). The orange, red and black staining and mottling is possibly the result of the oxidation of iron caused by the movement of groundwater though the sediment. Markers of paleogroundwater levels could potentially be used to investigate past environmental conditions related to changes in groundwater, which can be linked to climate change. This line of investigation was not pursued as a part of the present study. In no cases does mottling appear to follow stratigraphic boundaries and it made defining different strata more difficult. The nature of the mottling becomes more consistent and uniform across the exposed section with increased depth.

Stratum IX (samples 1-2-31 through 1-2-35) represents a spike in sand content; the peak in percent sand comprises the highest sand content below the aeolian stratum I. Sand fractions range from 75.99% to 90.80% and are all well sorted, consisting of between 69.16% to 75.52% fine sand. As with the increased sand content in strata V and VII mentioned above, this spike in sand content may represent a distinct individual flood event. Stratum IX is notable in that its lower contact appears concave up, with the left side reaching an angle of approximately 45 degrees (Figure 4.5). It is possible that this represents channelization, which would be related to the higher energy movement of water that presumably caused this level's increased coarseness. It is also possible that the influx of well-sorted fine sand is from an aeolian source. A single manuport/fired altered rock of approximately 7 cm visible length, similar in nature to those in stratum VIII, was found just below stratum IX's upper contact with stratum VIII embedded in the surface exposed by removing sample 1-2-31. The artifact partially extended into sample 1-2-31, but it was not collected with the sample as it was embedded deeply in the wall.

Stratum X (samples 1-2-36 through 1-2-45) consists of relatively consistent gravelly muddy moderately sorted medium sand. It is among the most poorly sorted layers at the site. Sample 1-2-36, the uppermost sample collected from the level, has a significantly higher sand content than the rest of the stratum (possible due to some mixing of the sample with the sandier deposit of stratum IX above during sampling) with approximately 74.41% moderately sorted medium sand, 20.50% silt/clay and 5.09% gravel. The rest of stratum X ranges from 46.46% to 55.94% moderately sorted medium sand, 40.11% to 50.23% silt/clay and 1.40% to 12.02% gravel. One gravel-sized particle, approximately 1.9 cm in diameter, found in sample 1-2-42, represents the largest piece of gravel found in any of the samples and showed the same evidence of fire alteration as the manuports/fire altered rocks found in strata VIII and IX. Additionally, what appeared to be the rock's cortex was blackened. As with those larger artifacts, it is extremely unlikely that this gravel particle would have been deposited by natural processes and it is almost certainly a human artifact. This is the lowest level at which any indication of human occupation was identified. As this artifact was found in a sample it was included in the textural analysis for purposes of methodological consistency.

Stratum X has some of the strong rust-colored and black staining or mottling, particularly in the lower half (Figure 4.4); this discoloration is more visually distinct from the surrounding matrix than any mottling found in other strata. Although it was not analyzed, manganese oxide is a common constituent of such black markings. In all of the samples from stratum X there are dark rust-colored concretions, possibly related to the same processes that cause the mottling. These concretions are found in all samples collected from below this level as well, but to a much lesser extent and they are rarely larger than one mm. Most clumps are smaller than 4 mm and none are large than 40 mm. It appears that post-depositional oxidation of the sediment caused some clumps of particles to adhere together; these clumps are often relatively hard and did not always disaggregate during wet screening. The gravel fraction and the coarse and very coarse sand fractions appeared to consist mostly of these concretions. For this reason, at the time of original deposition stratum X probably contained a much smaller gravel fraction and a slightly finer and more well sorted sand fraction. These concretions are found in all samples collected from below stratum X as well, but to a much lesser extent and they are rarely larger than one mm.

Figure 4.4. Rust colored and black staining/mottling in stratum X. Column sample visible in center of photo.

Below stratum X the first two samples (1-2-46, stratum XI and 1-2-47, stratum XIII; stratum XII is a lens that did not cross the sample column and thus was not sampled) maintain sand and silt/clay contents relatively similar to those in stratum X, but there is a drop in gravel content to less than 0.2%. Samples 1-2-48 (stratum XIV) and 1-2-49 (XIII) are finer in nature, consisting of sandy mud with 37.34% and 40.11% sand and 62.66% and 59.57% silt/clay respectively. Mottling/staining in all levels below stratum X is only orange and gray in color.

Below stratum XIII the coarseness continues to decrease. Stratum XV (samples 1-2-50 through 1-2-53) consists of 89.17% to 96.42% silt/clay with 3.58% to 10.83% sand. The small sand fractions in these samples appear to consist primarily of sand-sized grains of mica. Strata XVI (sample 1-2-53) and XVII (1-2-54), located directly below stratum XV, represent a short spike in coarseness. Both are muddy sands. Below this spike, the lowest three strata sampled, stratum XIX (1-2-55), stratum XX (1-2-56) and stratum XXI (1-2-56) all consist of silt/clay (89.79% to 97.00%) with only a very small amount of sand, mostly consisting of mica, similar to stratum XV.

Stratum XXI (sample 1-2-57) is the lowest stratum sampled. Based on observation of the profile, all levels below this point consist of silt/clay. It is estimated that textural analyses would yield sand contents of less than 10%. Strata XXII, XXIII, XXIV, XXV and XXVI (all located in the bottom 20 cm of our profile, below the depth of our column sample) all have completely uniform orange and gray mottling and were only able to be distinguished by very slight but well defined variations in darkness.

We collected four samples for OSL dating from the profile at Huaca del Sol. One additional OSL sample was collected from an adobe brick; the brick was located in lowest adobe level directly adjacent to our unit. Analysis of the samples is incomplete at the time of writing but we have received some preliminary data. The preliminary minimum ages indicate the adobe brick dates to approximately AD 400 and the lowest OSL sample in our profile (start XIII adjacent to sample 1-2-47) dates to approximately AD 0 (James K. Feathers, personal communication 2014).

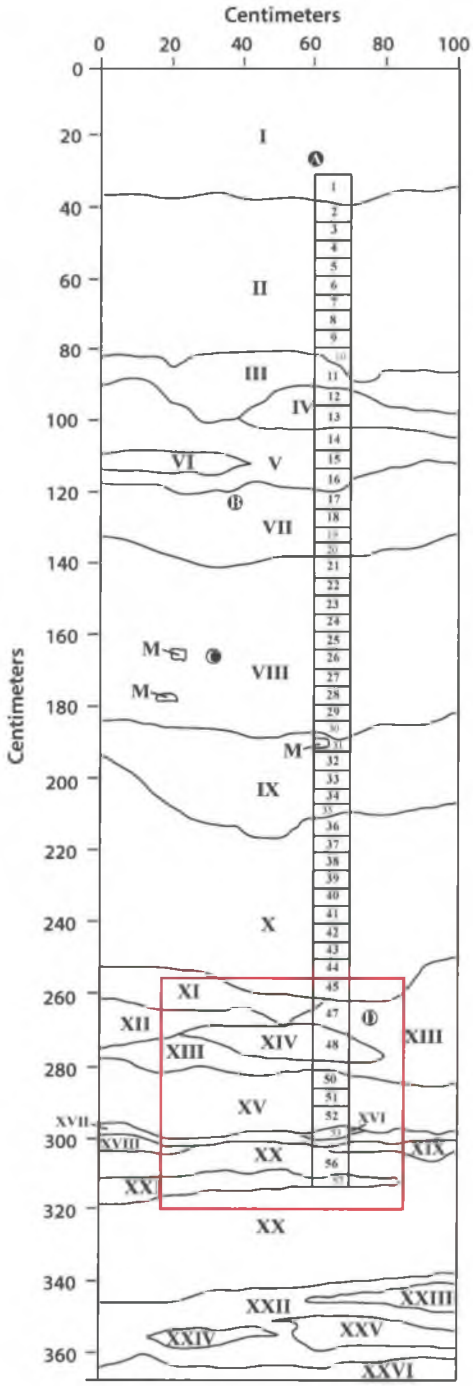

Key	
M	Manuport/Fire Altered Rock
A	OSL Sample 1-2-61
B	OSL Sample 1-2-60
C	OSL Sample 1-2-59
D	OSL Sample 1-2-58
Roman numerals represent stratigraphic designations	
Arabic numerals represent the last number in our three number sample naming system (example: "43" represents sample 1-2-43)	

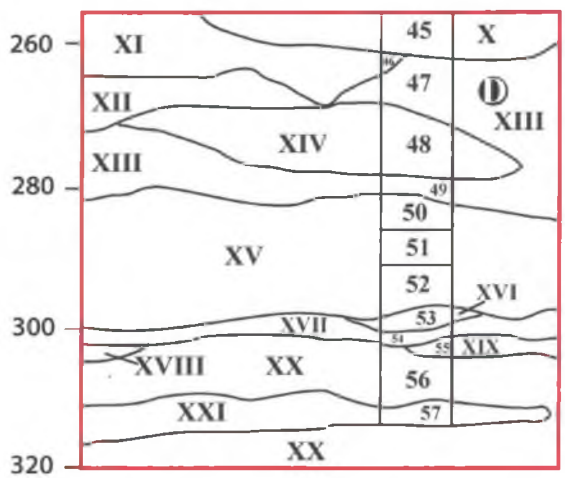

Figure 4.5. Profile Drawing at Huaca del Sol.

Stratum	Description
I	Fine sand; 10YR 5/3; Massive, well sorted.
II	Very fine sand; Gradient between 10YR 4/4 at top and 10YR 5/4 at bottom; Massive, very well sorted; Unclear boundary with strat III.
III	Very fine silty sand; 10YR 5/4; Massive, very well sorted; Unclear boundary with strat II.
IV	Sandy silt; 10YR 5/4; Massive; Unclear boundaries with surrounding units.
V	Very fine silt/sand; 10YR 5/3; Massive.
VI	Lens of fine sand; 10YR 5/4; Massive, well sorted.
VII	Gravelly silty sand; 10YR 5/3; Poorly sorted, Fining; Contains gravel up to ~3cm.
VIII	Very fine silty sand; 10YR 5/4; Massive, well sorted; Contains manuports/fire altered rock up to ~5cm; Occasional white specks up to <1mm; Slight orangeish mottling throughout, light tan mottling towards bottom.
IX	Silty fine sand; 10YR 5/4; massive, well sorted; red (7.5YR 3/4) and black (7.5YR 2.5/1) staining/mottling towards bottom of strata; single manuport/fire altered rock ~7cm.
X	Silt/clay; 10YR 3/3; Massive; Red and black staining/mottling continues into upper part of level from strat IX; Small fragments of manuports/fire altered rock up to ~2cm; Possible charcoal.
XI	Silt; 10YR 4/4; Massive, well sorted; Orange and gray mottling.
XII	Silt; 10YR 3/4; Massive, well sorted; Occasional small specks of white material (calcium carbonate?); Orange and gray mottling.
XIII	Fine to very fine sand; Gradient between 10YR 5/6 at top and 10YR 5/4 at bottom; Massive, well sorted; Orange and gray mottling.
XIV	Silt/clay; 7.5YR 4/4; Massive, well sorted; Orange and gray mottling.
XV	Clay; 10YR 3/4; Massive, well sorted; Orange and gray mottling.
XVI	Fine sand; 10YR 4/6; Massive, well sorted; Orange and gray mottling.
XVII	Silt; 10YR 5/6; Massive, well sorted; Orange and gray mottling.
XVIII	Silty clay; 10YR 4/4; Massive, well sorted; Orange and gray mottling.
XIX	Clayey silt; 10YR 6/6; Massive, well sorted; Orange and gray mottling.
XX	Silty clay; 10YR 4/3; Massive, well sorted; Orange and gray mottling.
XXI	Silt; 10YR 5/6; Massive, well sorted; Orange and gray mottling.
XXII	Silty clay; Massive, well sorted; Orange and gray mottling.
XXIII	Clayey silt; Massive, well sorted; Orange and gray mottling.
XXIV	Clayey silt; Massive, well sorted; Orange and gray mottling.
XXV	Clayey silt; Massive, well sorted; Orange and gray mottling.
XXVI	Clayey silt; Massive, well sorted; Orange and gray mottling.

Table 4.1. Field descriptions of strata at Huaca del Sol.

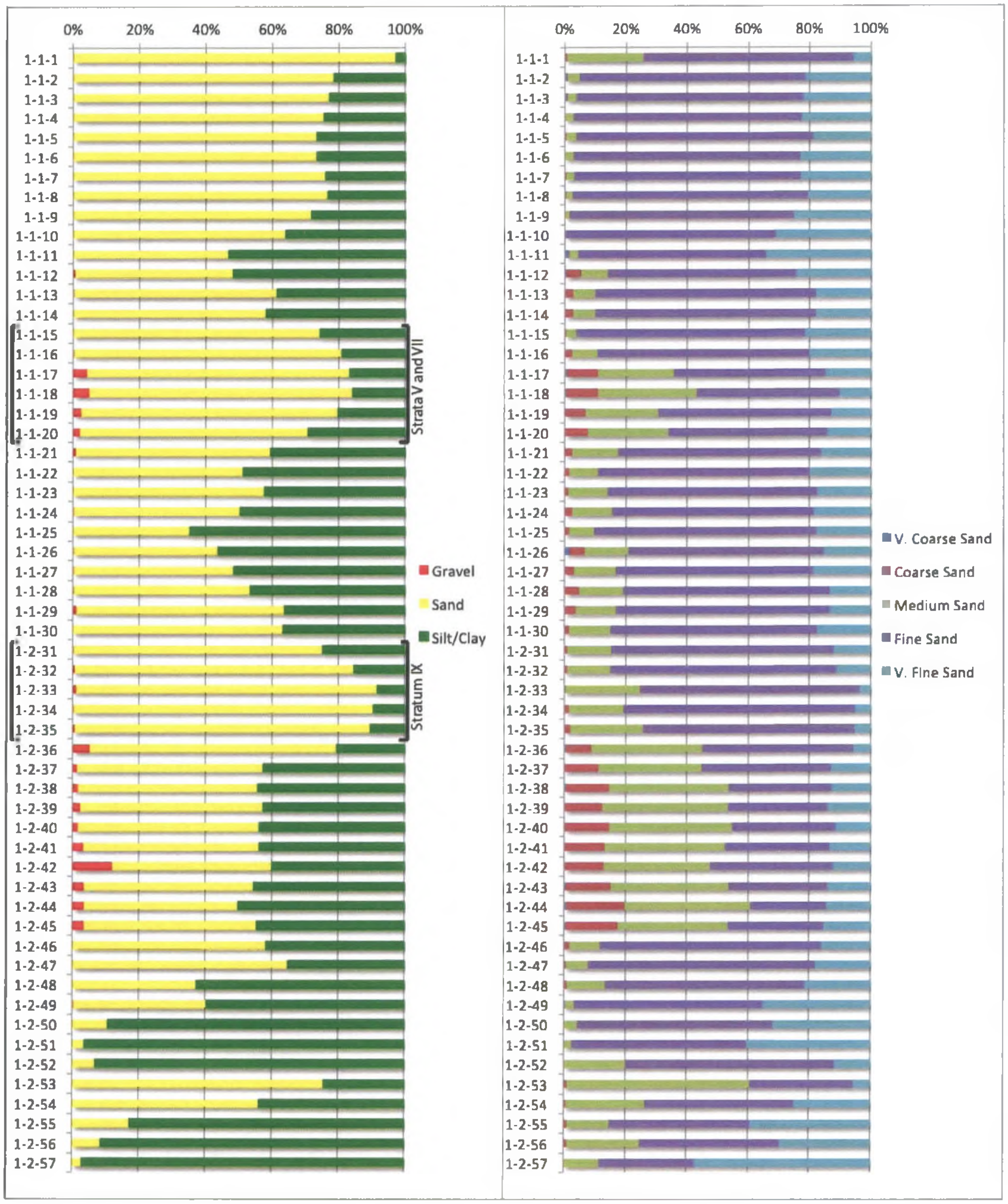

Figure 4.6. Results of textural analysis at Huaca del Sol. On the left is percent gravel, sand and silt/clay of the entire sample. On the right is the grain size distribution of the sand fraction. Black brackets show peaks in sand content at strata V and VII and stratum IX, which may represent individual flood events.

CHAPTER 5

DISCUSSION AND CONCLUSIONS

The stratigraphic sequences at San José de Moro and Huaca del Sol are both composed primarily of fluvial deposits consisting of muddy sands and sandy muds. They reflect the input of El Niño events as well as countless other environmental factors. The details of these environmental influences are essential to the interpretation of fluvial deposits in coastal Peru. Despite the complexity of the riverine/coastal systems involved, El Niño is undoubtedly one of the primary drivers of fluvial processes and deposits, through its extreme influence over precipitation regimes in coastal Peru. As mentioned in previous chapters, due to the small size of the Chamán River's drainage basin all waterlaid deposits at San José de Moro that date prior to 9,000 cal yr BP and after 5,800 cal year BP are believed to be El Niño related. At Huaca del Sol, non-El Niño sources of flooding are present, but El Niño is indubitably a major contributor to the alluvial record. In this chapter we consider the stratigraphic sequences described in the previous two chapters, and what these deposits can tell us about regional paleoenvironment and landscape formation, as well as about the effect of El Niño on the sedimentary record of this region.

At San José de Moro, the prominent shift from broad, relatively flat floodplain deposits to cross-bedded channelized deposits may have resulted from several causes, including channel avulsion, a change in local vegetation, a change in river base level, stream capture, or an increase in precipitation. Each of these factors needs to be considered in greater detail to understand their potential for influencing stratigraphic sequence at the site.

Channels and bars of braided streams can be created, destroyed and/or shift positions during high flow stages. Changes in grain size within the stratigraphic profile at San José de Moro may represent the changing proximity of channels as they moved laterally across the floodplain. The channelized upper deposits may have been caused by the movement and/or creation of channels at the location of the site simply due to the normal processes of channel avulsion. It should be noted that because channel avulsion occurs primarily under high flow stages, channels are more prone to shift under higher discharge floods. Therefore, channel avulsion takes place under the normal conditions of a braided stream, but higher flood velocities caused by any of the processes described below may contribute to increased channel avulsion.

Local vegetation is an important factor in determining stream character. Vegetation can act to stabilize stream banks and limit channel migration and avulsion. Unvegetated banks are more susceptible to rapid migration and the formation of braided systems (e.g., Hupp and Osterkamp 1996). It is therefore possible that a change in vegetation along the banks of the Chamán River could have allowed for a change in stream character resulting in the shift seen in the sequence of fluvial deposition at San José de Moro. A decrease in vegetation could have led to destabilization, allowing for increased channel migration and avulsion. Changes in vegetation may be linked to water availability due to climate variability or related to human land use.

A change in base level could also have caused a shift in the nature of fluvial deposits. Eustatic sea level stabilization occurred between approximately 6,000 and 7,000 cal year BP. Records from the Santa Valley indicate that local sea levels probably rose during the early to middle Holocene, reached a highstand at approximately 4,000 cal yr BP and subsequently remained stable or fell slowly (Sandweiss et al. 1998). The current lack of secure dates for the stratigraphic sequence at San José de Moro means that it is unable to be correlated with sea level at this time. The nature of the shift between broad overbank deposits and channelized deposits, however, is rather abrupt; if this shift resulted from a change in sea level we would expect it to consist of a much more gradual change. It is possible, however, that abrupt change may have occurred if the river breached the local baselevel somewhere downstream.

Tectonic activity is another potential cause of base-level change (Bull and McFadden 1977; Leopold and Bull 1979). The Peruvian Andes are the result of the subduction of the oceanic Nasca Plate beneath the continental South American Plate, and much of the South American coast has experienced tectonic uplift during the Holocene. There is little unambiguous evidence for Holocene uplift in the vicinity of the Jequetepeque Valley. It has been argued that between 6°S and 14°S there are no pre-Holocene coastal or marine sediments above sea level and that tectonic studies indicate the region has a near neutral state of stress (Wells 1988; Mercier et al. 1992; Noller 1993; Noller and Sebrier 1998; Wells and Noller 1999). DeVries and Wells (1990), however, do suggest that tectonic uplift may be evidenced by the emptying of the Santa lagoon, and that several other areas may exhibit similar situations. It is therefore possible that tectonic uplift was a cause of variation within the stratigraphic profile at San José de Moro, although there is no strong evidence for its likelihood.

Stream capture is another possible cause for the shift seen at San José de Moro. Fluvial erosion can cause a tributary to shift its course to a neighboring drainage basin (e.g., Prince et al. 2011). This alters the boundaries of both basins; the basin that has captured the tributary becomes larger, therefore increasing its overall discharge and flood velocity independently of other environmental changes. However, in the case of the Chamán River at San José de Moro, the river basin is currently very small, and sharply delineated. It does not appear that the Chamán captured an adjacent stream. The larger Moche River has a significantly larger drainage, and may have experienced changes in drainage patterns. However, at this time this has not been investigated.

The final possibility is that an increase in precipitation is the cause of the depositional shift at San José de Moro. More precipitation, particularly in the form of increased intensity of precipitation events, would result in a higher discharge and higher velocity flow, both increasing the competency and capacity of the river. In coastal Peru the most likely cause for this increase in precipitation is El Niño, particularly after 5,800 cal yr BP when sea-surface temperatures fell and El Niño once again became a cyclical phenomenon. As discussed in Chapter 1, between approximately 9,000 and 5,800 cal yr BP most evidence indicates that El Niño was absent, or only occurred at a very low frequency. Warmer sea-surface temperatures during this time would result in seasonal but limited precipitation north of 12°S. San José de Moro lies within this area and almost certainly experienced some periodic rainfall (Rollins et al. 1986; Sandweiss et al. 2007). It is therefore possible that the sequence of fluvial deposition at San José de Moro is related to precipitation during this pre-El Niño period. It is more likely, however, that the sequence was deposited primarily by El Niño rainfall and the shift represents in increase in the intensity of El Niño activity. Only detailed chronological analysis can address this issue.

To summarize, a consideration of the shift from broad, relatively flat floodplain deposits to cross-bedded channelized deposits indicates it was most likely not caused by sea-level change but is instead the result of one of five distinct possibilities: 1) with no other environmental influence the process of channel avulsion resulted in the creation of channels directly on the site; 2) a decrease in local vegetation destabilized the stream making it more susceptible to rapid migration and avulsion; 3) tectonic uplift resulted in an abrupt change in relative base level; 4) fluvial erosion upstream from the site resulted in a tributary shifting its course from an adjacent basin to the Chamán River basin, resulting in an enlargement of the Chamán's drainage area; or 5) a change in climate resulted in an increase in the intensity of precipitation events. Secure dating would provide the means for a better understanding the fluvial record at San José de Moro. The sequence could then be correlated with other proxies. It is possible that the shift from broad floodplain deposits to channelized deposits is the result of El Niño's return from its hiatus at around 5800 cal yr BP, or the increase in frequency, and perhaps intensity, that occurs at 3000 cal yr BP. If the shift at San José de Moro is shown to have occurred at either of these times it would suggest a potential correlation with changes in past El Niño intensity.

As at San José de Moro, the stratigraphic sequence at Huaca del Sol has significant textural variation. This is consistent with variation that should be expected to correspond with the shifting and avulsion of the Moche River over time. Unlike the upper part of the sequence at San José de Moro, the sequence at Huaca del Sol does not contain any clear channelization (with the possible exception of stratum IX) and no strata contain cross-bedding or flat-bedding; this suggests that the sequence primarily represents overbank flood deposits. There is no clear evidence of any changes in climate or any other environmental factors having a significant effect on the stratigraphic sequence at the site.

Stratum I at Huaca del Sol appears to be aeolian in nature, consisting of very well sorted fine sand. Other strata are very well sorted and consist of fine to medium sand and also may potentially represent aeolian deposition (e.g., stratum IX), but stratum I stands out as the most well sorted stratum with the least amount of silt/clay. Textural analysis alone cannot verify the aeolian nature of a deposit; particle shape, sedimentary structures and several other factors can also provide evidence of an aeolian origin (Collinson 1986b). There were no visible sedimentary structures in stratum I or in other sandy deposits at Huaca del Sol, and other forms of analysis were beyond the scope of this project. It therefore cannot be said that stratum I, or any other stratum, are conclusively aeolian. It is important to note that mica was found in every sample collected from Huaca del Sol, including the single sample taken from the bottom of stratum I (sample 1-1-1). Due to the shape of its particles, mica is generally not found in aeolian sand (Collinson 1986b). If stratum I, or any other stratum, is in fact aeolian then the presence of mica may indicate immaturity of the sand.

Additionally, strata V and VII (samples 1-1-15 to 1-1-20) and stratum IX (samples 1-1-27 to 1-1-35), both represent prominent peaks in sand content within the sequence at Huaca del Sol. It is possible that these two strata represent distinct individual flood events.

Human Occupation

The stratigraphic profiles at San José de Moro and Huaca del Sol both contain evidence of human presence below what was previously recognized as the earliest occupations at each site. At San José de Moro probable agricultural furrows were found directly below the lowest previously recognized archaeological level, which contained artifacts diagnostic of Middle Moche (Zevallos 2012). Botanical analysis revealed the presence of possible maize starch grains and possibly human damaged starch grains within and below the furrows (Linda Perry, personal communication 2013). Microscopic fragments of charcoal were found in several locations including the lowest sample collected from the profile. Although the agricultural furrows indicate use of the site of San José de Moro by humans earlier than previously thought, the botanical remains and charcoal could have travelled to the site through alluvial processes. This does not necessarily indicate human presence at the site itself, but at a minimum indicates human utilization of the Chamán River Basin at or upstream from the site.

At Huaca del Sol several cobble fragments, which may represent fire-altered rock, were found in the profile as far as 2.45 m below the earliest recognized Moche occupation. As these were too large to have been deposited by the same source as the surrounding alluvial sediment, they almost certainly were transported to the site by humans, indicating utilization of the site prior to the construction of the adobe structure. They occur between the two preliminary OSL dates of AD 0 and AD 400.

Landscape Construction

The profiles at San José de Moro and Huaca del Sol reveal two significant commonalities between the sites. First, at both sites the intensive Moche occupations directly overlay agricultural features. At San José de Moro we discovered agricultural furrows less than half a meter below highly disturbed soil that was previously thought to represent the first occupation of the site. Microbotanic evidence for agriculture exists as far as one meter below the furrows. Huaca del Sol sits directly on what Santiago Uceda describes as agricultural soil (personal communication, 2013).

The second major commonality between the two sites is that they both sit on landscapes built largely by El Niño-driven aggradation. As the Chamán River only floods during El Niño events, the ground surface on which San José de Moro sits is essentially a creation of El Niño. The Moche River floods from sources other than El Niño, but El Niño is one of the most significant sources of flooding in the valley and has certainly contributed to the aggradation of its floodplain.

San José de Moro and Huaca del Sol thus share a basic story. Before aggradation created the sedimentary sequences, the lower elevation of their floodplains meant that the risks associated with flood events of the same magnitude would have been higher than today. As aggradation raised the elevation of the floodplain the risks of flooding would have decreased with time. During this period humans utilized the sites or the surrounding region, but there is no evidence of concentrated occupation at the sites. Eventually, people began to use the sites for agriculture. This would not have happened before the landscape was perceived to have a sufficiently low risk of flood damage. Perhaps the initial utilization of the sites for agriculture was opportunistic, using the temporary increase in available water during El Niño events to grow crops in areas that were not normally able to be cultivated. Whether this is true or a more sustained use of the land began immediately, an agricultural landscape was created.

Within this landscape prehistoric people decided that the two sites were suitable for use for intensive occupation and ceremonialism. At San José de Moro, people began to lay their dead in the ground, including elite and prominent members of society. The site also began to be used to produce and consume chicha, which may have been consumed as part of ritual activities. At Huaca del Sol, people constructed an adobe structure larger than any they had seen before. In addition to the original mound, an urban center developed, as well as a second smaller but no less significant monumental adobe structure used for rituals, including sacrifice ceremonies.

El Niño was thus a force of great significance in constructing the landscapes found to be propitious for at least two Moche sites of great importance based on the size of the structures and the richness of the recovered burial materials. El Niño should therefore be seen not only as a cause for weather variation with potential for human impact, but also as an essential part of forming the physical setting of prehistoric settlements.

Future Work

The utilization of El Niño-influenced and created landscapes for agriculture, occupation and ceremonialism needs to be investigated at other sites in the north coast. Future work should address which other types of sites in the region are built on fluvial deposits and when these sites first begin to appear in these settings. A similar formation chronology may have both climatic and social implications. In particular, important Moche ceremonial sites should be examined within this framework to see which others, if any, are positioned on similar landscapes. The timing of aggradation and the relative safety from El Niño flooding must have been of great importance to the past inhabitants of the region, and this may be reflected in culture change in the region, perhaps including the development of Moche ceremonialism

The profiles we investigated at San José de Moro and Huaca del Sol would be more informative with secure dating. At the time of writing, results of OSL analysis are pending and other dating options are being investigated. If successful, absolute dating will allow for a better understanding of the timing of events at the sites. This is particularly important at San José de Moro where we discovered a shift in the nature of sedimentary deposits that may be related to a significant environmental change. With absolute dating, we will furthermore be able to compare the profiles at both sites to coeval cultural and environmental developments that occurred throughout the region.

The stratigraphic sequences at San José de Moro and Huaca del Sol, along with the work of Wells (1987, 1990) in the Casma Valley, illustrate the great potential for fluvial deposits to provide evidence of past El Niño activity. The investigation of more undisturbed fluvial sequences throughout coastal Peru would prove highly valuable in developing a detailed record of changes in El Niño intensity and frequency over time.

At both San José de Moro and Huaca del Sol evidence of human presence was discovered below what was previously the earliest known occupation of each site. This suggests that valuable information is still located below both of these significant sites and may warrant excavation of more area of the sites to these deeper levels. Stratigraphic excavations in these fluvial contexts combined with regional surveys could provide a wealth of information on how the Moche and the poorly understood earlier inhabitants of the Jequetepeque and Moche Valleys came to occupy these areas and how they may have responded to changes in the landscape and environment over time.

The probable furrows and the starch grains found at San José de Moro indicate potential for the site to reveal data related to middle, early or pre-Moche agriculture. An investigation of the structure and extent of the furrows as well as any artifacts that may be associated with these levels could provide important details about farming methods. Further botanical analysis would prove highly valuable in showing what types of plants were being grown and utilized in the Jequetepeque Valley.

Conclusions

The work undertaken for this thesis represents several significant contributions. First, the stratigraphic sequences investigated underneath San José de Moro and Huaca del Sol provide important information on the nature and development of the landscapes on which these sites were constructed. The primarily fluvial nature of both contexts was fully supported by the data collected. Second, the sequence at San José de Moro revealed a major shift from broad, finer-grained floodplain deposits to higher energy, coarser-grained, cross-bedded and flat-bedded channelized deposits. This may have occurred due to channel avulsion or an increase in flood velocity at the site. Either case is potentially the result of a significant increase in the strength of El Niño events. Third, within the stratigraphic sequences at both sites there was clear evidence of human presence below what was previously the earliest recognized occupation of the site. At San José de Moro these finds were particularly significant as they revealed evidence of early/middle Moche or pre-Moche agriculture including potential agricultural furrows. Finally, a consideration of the strong El Niño influence on fluvial systems in coastal Peru suggests that El Niño should be seen not only as a cause of weather variation and catastrophism, but also as a constructor of landscapes utilized and inhabited by prehistoric people. San José de Moro and Huaca del Sol, two of the region's most important sites, were both built on broad, elevated areas with decreased risk of El Niño flooding. These surfaces were created at least in part by El Niño-driven aggradation. Thus, it is clear that reconstructing past patterns of El Niño activity is essential not only for understanding the climatological context of prehistoric human settlements, but also for understanding the nature and development of their physical setting.

REFERENCES

Andrus, C. F. T., D. E. Crowe, E. J. Reitz, and C. S. Romanek
2002 Otolith $\delta^{18}O$ record of Mid-Holocene Sea Surface Temperatures in Peru. Science 295:1508-1511.

Andrus, C. F. T., D. E. Crowe, D. H. Sandweiss, E. J. Reitz C. S. Romanek, and K. A. Maasch
2003 Response to comment on "Otolith $\delta^{18}O$ record of Mid-Holocene Sea Surface Temperatures in Peru". Science 209:203b.

Andrus, C. F. T., G. G. L. Hodgins, D. H. Sandweiss, and D. E. Crowe.
2005 Molluscan radiocarbon as a proxy for El Niño-related upwelling variations in Peru. In, Isotopic and Elemental Tracers of Cenozoic Climate Change, edited by G. Mora and D. Surge, pp. 13-20. Geological Society of America Special Paper 395, Boulder, CO.

Bagnold, B. A.
1941 The physics of blown sand and desert dunes. William Morrow and Co., New York.

Belknap, D. F.
n.d. Folk Textural Classification of Sediments. Unpublished teaching diagram. University of Maine, Orono.

Boggs, S.
2012 Principles of sedimentology and stratigraphy, 5th edition. Prentice Hall, Upper Saddle River, New Jersey.

Brennan, C.
1982 Cerro Arena: origins of the urban tradition on the Peruvian north coast. Current Anthropology 23(3):247-254.

Bridge, J. S.
2003 Rivers and floodplains. Blackwell, Oxford.

Bull, W. B., and L. D. McFadden
1977 Tectonic geomorphology north and south of the Gerlock fault, California. Eighth Annual Geomorphology Symposia Series, pp. 115-137, Binghamton, New York.

Burger, R. L.
1992 Chavín and the origins of Andean civilization. Thames and Hudson, New York.

Carré, M., J. P. Sachs, S. Purca, A. J. Schauer, P. Bracannot, R. Angeles F., M. Julien, and D. Lavallée.
2014 Holocene history of ENSO variance and asymmetry in the eastern tropical Pacific. Science 345:1045-1048.

Castillo B., L. J.
2008 Generalidades. In Programa arquelógico San José de Moro, informe de excavaciones temporada 2008, edited by L. J. Castillo B. pp. 3-17. Pontificia Universidad Católica del Perú, Lima.

2009 Gallinazo, Vicús, and Moche in the development of complex societies along the north coast of Peru. In Gallinazo: an early cultural tradition on the Peruvian north coast, edited by J. F. Millaire with M. Morlion, pp. 223-232. Cotsen Institute, Los Angeles.

Castillo B., L. J., J. Rucabado Y., M. del Carpio P., K. Bernuy Q., K. Ruiz R., C. Rengifo C., G. Prieto B., and C. Fraresso
2008 Ideología y poder en la consolidación, colapso u reconstruction del Estato Mochica del Jequetepeque: El Proyecto Arqueológico San José de Moro (1991-2006). Ñawpa Pacha 26:1-86.

Castillo B., L. J., and S. Uceda C.
2008 The Mochicas. In The Handbook of South American archaeology, edited by H. Silverman and W. Isbell, pp. 707-730. Springer, New York.

Collinson, J. D.
1986a Alluvial Sediments. In Sedimentary Environments and Facies, second edition, edited by H.G. Reading, pp. 20-62. Blackwell Scientific Publications, Oxford.

1986b Deserts. In Sedimentary Environments and Facies, second edition, edited by H.G. Reading, pp. 95-112. Blackwell Scientific Publications, Oxford.

Cusicanqui, S., and R. Barrazueta
2008 Informe téchnico de las excavaciones en el área 35-temporada 2008. In Programa arquelógico San José de Moro, informe de excavaciones temporada 2008, edited by L. J. Castillo B. pp. 36-71. Pontificia Universidad Católica del Perú, Lima.

Del Carpio P., M.
2009 Middle Moche and Gallinazo Ceramic Styles at San José de Moro. In Gallinazo: an early cultural tradition on the Peruvian north coast, edited by J. F. Millaire with M. Morlion, pp. 61-76. Cotsen Institute, Los Angeles.

DeVries, T. J., and L. E. Wells
1990 Thermally-anomalous Holocene molluscan assemblages from coastal Peru: evidence for paleogeographic, not climatic change. Paleogeography, Paleoclimatology, Paleoecology 81:11-32.

Elera, C. G.
1993 El Complejo Cultural Cupisnique: Antecedentes y Desarrollo de su Ideología Religiosa. Senri Ethnological Studies 37:229-257.
1998 The Puémape Site and the Cupisnique Culture: A Case Study on the Origins and Development ad Complex Society in the Central Andes, Perú. PhD Dissertation, Department of Archaeology, University of Calgary, Calgary.

Fogel, H.
1993 Settlements in time: a study of social and political developments during the Gallinazo Occupation of the north coast of Peru. PhD dissertation, Yale University.

Folk, R. L.
1954 The distinction between grain size and mineral composition in sedimentary rock nomenclature. Journal of Geology 62:344-359.

1974 Petrology of sedimentary rocks. Hemphill Publishing Company, Austin.

Fontugne, M., P. Usselmann, D. Lavallée, M. Julien, and C. Hatté
1999 El Niño Variability in the Coastal Desert of Southern Peru during the Mid-Holocene. Quaternary Research 52:171-179.

Haas, J., Creamer, W., and Ruiz, A.
2004 Dating the Late Archaic Occupation of the Norte Chico Region in Peru. Nature 432:1020-1023.

Hastings, C. M., and M. E. Moseley
1975 The adobes of Huaca del Sol and Huaca de la Luna. American Antiquity 40(2):196-203.

Hupp, C. R. and W. R. Osterkamp
1996 Riparian vegetation and fluvial geomorphic processes. Geomorphology 14:277-295.

Keefer, D. K., S. D. deFrance, M. E. Moseley, J. B. Richardson III, D. R. Satterlee, and A. Day-Lewis
1998 Early Maritime Economy and El Niño Events at Quebrada Tacahuay, Peru. Science 281:1833-1835.

Keefer, D. K., M. E. Moseley, and S. D. deFrance
2003 A 38,000-year record of floods and debris flows in the Ilo region of southern Peru and its relation to El Niño events and great earthquakes. Palaeogeography, Palaeoclimatology, Palaeoecology 194:41-77.

Leopold, L. B., and W. B. Bull
1979 Base level, aggradation, and grade. Proceedings of the American Philosophical Society 123(3):168-202.

Maasch, K. A.
2009 El Niño and interannual variable of climate in the western hemisphere. In El Niño, Catastrophes, and Culture Change in Ancient America, edited by J. Quilter and D. H. Sandweiss, pp. 33-55. Dumbarton Oaks, Washington, D.C.

Mercier, J. L., M. Serbrier, A. Lavenu, J. Cabrera, O. Bellier, J. F. Dumont, and J. Machare
1992 Changes in the tectonic regime above a subduction zone of the Andean type: The Andes of Peru and Bolivia during the Pliocene-Pleistocene. Journal of Geophysical Research 97:11,945-11,982.

Miall, A. D.
1977 Fluvial Sedimentology. Canadian Society of Petroleum Geologists, Calgary.

MINEM
1997 Estudio de Evaluación ambiental territorial y de planteaminientos para la reducción o eliminación origen minero en la cuanca del río Moche. Lima: Minesterio de Energia y Minas.

Moseley, M. E.
2001 The Incas and their Ancestors: The Archaeology of Peru. 2nd Edition. Thames and Hudson, London and New York.

Moy, C. M., G. O. Seltzer, D. T. Rodbell, and D. M. Anderson
2002 Variability of El Niño/southern oscillation activity at millennial timescales during the Holocene epoch. Nature 420:162-165.

Nesbitt, J.
2012 Excavations at Caballo Muerto: an investigation into the origins of the Cupisnique culture. PhD dissertation, Yale University.

Noller, J. S.
1993 Late Cenozoic stratigraphy and soil geomorphology of the Peruvian desert, 3 degrees-18 S: a long-term record of hyperaridity and El Niño. Unpublished PhD. Dissertation, University of Colorado, Boulder.

Noller, J. S., and M. Sebrier
1998 Peru. In Active fault map of the world, Western Hemisphere, edited by M. Machette. International Lithoshpere Programme.

Philander, S. G. H.
1985 El Niño and La Niña. Journal of the Atmospheric Sciences. 42(23):2652-2662.

Pozorski, S.
1983 Changing subsistence priorities and early settlement patterns on the north coast of Peru. Journal of Ethnobiology 3:15-38.

Prince, P. S., J. A. Spotila, and W. S. Henika
2011 Stream capture as driver of transient landscape evolution in a tectonically quiescent setting. Geology 39(9):823-826.

Quilter, J.
1991 Late Preceramic Peru. Journal of World Prehistory, 5(4):387-438.

2002 Moche politics, religion, and warfare. Journal of World Prehistory 16(2):145-195.

2010 Moche: archaeology, ethnicity, identity. Buletin de l'Institut Français d'Études Andines 39(2):225-241.

Rein, B., A. Lückge, and F. Sirocko
2004 A major Holocene ENSO anomaly during the Medieval period. Geophysical Research Letters 31.

Rein, B., A. Lückge, L. Reinhardt, F. Sirocko, A. Wolf, and W. Dullo
2005 El Niño variability off Peru during the last 20,000 years. Paleoceanography 20.

Reitz, E. J., and D. H. Sandweiss
2001 Environmental Change at Ostra Base Camp, A Peruvian Preceramic Site. Journal of Archaeological Science 28:1085-1100.

Rodbell, D. T., G. O. Seltzer, D. M. Anderson, M. B. Abbott, D. B. Enfield, and J. H. Newman
1999 An ~15,000-year record of El Niño-driven Alluviation in Southwestern Ecuador. Science, 283:516-520.

Rollins, H. B., J. B. Richardson III, and D. H. Sandweiss
1986 The birth of El Niño: geoarchaeological evidence and implications. Geoarchaeology 1:3-15.

Salazar-Burger, L., and R. L. Burger
1996 Cupisnique. In Andean art at Dumbarton Oaks, edited by E. H Boone, pp. 87-100. Dumbarton Oaks, Washington, D.C.

Sandweiss, D. H.
2003 Terminal Pleistocene through Mid-Holocene archaeological sites as paleoclimatic archives for the Peruvian coast. Palaeogeography, Palaeoclimatology, Palaeoecology 194:23-40.

Sandweiss, D. H., A. R. Kelley, D. F. Belknap, J. T. Kelley, K. Rademaker, and D. A. Reid
2010 GPR Identification of an Early Monument at Los Morteros in the Peruvian Coastal Desert. Quaternary Research 73:439-448.

Sandweiss, D. H., K. A. Maasch, C. F. T. Andrus, E. J. Reitz, J. B. Richardson III, M. Riedinger-Whitmore, and H. B. Rollins
2007 Mid-Holocene climate and culture change in coastal Peru, In, Climate Change and Cultural Dynamics: A Global Perspective on Mid-Holocene Transitions, edited by David G. Anderson, Kirk A. Maasch and Daniel H. Sandweiss, pp. 25-50. Academic Press, London.

Sandweiss, D. H., K. A. Maasch, D. F. Belknap, J. B. Richardson III, and H. B. Rollins.
1998 Discussion of: Lisa E. Wells, 1996. The Santa Beach Ridge Complex, Journal of Coastal Research, 12(1), 1-17. Journal of Coastal Research 14(1):367-373.

Sandweiss, D. H., K. A. Maasch, R. L. Burger, J. B. Richardson III, H. B. Rollins, and A. Clament
2001 Variation in Holocene El Niño frequencies: Climate records and cultural consequences in ancient Peru. Geology 29:603-606.

Sandweiss, D. H., and J. Quilter
2012 Collation, correlation, and causation in the prehistory of coastal Peru. In Surviving sudden environmental change: understanding hazards, mitigating impacts, avoiding disasters, edited by J. Cooper and P. Sheets, pp. 117-139. University Press of Colorado, Boulder.

Sandweiss, D. H., R. Shady S., M. E. Moseley, D. K. Keefer, and C. R. Ortloff
2009 Environmental change and economic development in coastal Peru between 5,800 and 3,600 years ago. Proceedings of National Academy of Sciences 106:1359-1363.

Sandweiss, D. H., J. B. Richardson III, E. J. Reitz, H. B. Rollins, and K. A. Maasch
1996 Geoarchaeological Evidence from Peru for a 5000 Years B.P. Onset of El Niño. Science 273:1531-1533.

Sandweiss, D. H., J. B. Richardson III, E. J. Reitz, H. B. Rollins, and K. A. Maasch
1997 Determining the Early History of El Niño: Response. Science 276:966-967.

Shimada, I.
1994 Pampa Grande and the Mochica Culture. University of Texas Press, Austin.

Stewart, R. M.
2002 Archaeology: Basic field methods. Kendall/Hunt Publishing, Dubuque, Iowa

Uceda C., S.
2010 Los contextos urbanos de producción artisanal en el complejo archeólogico de las huacas del Sol y de la Luna. Buletin de I'Institut Français d'Études Andines 39(2):243-297.

Uceda C, S., H. Gayoso R., and N. Gamarra C.
2009 The Gallinazo at Huacas de Moche: style or culture? In Gallinazo: an early cultural tradition on the Peruvian north coast, edited by J. F. Millaire with M. Morlion, pp. 105-124. Cotsen Institute, Los Angeles.

Víchez M., M. S., S. P. Villacorta C., J. E. Chira F., F. Peña L, and W. Pari P.
2007 Estudio Geoambiental de la Cuanca de los Ríos Jequetepeque y Loco de Chamán. INGEMMET, Serie C. Geodinámica e Ingeniería Geológica, No. 36. Lima: Instituto Geológico, Minero y Metalúrgico.

Warner, J. P.
2010 Interpreting the Architectonics of Power and Memory at the Late Formative Center of Jatanca, Jequetepeque Valley, Peru. PhD Dissertation, Department of Anthropology, University of Kentucky, Lexington.

Waters, M. R.
1992 Principles of geoarchaeology. The University of Arizona Press, Tuscon.

Wells, L. E.
1987 An alluvial record of El Niño events from northern coastal Peru. Journal of Geophysical Research 92(C13):14,463-14,470.

1988 Holocene fluvial and shoreline history as a function of human and geological factors in arid northern Peru. PhD dissertation, Stanford University, California.

1990 Holocene history of El Niño phenomenon as recorded in flood sediments of northern coastal Peru. Geology 18:1134-1137.

Wells, L. E., and J. S. Noller
1999 Holocene coevolution of the physical landscape and human settlement in northern coastal Peru. Geoarchaeology 14(8):755-789.

Zevallos C., D.
2012 Informe téchnico de las excavaciones en el área 35 - temporada 2012. In Programa arquelógico San José de Moro, informe de excavacion temporada 2012, edited by L. J. Castillo B. pp. 82-143. Pontificia Universidad Católica del Perú, Lima.

APPENDIX A

INDIVIDUAL SAMPLE RESULTS OF TEXTURAL ANALYSIS OF UNITS 1 AND 2 AT SAN JOSÉ DE MORO

Sample:	SJM 1-1-1	% Gravel:	0.57
Depth:	0-5	% Sand:	27.33
Level:	I	% Silt/Clay:	72.10

PHI	Weight as Percentage of Cumulative Total
-1.00	0.00
-0.75	0.00
-0.50	0.00
-0.25	0.00
0.00	0.00
+0.25	0.50
+0.50	0.75
+0.75	1.00
+1.00	1.50
+1.25	2.00
+1.50	3.00
+1.75	4.25
+2.00	5.75
+2.25	8.25
+2.50	28.00
+2.75	48.50
+3.00	67.00
+3.25	82.75
+3.50	93.50
+3.75	98.50
+4.00	100.00

Percent Weight Error:	-4.3340	
Folk-Ward Statistical Parameters		
Graphic Mean:	2.7991	:Fine Sand
Incl Graph Standard Deviation:	0.4903	:Well Sorted
Incl Graph Skewness:	0.0199	:Near Symmetrical
Graphic Kurtosis:	1.0478	:Mesokurtic
Normalized Kurtosis:	0.5117	

Parameter by the Method of Moments	
Mean X:	2.8869
Varience:	0.3017
Skewness:	-1.1710
Standard Deviation:	0.5493
Kurtosis:	6.7965

Notes: Mica present; clumps up to 2.3 cm; root casts

Sample:	SJM 1-1-2	% Gravel:	0.58
Depth:	5-10	% Sand:	37.38
Level:	I	% Silt/Clay:	62.04

PHI	Weight as Percentage of Cumulative Total
-1.00	0.00
-0.75	0.00
-0.50	0.00
-0.25	0.00
0.00	0.00
+0.25	0.00
+0.50	0.00
+0.75	0.20
+1.00	0.39
+1.25	0.59
+1.50	0.99
+1.75	1.78
+2.00	3.75
+2.25	8.09
+2.50	26.43
+2.75	50.30
+3.00	70.22
+3.25	85.01
+3.50	94.48
+3.75	99.01
+4.00	100.00

Percent Weight Error:	-1.9101

Folk-Ward Statistical Parameters		
Graphic Mean:	2.7792	:Fine Sand
Incl Graph Standard Deviation:	0.4395	:Well Sorted
Incl Graph Skewness:	0.0922	:Near Symmetrical
Graphic Kurtosis:	0.9944	:Mesokurtic
Normalized Kurtosis:	0.4986	

Parameter by the Method of Moments	
Mean X:	2.8969
Varience:	0.2077
Skewness:	0.3568
Standard Deviation:	0.4557
Kurtosis:	4.3843

Notes: Mica present; clumps up to 1.5 cm; root casts

Sample:	SJM 1-1-3	% Gravel:	0.00
Depth:	10-13	% Sand:	48.56
Level:	I	% Silt/Clay:	51.44

PHI	Weight as Percentage of Cumulative Total
-1.00	0.00
-0.75	0.00
-0.50	0.00
-0.25	0.00
0.00	0.13
+0.25	0.13
+0.50	0.13
+0.75	0.13
+1.00	0.27
+1.25	0.27
+1.50	0.27
+1.75	0.27
+2.00	1.35
+2.25	7.40
+2.50	33.24
+2.75	58.82
+3.00	77.93
+3.25	90.17
+3.50	96.77
+3.75	99.19
+4.00	100.00

Percent Weight Error:	-3.5255

Folk-Ward Statistical Parameters		
Graphic Mean:	2.7070	:Fine Sand
Incl Graph Standard Deviation:	0.3919	:Well Sorted
Incl Graph Skewness:	0.1010	:Fine Skewed
Graphic Kurtosis:	0.9704	:Mesokurtic
Normalized Kurtosis:	0.4925	

Parameter by the Method of Moments	
Mean X:	2.8338
Varience:	0.1611
Skewness:	-0.0978
Standard Deviation:	0.1611
Kurtosis:	6.4047

Notes: Mica present; clumps up to 2.5 cm

Sample:	SJM 1-1-4	% Gravel:	0.00
Depth:	13-18	% Sand:	72.73
Level:	IIa	% Silt/Clay:	27.27

PHI	Weight as Percentage of Cumulative Total
-1.00	0.20
-0.75	0.20
-0.50	0.20
-0.25	0.20
0.00	0.20
+0.25	0.20
+0.50	0.39
+0.75	0.39
+1.00	0.59
+1.25	0.59
+1.50	0.78
+1.75	1.37
+2.00	2.75
+2.25	5.49
+2.50	24.51
+2.75	56.86
+3.00	77.06
+3.25	88.63
+3.50	94.90
+3.75	98.63
+4.00	100.00

Percent Weight Error:	1.9246	
Folk-Ward Statistical Parameters		
Graphic Mean:	2.7450	:Fine Sand
Incl Graph Standard Deviation:	0.3876	:Well Sorted
Incl Graph Skewness:	0.2168	:Fine Skewed
Graphic Kurtosis:	1.1329	:Leptokurtic
Normalized Kurtosis:	0.5312	
Parameter by the Method of Moments		
Mean X:	2.8647	
Varience:	0.2013	
Skewness:	-1.3373	
Standard Deviation:	0.4487	
Kurtosis:	15.0989	
Notes: Mica present		

Sample:	SJM 1-1-5	% Gravel:	0.00
Depth:	18-23	% Sand:	79.25
Level:	IIa	% Silt/Clay:	20.75

PHI	Weight as Percentage of Cumulative Total
-1.00	0.16
-0.75	0.16
-0.50	0.16
-0.25	0.24
0.00	0.24
+0.25	0.24
+0.50	0.24
+0.75	0.24
+1.00	0.24
+1.25	0.24
+1.50	0.24
+1.75	0.32
+2.00	0.72
+2.25	7.27
+2.50	33.15
+2.75	55.91
+3.00	76.36
+3.25	88.74
+3.50	94.85
+3.75	99.12
+4.00	100.00

Percent Weight Error:	-2.6255	
Folk-Ward Statistical Parameters		
Graphic Mean:	2.7246	:Fine Sand
Incl Graph Standard Deviation:	0.4030	:Well Sorted
Incl Graph Skewness:	0.1731	:Fine Skewed
Graphic Kurtosis:	0.9528	:Mesokurtic
Normalized Kurtosis:	0.4879	
Parameter by the Method of Moments		
Mean X:	2.8504	
Varience:	0.1853	
Skewness:	-0.9877	
Standard Deviation:	0.4305	
Kurtosis:	14.3602	
Notes: Mica present; very few clumps, up to 0.4 cm		

Sample:	SJM 1-1-6	% Gravel:	0.00
Depth:	23-28	% Sand:	81.93
Level:	IIa	% Silt/Clay:	18.07

PHI	Weight as Percentage of Cumulative Total
-1.00	0.00
-0.75	0.00
-0.50	0.00
-0.25	0.00
0.00	0.00
+0.25	0.00
+0.50	0.00
+0.75	0.13
+1.00	0.13
+1.25	0.13
+1.50	0.13
+1.75	0.13
+2.00	1.26
+2.25	9.22
+2.50	39.87
+2.75	61.99
+3.00	79.55
+3.25	90.40
+3.50	96.34
+3.75	99.12
+4.00	100.00

Percent Weight Error:	-2.0008

Folk-Ward Statistical Parameters		
Graphic Mean:	2.6815	:Fine Sand
Incl Graph Standard Deviation:	0.3987	:Well Sorted
Incl Graph Skewness:	0.2094	:Fine Skewed
Graphic Kurtosis:	1.0017	:Mesokurtic
Normalized Kurtosis:	0.5004	

Parameter by the Method of Moments	
Mean X:	2.0116
Varience:	0.1579
Skewness:	0.4437
Standard Deviation:	0.3974
Kurtosis:	3.8098

Notes: Mica present; very few clumps, up to 0.4 cm

Sample:	SJM 1-1-7	% Gravel:	0.00
Depth:	28-33	% Sand:	78.23
Level:	IIa	% Silt/Clay:	21.77

PHI	Weight as Percentage of Cumulative Total
-1.00	0.00
-0.75	0.00
-0.50	0.00
-0.25	0.00
0.00	0.00
+0.25	0.00
+0.50	0.00
+0.75	0.00
+1.00	0.00
+1.25	0.00
+1.50	0.00
+1.75	0.10
+2.00	1.16
+2.25	9.11
+2.50	34.88
+2.75	58.62
+3.00	79.07
+3.25	90.50
+3.50	96.32
+3.75	99.32
+4.00	100.00

Percent Weight Error:	1.7279

Folk-Ward Statistical Parameters		
Graphic Mean:	2.6946	:Fine Sand
Incl Graph Standard Deviation:	0.3981	:Well Sorted
Incl Graph Skewness:	0.1601	:Fine Skewed
Graphic Kurtosis:	0.9926	:Mesokurtic
Normalized Kurtosis:	0.4981	

Parameter by the Method of Moments	
Mean X:	2.8273
Varience:	0.1517
Skewness:	0.5122
Standard Deviation:	0.3894
Kurtosis:	2.9748

Notes: Mica present; very few clumps, up to 0.4 cm

Sample:	SJM 1-1-8	% Gravel:	0.00
Depth:	33-38	% Sand:	77.46
Level:	IIa	% Silt/Clay:	22.54

PHI	Weight as Percentage of Cumulative Total
-1.00	0.00
-0.75	0.00
-0.50	0.00
-0.25	0.00
0.00	0.00
+0.25	0.00
+0.50	0.00
+0.75	0.00
+1.00	0.10
+1.25	0.10
+1.50	0.10
+1.75	0.10
+2.00	0.51
+2.25	8.19
+2.50	35.01
+2.75	57.11
+3.00	77.89
+3.25	90.28
+3.50	96.52
+3.75	99.28
+4.00	100.00

Percent Weight Error:	-1.6407	
Folk-Ward Statistical Parameters		
Graphic Mean:	2.7052	:Fine Sand
Incl Graph Standard Deviation:	0.3960	:Well Sorted
Incl Graph Skewness:	0.1620	:Fine Skewed
Graphic Kurtosis:	0.9488	:Mesokurtic
Normalized Kurtosis:	0.4869	
Parameter by the Method of Moments		
Mean X:	2.8370	
Varience:	0.1517	
Skewness:	0.4305	
Standard Deviation:	0.3895	
Kurtosis:	3.2310	

Notes: Mica present

Sample:	SJM 1-1-9	% Gravel:	0.00
Depth:	38-43	% Sand:	79.73
Level:	IIa	% Silt/Clay:	20.27

PHI	Weight as Percentage of Cumulative Total
-1.00	0.19
-0.75	0.19
-0.50	0.19
-0.25	0.19
0.00	0.19
+0.25	0.19
+0.50	0.19
+0.75	0.19
+1.00	0.38
+1.25	0.58
+1.50	1.06
+1.75	2.98
+2.00	7.31
+2.25	27.33
+2.50	47.26
+2.75	65.93
+3.00	82.48
+3.25	92.40
+3.50	97.40
+3.75	99.52
+4.00	100.00

Percent Weight Error:	-1.9862

Folk-Ward Statistical Parameters		
Graphic Mean:	2.5611	:Fine Sand
Incl Graph Standard Deviation:	0.4618	:Well Sorted
Incl Graph Skewness:	0.0965	:Near Symmetrical
Graphic Kurtosis:	0.9313	: Mesokurtic
Normalized Kurtosis:	0.4822	

Parameter by the Method of Moments	
Mean X:	2.6846
Varience:	0.2386
Skewness:	-0.6828
Standard Deviation:	0.4885
Kurtosis:	8.6948

Notes: Mica present; very few clumps, up to 0.5 cm

Sample:	SJM 1-1-10	% Gravel:	0.00
Depth:	43-48	% Sand:	82.01
Level:	IIa	% Silt/Clay:	18.00

PHI	Weight as Percentage of Cumulative Total
-1.00	0.00
-0.75	0.00
-0.50	0.00
-0.25	0.00
0.00	0.13
+0.25	0.13
+0.50	0.26
+0.75	0.26
+1.00	0.93
+1.25	1.85
+1.50	3.84
+1.75	9.39
+2.00	23.54
+2.25	45.63
+2.50	63.10
+2.75	76.19
+3.00	86.24
+3.25	92.99
+3.50	96.96
+3.75	99.34
+4.00	100.00

Percent Weight Error:	2.9488	
Folk-Ward Statistical Parameters		
Graphic Mean:	2.3745	:Fine Sand
Incl Graph Standard Deviation:	0.5458	:Moderately Well Sorted
Incl Graph Skewness:	0.1696	:Fine Skewed
Graphic Kurtosis:	1.0518	:Mesokurtic
Normalized Kurtosis:	0.5126	
Parameter by the Method of Moments		
Mean X:	2.4980	
Varience:	0.3062	
Skewness:	0.1022	
Standard Deviation:	0.5534	
Kurtosis:	3.5792	
Notes: Mica present		

Sample:	SJM 1-1-11	% Gravel:	0.00
Depth:	48-53	% Sand:	84.91
Level:	IIc	% Silt/Clay:	15.09

PHI	Weight as Percentage of Cumulative Total
-1.00	0.00
-0.75	0.11
-0.50	0.11
-0.25	0.11
0.00	0.11
+0.25	0.21
+0.50	0.21
+0.75	0.21
+1.00	0.32
+1.25	0.96
+1.50	3.32
+1.75	11.99
+2.00	33.94
+2.25	54.28
+2.50	70.45
+2.75	82.44
+3.00	90.69
+3.25	95.61
+3.50	98.29
+3.75	99.68
+4.00	100.00

Percent Weight Error:	-0.4155

Folk-Ward Statistical Parameters		
Graphic Mean:	2.2634	:Fine Sand
Incl Graph Standard Deviation:	0.5035	:Moderately Well Sorted
Incl Graph Skewness:	0.2105	:Fine Skewed
Graphic Kurtosis:	0.9827	:Mesokurtic
Normalized Kurtosis:	0.4956	

Parameter by the Method of Moments	
Mean X:	2.3924
Varience:	0.2691
Skewness:	0.2148
Standard Deviation:	0.5187
Kurtosis:	4.5000

Notes: Mica present; white flakes

Sample:	SJM 1-1-12	% Gravel:	0.00
Depth:	53-58	% Sand:	86.26
Level:	IIc	% Silt/Clay:	13.74

PHI	Weight as Percentage of Cumulative Total
-1.00	0.10
-0.75	0.10
-0.50	0.10
-0.25	0.10
0.00	0.10
+0.25	0.10
+0.50	0.10
+0.75	0.10
+1.00	0.21
+1.25	0.84
+1.50	4.28
+1.75	13.67
+2.00	35.39
+2.25	56.78
+2.50	71.92
+2.75	82.25
+3.00	90.08
+3.25	95.41
+3.50	98.23
+3.75	99.48
+4.00	100.00

Percent Weight Error:	-2.0031

Folk-Ward Statistical Parameters		
Graphic Mean:	2.2511	:Fine Sand
Incl Graph Standard Deviation:	0.5166	:Moderately Well Sorted
Incl Graph Skewness:	0.2365	:Fine Skewed
Graphic Kurtosis:	1.0107	:Mesokurtic
Normalized Kurtosis:	0.5027	

Parameter by the Method of Moments	
Mean X:	2.3766
Varience:	0.2801
Skewness:	0.3012
Standard Deviation:	0.5293
Kurtosis:	4.5798

Notes: Mica present

Sample:	SJM 1-1-13	% Gravel:	0.00
Depth:	58-63	% Sand:	90.24
Level:	IIc	% Silt/Clay:	9.76

PHI	Weight as Percentage of Cumulative Total
-1.00	0.00
-0.75	0.00
-0.50	0.00
-0.25	0.00
0.00	0.00
+0.25	0.00
+0.50	0.00
+0.75	0.16
+1.00	0.33
+1.25	0.90
+1.50	3.43
+1.75	11.27
+2.00	32.98
+2.25	57.06
+2.50	74.94
+2.75	87.02
+3.00	93.96
+3.25	97.63
+3.50	99.27
+3.75	100.00
+4.00	100.00

Percent Weight Error:	-3.2636	
Folk-Ward Statistical Parameters		
Graphic Mean:	2.2229	:Fine Sand
Incl Graph Standard Deviation:	0.4512	:Well Sorted
Incl Graph Skewness:	0.1665	:Fine Skewed
Graphic Kurtosis:	1.0508	:Mesokurtic
Normalized Kurtosis:	0.5124	
Parameter by the Method of Moments		
Mean X:	2.3527	
Varience:	0.2080	
Skewness:	0.3920	
Standard Deviation:	0.4561	
Kurtosis:	3.4026	

Notes: Mica present; very few clumps, up to 0.4 cm

Sample:	SJM 1-1-14	% Gravel:	0.00
Depth:	63-68	% Sand:	88.89
Level:	IIc	% Silt/Clay:	11.11

PHI	Weight as Percentage of Cumulative Total
-1.00	0.00
-0.75	0.00
-0.50	0.00
-0.25	0.00
0.00	0.00
+0.25	0.00
+0.50	0.00
+0.75	0.13
+1.00	0.13
+1.25	0.39
+1.50	1.04
+1.75	4.05
+2.00	18.02
+2.25	45.17
+2.50	69.84
+2.75	84.07
+3.00	92.69
+3.25	97.13
+3.50	99.48
+3.75	100.00
+4.00	100.00

Percent Weight Error:	-4.3000

Folk-Ward Statistical Parameters		
Graphic Mean:	2.3372	:Fine Sand
Incl Graph Standard Deviation:	0.4027	:Well Sorted
Incl Graph Skewness:	0.1829	:Fine Skewed
Graphic Kurtosis:	1.0615	:Mesokurtic
Normalized Kurtosis:	0.5149	

Parameter by the Method of Moments	
Mean X:	2.4696
Varience:	0.1695
Skewness:	0.3995
Standard Deviation:	0.4117
Kurtosis:	3.5881

Notes: Mica present; clumps up to 1.5 cm

Sample:	SJM 1-1-15	% Gravel:	0.00
Depth:	68-72	% Sand:	79.27
Level:	IIc	% Silt/Clay:	20.73

PHI	Weight as Percentage of Cumulative Total
-1.00	0.00
-0.75	0.00
-0.50	0.00
-0.25	0.00
0.00	0.17
+0.25	0.17
+0.50	0.17
+0.75	0.35
+1.00	0.35
+1.25	0.52
+1.50	0.70
+1.75	1.40
+2.00	4.89
+2.25	21.29
+2.50	55.85
+2.75	77.31
+3.00	88.83
+3.25	94.94
+3.50	97.91
+3.75	99.30
+4.00	100.00

Percent Weight Error:	-1.8122

Folk-Ward Statistical Parameters		
Graphic Mean:	2.5074	:Fine Sand
Incl Graph Standard Deviation:	0.3714	:Well Sorted
Incl Graph Skewness:	0.2389	:Fine Skewed
Graphic Kurtosis:	1.1512	:Leptokurtic
Normalized Kurtosis:	0.5351	

Parameter by the Method of Moments	
Mean X:	2.6396
Varience:	0.1679
Skewness:	-0.0098
Standard Deviation:	0.4098
Kurtosis:	7.1797

Notes: Mica present

Sample:	SJM 1-1-16	% Gravel:	0.61
Depth:	72-73	% Sand:	67.17
Level:	V	% Silt/Clay:	32.23

PHI	Weight as Percentage of Cumulative Total
-1.00	0.00
-0.75	0.00
-0.50	0.00
-0.25	0.00
0.00	0.00
+0.25	0.00
+0.50	0.00
+0.75	0.00
+1.00	0.17
+1.25	0.17
+1.50	0.17
+1.75	0.17
+2.00	0.17
+2.25	0.67
+2.50	16.16
+2.75	49.66
+3.00	74.24
+3.25	89.73
+3.50	97.14
+3.75	99.66
+4.00	100.00

Percent Weight Error:	-6.1495

Folk-Ward Statistical Parameters		
Graphic Mean:	2.8028	:Fine Sand
Incl Graph Standard Deviation:	0.3329	:Very Well Sorted
Incl Graph Skewness:	0.2208	:Fine Skewed
Graphic Kurtosis:	1.0175	:Mesokurtic
Normalized Kurtosis:	0.5043	

Parameter by the Method of Moments	
Mean X:	2.9297
Varience:	0.1101
Skewness:	0.2482
Standard Deviation:	0.3318
Kurtosis:	4.5711

Notes: Mica present; clumps up to 1 cm; root casts

Sample:	SJM 1-1-17	% Gravel:	0.36
Depth:	73-74	% Sand:	56.77
Level:	VI	% Silt/Clay:	42.87

PHI	Weight as Percentage of Cumulative Total
-1.00	0.00
-0.75	0.00
-0.50	0.00
-0.25	0.00
0.00	0.00
+0.25	0.21
+0.50	0.42
+0.75	0.42
+1.00	0.42
+1.25	0.42
+1.50	0.42
+1.75	0.85
+2.00	1.69
+2.25	5.07
+2.50	25.58
+2.75	53.07
+3.00	73.36
+3.25	86.68
+3.50	95.56
+3.75	99.37
+4.00	100.00

Percent Weight Error:	-7.0063

Folk-Ward Statistical Parameters		
Graphic Mean:	2.7683	:Fine Sand
Incl Graph Standard Deviation:	0.3920	:Well Sorted
Incl Graph Skewness:	0.1997	:Fine Skewed
Graphic Kurtosis:	0.9446	:Mesookurtic
Normalized Kurtosis:	0.4858	

Parameter by the Method of Moments	
Mean X:	2.8911
Varience:	0.1782
Skewness:	-0.5699
Standard Deviation:	0.4221
Kurtosis:	7.5567

Notes: Mica present; clumps up to 0.7 cm; root casts

Sample:	SJM 1-1-18	% Gravel:	2.06
Depth:	74-76	% Sand:	18.91
Level:	VII	% Silt/Clay:	79.03

PHI	Weight as Percentage of Cumulative Total
-1.00	0.00
-0.75	0.00
-0.50	0.00
-0.25	0.00
0.00	0.00
+0.25	0.00
+0.50	1.00
+0.75	2.00
+1.00	4.50
+1.25	6.00
+1.50	8.00
+1.75	10.50
+2.00	12.00
+2.25	17.00
+2.50	29.00
+2.75	47.00
+3.00	64.50
+3.25	78.00
+3.50	88.50
+3.75	95.00
+4.00	100.00

Percent Weight Error:	-6.1860

Folk-Ward Statistical Parameters		
Graphic Mean:	2.7952	:Fine Sand
Incl Graph Standard Deviation:	0.7023	:Moderately Well Sorted
Incl Graph Skewness:	-0.1381	:Coarse Skewed
Graphic Kurtosis:	1.4052	:Leptokurtic
Normalized Kurtosis:	0.5842	

Parameter by the Method of Moments	
Mean X:	2.8425
Varience:	0.5239
Skewness:	-0.9932
Standard Deviation:	0.7238
Kurtosis:	4.1916

Notes: Mica present; clumps up to 2.4 cm; root casts

Sample:	SJM 1-1-19	% Gravel:	1.06
Depth:	76-81	% Sand:	16.79
Level:	VIIIa	% Silt/Clay:	82.15

PHI	Weight as Percentage of Cumulative Total
-1.00	0.00
-0.75	0.00
-0.50	0.00
-0.25	0.00
0.00	0.00
+0.25	0.28
+0.50	1.10
+0.75	2.49
+1.00	3.87
+1.25	5.25
+1.50	6.63
+1.75	7.73
+2.00	9.12
+2.25	15.19
+2.50	23.20
+2.75	38.95
+3.00	56.63
+3.25	72.10
+3.50	85.08
+3.75	95.30
+4.00	100.00

Percent Weight Error:	-5.1287	
Folk-Ward Statistical Parameters		
Graphic Mean:	2.8869	:Fine Sand
Incl Graph Standard Deviation:	0.6855	:Moderately Well Sorted
Incl Graph Skewness:	-0.1946	:Coarse Skewed
Graphic Kurtosis:	1.3379	:Leptokurtic
Normalized Kurtosis:	0.5723	
Parameter by the Method of Moments		
Mean X:	2.9427	
Varience:	0.5097	
Skewness:	-1.2432	
Standard Deviation:	0.7139	
Kurtosis:	4.9895	
Notes: Mica present; clumps up to 2.3 cm; root casts		

Sample:	SJM 1-1-20	% Gravel:	0.00
Depth:	81-86	% Sand:	48.95
Level:	VIIIf	% Silt/Clay:	51.05

PHI	Weight as Percentage of Cumulative Total
-1.00	0.28
-0.75	0.28
-0.50	0.28
-0.25	0.28
0.00	0.28
+0.25	0.28
+0.50	0.28
+0.75	0.28
+1.00	0.46
+1.25	0.65
+1.50	0.83
+1.75	1.29
+2.00	2.13
+2.25	8.23
+2.50	29.48
+2.75	50.55
+3.00	70.24
+3.25	84.38
+3.50	93.35
+3.75	98.43
+4.00	100.00

Percent Weight Error:	-2.4607

Folk-Ward Statistical Parameters		
Graphic Mean:	2.7760	:Fine Sand
Incl Graph Standard Deviation:	0.4472	:Well Sorted
Incl Graph Skewness:	0.1268	:Fine Skewed
Graphic Kurtosis:	0.9418	:Mesokurtic
Normalized Kurtosis:	0.4850	

Parameter by the Method of Moments	
Mean X:	2.8944
Varience:	0.2421
Skewness:	-1.2829
Standard Deviation:	0.4921
Kurtosis:	13.2371

Notes: Mica present

Sample:	SJM 1-1-21	% Gravel:	0.18
Depth:	86-91	% Sand:	52.06
Level:	VIIIf	% Silt/Clay:	47.76

PHI	Weight as Percentage of Cumulative Total
-1.00	0.00
-0.75	0.00
-0.50	0.15
-0.25	0.15
0.00	0.15
+0.25	0.15
+0.50	0.15
+0.75	0.15
+1.00	0.15
+1.25	0.15
+1.50	0.15
+1.75	0.15
+2.00	0.15
+2.25	1.24
+2.50	11.46
+2.75	39.16
+3.00	61.46
+3.25	78.95
+3.50	91.33
+3.75	97.83
+4.00	100.00

Percent Weight Error:	-5.0288

Folk-Ward Statistical Parameters		
Graphic Mean:	2.9215	:Fine Sand
Incl Graph Standard Deviation:	0.3996	:Well Sorted
Incl Graph Skewness:	0.1848	:Fine Skewed
Graphic Kurtosis:	0.9318	:Mesokurtic
Normalized Kurtosis:	0.4823	

Parameter by the Method of Moments	
Mean X:	3.0422
Varience:	0.1663
Skewness:	-0.6172
Standard Deviation:	0.4078
Kurtosis:	10.8200

Notes: Mica present; clumps up to 1.8 cm; root casts

Sample:	SJM 1-1-22	% Gravel:	0.72
Depth:	91-96	% Sand:	37.79
Level:	VIIIf	% Silt/Clay:	61.49

PHI	Weight as Percentage of Cumulative Total
-1.00	0.00
-0.75	0.00
-0.50	0.00
-0.25	0.00
0.00	0.00
+0.25	0.00
+0.50	0.00
+0.75	0.00
+1.00	0.00
+1.25	0.00
+1.50	0.00
+1.75	0.00
+2.00	0.00
+2.25	0.97
+2.50	8.12
+2.75	32.11
+3.00	51.84
+3.25	73.69
+3.50	89.17
+3.75	97.49
+4.00	100.00

Percent Weight Error:	-5.8984

Folk-Ward Statistical Parameters		
Graphic Mean:	2.9918	:Fine Sand
Incl Graph Standard Deviation:	0.4032	:Well Sorted
Incl Graph Skewness:	0.0710	:Near Symmetrical
Graphic Kurtosis:	0.8844	:Platykurtic
Normalized Kurtosis:	0.4693	

Parameter by the Method of Moments	
Mean X:	3.1165
Varience:	0.1490
Skewness:	0.2179
Standard Deviation:	0.3860
Kurtosis:	2.3546

Notes: Mica present; clumps up to 1.2 cm; root casts

Sample:	SJM 1-1-23	% Gravel:	0.64
Depth:	96-101	% Sand:	14.73
Level:	VIIIc	% Silt/Clay:	84.63

PHI	Weight as Percentage of Cumulative Total
-1.00	0.00
-0.75	0.00
-0.50	0.00
-0.25	0.00
0.00	0.00
+0.25	0.37
+0.50	1.85
+0.75	3.32
+1.00	4.80
+1.25	6.27
+1.50	9.23
+1.75	10.70
+2.00	13.28
+2.25	18.45
+2.50	31.00
+2.75	48.71
+3.00	64.94
+3.25	77.12
+3.50	87.08
+3.75	94.83
+4.00	100.00

Percent Weight Error:	-6.0688

Folk-Ward Statistical Parameters		
Graphic Mean:	2.7746	:Fine Sand
Incl Graph Standard Deviation:	0.7355	:Moderately Well Sorted
Incl Graph Skewness:	-0.1317	:Near Symmetrical
Graphic Kurtosis:	1.3515	:Leptokurtic
Normalized Kurtosis:	0.0575	

Parameter by the Method of Moments	
Mean X:	2.8201
Varience:	0.5813
Skewness:	-1.0129
Standard Deviation:	0.7625
Kurtosis:	4.2094

Notes: Mica present; hard clumps up to 2.1 cm; root casts

Sample:	SJM 1-1-24	% Gravel:	1.27
Depth:	101-104	% Sand:	11.92
Level:	VIIIc	% Silt/Clay:	86.81

PHI	Weight as Percentage of Cumulative Total
-1.00	0.00
-0.75	0.00
-0.50	0.00
-0.25	0.00
0.00	1.02
+0.25	1.71
+0.50	4.10
+0.75	7.51
+1.00	10.24
+1.25	13.31
+1.50	15.36
+1.75	18.36
+2.00	20.48
+2.25	30.03
+2.50	44.03
+2.75	58.02
+3.00	69.97
+3.25	80.20
+3.50	90.10
+3.75	96.93
+4.00	100.00

Percent Weight Error:	-7.5515

Folk-Ward Statistical Parameters		
Graphic Mean:	2.5038	:Fine Sand
Incl Graph Standard Deviation:	0.9185	:Moderately Sorted
Incl Graph Skewness:	-0.2418	:Coarse Skewed
Graphic Kurtosis:	1.2700	:Leptokurtic
Normalized Kurtosis:	0.5595	

Parameter by the Method of Moments	
Mean X:	2.5973
Varience:	0.8173
Skewness:	-0.9041
Standard Deviation:	0.9041
Kurtosis:	3.2736

Notes: Mica present; clumps up to 1 cm; root casts

Sample:	SJM 1-1-25	% Gravel:	3.02
Depth:	104-109	% Sand:	14.90
Level:	VIIId	% Silt/Clay:	82.08

PHI	Weight as Percentage of Cumulative Total
-1.00	0.00
-0.75	0.00
-0.50	0.00
-0.25	0.00
0.00	0.00
+0.25	0.63
+0.50	3.75
+0.75	6.88
+1.00	9.38
+1.25	14.38
+1.50	16.25
+1.75	17.50
+2.00	22.50
+2.25	32.50
+2.50	43.13
+2.75	60.63
+3.00	75.63
+3.25	85.00
+3.50	91.25
+3.75	96.87
+4.00	100.00

Percent Weight Error:	-4.3825

Folk-Ward Statistical Parameters		
Graphic Mean:	2.4294	:Fine Sand
Incl Graph Standard Deviation:	0.9038	:Moderately Sorted
Incl Graph Skewness:	-1.2957	:Coarse Skewed
Graphic Kurtosis:	1.3557	:Leptokurtic
Normalized Kurtosis:	0.5755	

Parameter by the Method of Moments	
Mean X:	2.5594
Varience:	0.7496
Skewness:	-1.7664
Standard Deviation:	0.8658
Kurtosis:	3.0755

Notes: Mica present; clumps up to 3.1 cm; root casts

Sample:	SJM 1-1-26	% Gravel:	0.15
Depth:	109-115	% Sand:	57.81
Level:	VIIIe	% Silt/Clay:	42.04

PHI	Weight as Percentage of Cumulative Total
-1.00	0.00
-0.75	0.00
-0.50	0.00
-0.25	0.00
0.00	0.00
+0.25	0.11
+0.50	0.22
+0.75	0.43
+1.00	0.06
+1.25	1.72
+1.50	2.91
+1.75	4.31
+2.00	6.78
+2.25	18.51
+2.50	41.98
+2.75	61.79
+3.00	78.26
+3.25	88.70
+3.50	95.80
+3.75	99.46
+4.00	100.00

Percent Weight Error:	-2.9006

Folk-Ward Statistical Parameters		
Graphic Mean:	2.6451	:Fine Sand
Incl Graph Standard Deviation:	0.4855	:Well Sorted
Incl Graph Skewness:	0.0969	:Near Symmetrical
Graphic Kurtosis:	1.0720	:Mesokurtic
Normalized Kurtosis:	0.5174	

Parameter by the Method of Moments	
Mean X:	2.7454
Varience:	0.2651
Skewness:	-0.4981
Standard Deviation:	0.5149
Kurtosis:	4.6261

Notes: Mica present; clumps up to 1.9 cm; root casts

Sample:	SJM 1-1-27	% Gravel:	0.00
Depth:	115-120	% Sand:	89.81
Level:	XIII	% Silt/Clay:	10.19

PHI	Weight as Percentage of Cumulative Total
-1.00	0.00
-0.75	0.00
-0.50	0.00
-0.25	0.00
0.00	0.00
+0.25	0.00
+0.50	0.14
+0.75	0.14
+1.00	0.14
+1.25	0.14
+1.50	0.14
+1.75	0.43
+2.00	0.58
+2.25	4.61
+2.50	33.29
+2.75	62.68
+3.00	81.56
+3.25	92.36
+3.50	97.41
+3.75	99.42
+4.00	100.00

Percent Weight Error:	-3.0472

Folk-Ward Statistical Parameters		
Graphic Mean:	2.6827	:Fine Sand
Incl Graph Standard Deviation:	0.3476	:Very Well Sorted
Incl Graph Skewness:	0.2411	:Fine Skewed
Graphic Kurtosis:	0.9518	:Mesokurtic
Normalized Kurtosis:	0.4877	

Parameter by the Method of Moments	
Mean X:	2.8174
Varience:	0.1308
Skewness:	2746.0000
Standard Deviation:	0.3617
Kurtosis:	5.5230

Notes: Mica present

Sample:	SJM 1-1-28	% Gravel:	0.00
Depth:	120-127	% Sand:	92.33
Level:	XIII	% Silt/Clay:	7.67

PHI	Weight as Percentage of Cumulative Total
-1.00	0.00
-0.75	0.00
-0.50	0.00
-0.25	0.12
0.00	0.12
+0.25	0.12
+0.50	0.12
+0.75	0.12
+1.00	0.12
+1.25	0.12
+1.50	0.12
+1.75	0.12
+2.00	0.12
+2.25	5.83
+2.50	35.36
+2.75	61.61
+3.00	82.26
+3.25	93.58
+3.50	98.02
+3.75	99.65
+4.00	100.00

Percent Weight Error:	-2.6123	
Folk-Ward Statistical Parameters		
Graphic Mean:	2.6713	:Fine Sand
Incl Graph Standard Deviation:	0.3447	:Very Well Sorted
Incl Graph Skewness:	0.1865	:Fine Skewed
Graphic Kurtosis:	0.9155	:Mesokurtic
Normalized Kurtosis:	0.4779	
Parameter by the Method of Moments		
Mean X:	2.8063	
Varience:	0.1280	
Skewness:	-0.1269	
Standard Deviation:	0.3578	
Kurtosis:	8.8399	

Notes: Mica present

Sample:	SJM 1-1-29	% Gravel:	0.00
Depth:	127-133.5	% Sand:	81.74
Level:	XIV	% Silt/Clay:	18.26

PHI	Weight as Percentage of Cumulative Total
-1.00	0.00
-0.75	0.00
-0.50	0.00
-0.25	0.00
0.00	0.00
+0.25	0.00
+0.50	0.00
+0.75	0.00
+1.00	0.00
+1.25	0.00
+1.50	0.00
+1.75	0.00
+2.00	0.00
+2.25	0.00
+2.50	11.68
+2.75	40.60
+3.00	65.81
+3.25	84.76
+3.50	94.73
+3.75	98.86
+4.00	100.00

Percent Weight Error:	-3.3840	
Folk-Ward Statistical Parameters		
Graphic Mean:	2.8735	:Fine Sand
Incl Graph Standard Deviation:	0.3513	: Well Sorted
Incl Graph Skewness:	0.1453	:Fine Skewed
Graphic Kurtosis:	0.9389	:Mesokurtic
Normalized Kurtosis:	0.4842	
Parameter by the Method of Moments		
Mean X:	3.0089	
Varience:	0.1186	
Skewness:	0.5377	
Standard Deviation:	0.3444	
Kurtosis:	2.7749	

Notes: Mica present; clumps up to 2 cm

Sample:	SJM 1-2-1	% Gravel:	0.28
Depth:	0-6	% Sand:	15.07
Level:	XVa	% Silt/Clay:	84.64

PHI	Weight as Percentage of Cumulative Total
-1.00	0.34
-0.75	0.34
-0.50	0.34
-0.25	0.34
0.00	0.34
+0.25	0.69
+0.50	1.38
+0.75	1.38
+1.00	2.07
+1.25	2.41
+1.50	3.45
+1.75	4.48
+2.00	5.86
+2.25	6.90
+2.50	11.03
+2.75	44.14
+3.00	70.34
+3.25	87.59
+3.50	96.21
+3.75	99.31
+4.00	100.00

Percent Weight Error:	-2.9648

Folk-Ward Statistical Parameters		
Graphic Mean:	2.8471	:Fine Sand
Incl Graph Standard Deviation:	0.4108	:Well Sorted
Incl Graph Skewness:	0.0001	:Near Symmetrical
Graphic Kurtosis:	1.4381	:Leptokurtic
Normalized Kurtosis:	0.5898	

Parameter by the Method of Moments	
Mean X:	2.9026
Varience:	0.2998
Skewness:	-2.6530
Standard Deviation:	0.5475
Kurtosis:	15.8743

Notes: Mica present; clumps up to 2.3 cm; root casts

Sample:	SJM 1-2-2	% Gravel:	0.27
Depth:	6-9	% Sand:	29.41
Level:	XVI	% Silt/Clay:	70.32

PHI	Weight as Percentage of Cumulative Total
-1.00	0.00
-0.75	0.00
-0.50	0.00
-0.25	0.00
0.00	0.00
+0.25	0.00
+0.50	0.90
+0.75	0.90
+1.00	1.49
+1.25	2.09
+1.50	2.39
+1.75	2.99
+2.00	3.88
+2.25	4.78
+2.50	14.33
+2.75	47.76
+3.00	68.66
+3.25	84.48
+3.50	93.43
+3.75	97.91
+4.00	100.00

Percent Weight Error:	-4.5023

Folk-Ward Statistical Parameters		
Graphic Mean:	2.8439	:Fine Sand
Incl Graph Standard Deviation:	0.3843	:Well Sorted
Incl Graph Skewness:	0.2468	:Fine Skewed
Graphic Kurtosis:	1.0486	:Mesokurtic
Normalized Kurtosis:	0.5119	

Parameter by the Method of Moments	
Mean X:	2.9351
Varience:	0.2471
Skewness:	-1.3797
Standard Deviation:	0.4971
Kurtosis:	8.8624

Notes: Mica present; clumps up to 2.8 cm; root casts

Sample:	SJM 1-2-3	% Gravel:	0.67
Depth:	9-10	% Sand:	24.07
Level:	XVIIa	% Silt/Clay:	75.26

PHI	Weight as Percentage of Cumulative Total
-1.00	0.00
-0.75	0.00
-0.50	0.00
-0.25	0.00
0.00	0.00
+0.25	0.00
+0.50	0.00
+0.75	0.00
+1.00	0.00
+1.25	0.34
+1.50	1.02
+1.75	2.03
+2.00	2.71
+2.25	3.39
+2.50	5.42
+2.75	34.24
+3.00	61.02
+3.25	80.34
+3.50	93.22
+3.75	98.98
+4.00	100.00

Percent Weight Error:	-2.7084

Folk-Ward Statistical Parameters		
Graphic Mean:	2.9367	:Fine Sand
Incl Graph Standard Deviation:	0.3534	:Well Sorted
Incl Graph Skewness:	0.1834	:Fine Skewed
Graphic Kurtosis:	0.9056	:Mesokurtic
Normalized Kurtosis:	0.4752	

Parameter by the Method of Moments	
Mean X:	3.0432
Varience:	0.1602
Skewness:	-0.6994
Standard Deviation:	0.4003
Kurtosis:	5.6660

Notes: Mica present; clumps up to 2.2 cm; rust colored specks in some clumps; root casts

Sample:	SJM 1-2-4	% Gravel:	0.41
Depth:	9-10	% Sand:	47.20
Level:	XVIIb	% Silt/Clay:	52.39

PHI	Weight as Percentage of Cumulative Total
-1.00	0.00
-0.75	0.00
-0.50	0.00
-0.25	0.00
0.00	0.22
+0.25	0.22
+0.50	0.22
+0.75	0.44
+1.00	0.44
+1.25	0.44
+1.50	0.44
+1.75	1.10
+2.00	1.10
+2.25	1.32
+2.50	7.02
+2.75	41.01
+3.00	66.89
+3.25	85.53
+3.50	95.18
+3.75	99.12
+4.00	100.00

Percent Weight Error:	-5.1712

Folk-Ward Statistical Parameters		
Graphic Mean:	2.8775	:Fine Sand
Incl Graph Standard Deviation:	0.3301	:Very Well Sorted
Incl Graph Skewness:	0.1994	:Fine Skewed
Graphic Kurtosis:	0.9321	:Mesokurtic
Normalized Kurtosis:	0.4824	

Parameter by the Method of Moments	
Mean X:	2.9984
Varience:	0.1446
Skewness:	-1.2602
Standard Deviation:	0.3803
Kurtosis:	13.5374

Notes: Mica present; clumps up to 1.9 cm

Sample:	SJM 1-2-5	% Gravel:	1.58
Depth:	10-12.5	% Sand:	57.23
Level:	XIIX	% Silt/Clay:	41.19

PHI	Weight as Percentage of Cumulative Total
-1.00	0.11
-0.75	0.11
-0.50	0.11
-0.25	0.11
0.00	0.11
+0.25	0.22
+0.50	0.22
+0.75	0.44
+1.00	0.55
+1.25	0.55
+1.50	0.77
+1.75	0.99
+2.00	1.33
+2.25	2.54
+2.50	23.98
+2.75	48.62
+3.00	70.83
+3.25	87.29
+3.50	95.91
+3.75	99.23
+4.00	100.00

Percent Weight Error:	-5.5347

Folk-Ward Statistical Parameters		
Graphic Mean:	2.7908	:Fine Sand
Incl Graph Standard Deviation:	0.3793	:Well Sorted
Incl Graph Skewness:	0.1404	:Fine Skewed
Graphic Kurtosis:	0.8856	:Platykurtic
Normalized Kurtosis:	0.4697	

Parameter by the Method of Moments	
Mean X:	2.9149
Varience:	0.1802
Skewness:	-1.2668
Standard Deviation:	0.4245
Kurtosis:	13.6095

Notes: Mica present; clumps up to 2.6 cm; some rust colered grains in clumps; root casts

Sample:	SJM 1-2-6	% Gravel:	3.00
Depth:	12.5-14	% Sand:	30.70
Level:	XIX, XX,XXI	% Silt/Clay:	66.30

PHI	Weight as Percentage of Cumulative Total
-1.00	0.00
-0.75	0.00
-0.50	0.00
-0.25	0.00
0.00	0.37
+0.25	1.11
+0.50	2.96
+0.75	8.89
+1.00	10.74
+1.25	12.22
+1.50	16.30
+1.75	25.19
+2.00	30.00
+2.25	37.41
+2.50	53.33
+2.75	68.52
+3.00	80.37
+3.25	90.00
+3.50	95.56
+3.75	98.89
+4.00	100.00

Percent Weight Error:	-5.8955	
Folk-Ward Statistical Parameters		
Graphic Mean:	2.3412	:Fine Sand
Incl Graph Standard Deviation:	0.8408	:Moderately Sorted
Incl Graph Skewness:	-0.2434	:Coarse Skewed
Graphic Kurtosis:	1.0369	:Mesokurtic
Normalized Kurtosis:	0.5091	

Parameter by the Method of Moments	
Mean X:	2.4284
Varience:	0.7080
Skewness:	-0.6701
Standard Deviation:	0.8414
Kurtosis:	2.9249

Notes: Mica present; rootcasts

Sample:	SJM 1-2-7	% Gravel:	1.45
Depth:	14-19	% Sand:	37.55
Level:	XXIIIa	% Silt/Clay:	61.01

PHI	Weight as Percentage of Cumulative Total
-1.00	0.00
-0.75	0.00
-0.50	0.00
-0.25	0.00
0.00	0.00
+0.25	0.00
+0.50	0.36
+0.75	1.08
+1.00	2.15
+1.25	2.51
+1.50	3.23
+1.75	5.38
+2.00	6.45
+2.25	7.89
+2.50	12.54
+2.75	30.82
+3.00	54.48
+3.25	73.84
+3.50	87.10
+3.75	95.70
+4.00	100.00

Percent Weight Error:	-4.4957

Folk-Ward Statistical Parameters		
Graphic Mean:	2.9805	:Fine Sand
Incl Graph Standard Deviation:	0.5302	:Moderately Well Sorted
Incl Graph Skewness:	-0.0693	:Near Symmetrical
Graphic Kurtosis:	1.3784	:Leptokurtic
Normalized Kurtosis:	0.5796	

Parameter by the Method of Moments	
Mean X:	3.0412
Varience:	0.3393
Skewness:	-1.4053
Standard Deviation:	0.5825
Kurtosis:	6.5921

Notes: Mica present; clumps up to 2 cm; root casts

Sample:	SJM 1-2-8	% Gravel:	2.03
Depth:	19-24	% Sand:	30.35
Level:	XXIIIa	% Silt/Clay:	67.62

PHI	Weight as Percentage of Cumulative Total
-1.00	0.00
-0.75	0.00
-0.50	0.00
-0.25	0.00
0.00	0.00
+0.25	0.00
+0.50	0.00
+0.75	0.30
+1.00	0.91
+1.25	1.22
+1.50	1.02
+1.75	2.74
+2.00	3.65
+2.25	4.56
+2.50	14.59
+2.75	39.51
+3.00	62.01
+3.25	79.03
+3.50	90.58
+3.75	97.57
+4.00	100.00

Percent Weight Error:	-2.2931

Folk-Ward Statistical Parameters		
Graphic Mean:	2.9128	:Fine Sand
Incl Graph Standard Deviation:	0.4226	:Well Sorted
Incl Graph Skewness:	0.1488	:Fine Skewed
Graphic Kurtosis:	0.9764	:Mesokurtic
Normalized Kurtosis:	0.4940	

Parameter by the Method of Moments	
Mean X:	3.0038
Varience:	0.2350
Skewness:	-0.8695
Standard Deviation:	0.4847
Kurtosis:	6.0085

Notes: Mica present; clumps up to 2 cm; root casts

Sample:	SJM 1-2-9	% Gravel:	1.04
Depth:	24-29	% Sand:	29.66
Level:	XXIIIa	% Silt/Clay:	69.30

PHI	Weight as Percentage of Cumulative Total
-1.00	0.00
-0.75	0.00
-0.50	0.00
-0.25	0.00
0.00	0.00
+0.25	0.00
+0.50	0.00
+0.75	0.00
+1.00	0.55
+1.25	1.94
+1.50	3.05
+1.75	3.88
+2.00	4.16
+2.25	5.54
+2.50	14.96
+2.75	38.78
+3.00	61.71
+3.25	78.39
+3.50	89.75
+3.75	97.78
+4.00	100.00

Percent Weight Error:	-3.1967

Folk-Ward Statistical Parameters		
Graphic Mean:	2.9188	:Fine Sand
Incl Graph Standard Deviation:	0.4445	:Well Sorted
Incl Graph Skewness:	0.1052	:Fine Skewed
Graphic Kurtosis:	1.0432	:Mesokurtic
Normalized Kurtosis:	0.5106	

Parameter by the Method of Moments	
Mean X:	2.9986
Varience:	0.2576
Skewness:	-0.9359
Standard Deviation:	0.5076
Kurtosis:	5.4778

Notes: Mica present; clumps up to 1.3 cm; root casts

Sample:	SJM 1-2-10	% Gravel:	0.96
Depth:	29-34	% Sand:	27.26
Level:	XXIIIa	% Silt/Clay:	71.78

PHI	Weight as Percentage of Cumulative Total
-1.00	0.00
-0.75	0.00
-0.50	0.00
-0.25	0.00
0.00	0.00
+0.25	0.00
+0.50	0.45
+0.75	1.36
+1.00	2.50
+1.25	3.41
+1.50	4.32
+1.75	5.32
+2.00	6.14
+2.25	7,73
+2.50	18.86
+2.75	42.05
+3.00	62.95
+3.25	79.09
+3.50	90.23
+3.75	97.50
+4.00	0.00

Percent Weight Error:	-4.3680

Folk-Ward Statistical Parameters		
Graphic Mean:	2.8803	:Fine Sand
Incl Graph Standard Deviation:	0.5306	:Moderately Well Sorted
Incl Graph Skewness:	-0.0285	:Near Symmetrical
Graphic Kurtosis:	1.3056	:Leptokurtic
Normalized Kurtosis:	0.5663	

Parameter by the Method of Moments	
Mean X:	2.9455
Varience:	0.3436
Skewness:	-1.3279
Standard Deviation:	0.5862
Kurtosis:	0.4278

Notes: Mica present; clumps up to 2.4 cm; root casts

Sample:	SJM 1-2-11	% Gravel:	0.81
Depth:	34-38	% Sand:	39.42
Level:	XXIIIa	% Silt/Clay:	59.78

PHI	Weight as Percentage of Cumulative Total
-1.00	0.00
-0.75	0.00
-0.50	0.00
-0.25	0.00
0.00	0.26
+0.25	0.52
+0.50	1.30
+0.75	2.34
+1.00	4.16
+1.25	7.01
+1.50	8.57
+1.75	10.91
+2.00	14.03
+2.25	23.90
+2.50	36.36
+2.75	51.95
+3.00	67.27
+3.25	80.78
+3.50	90.65
+3.75	97.14
+4.00	100.00

Percent Weight Error:	-2.1940

Folk-Ward Statistical Parameters		
Graphic Mean:	2.7001	:Fine Sand
Incl Graph Standard Deviation:	0.7134	:Moderately Sorted
Incl Graph Skewness:	-0.1560	:Coarse Skewed
Graphic Kurtosis:	1.2205	:Leptokurtic
Normalized Kurtosis:	0.5497	

Parameter by the Method of Moments	
Mean X:	2.7571
Varience:	0.5430
Skewness:	-0.9287
Standard Deviation:	0.7369
Kurtosis:	4.0516

Notes: Mica present; lots of root casts: gravel fraction only consists of root casts

Sample:	SJM 1-2-12	% Gravel:	0.00
Depth:	38-45	% Sand:	59.20
Level:	XXIIIc	% Silt/Clay:	40.80

PHI	Weight as Percentage of Cumulative Total
-1.00	0.00
-0.75	0.00
-0.50	0.00
-0.25	0.00
0.00	0.00
+0.25	0.00
+0.50	0.55
+0.75	2.74
+1.00	7.31
+1.25	11.52
+1.50	13.89
+1.75	16.09
+2.00	21.21
+2.25	37.29
+2.50	50.46
+2.75	65.08
+3.00	78.79
+3.25	88.85
+3.50	95.06
+3.75	98.72
+4.00	100.00

Percent Weight Error:	-1.1619

Folk-Ward Statistical Parameters		
Graphic Mean:	2.4536	:Fine Sand
Incl Graph Standard Deviation:	0.7449	:Moderately Sorted
Incl Graph Skewness:	-0.1573	:Coarse Skewed
Graphic Kurtosis:	1.2334	:Leptokurtic
Normalized Kurtosis:	0.5523	

Parameter by the Method of Moments	
Mean X:	2.5311
Varience:	0.5637
Skewness:	-0.5995
Standard Deviation:	0.7508
Kurtosis:	2.9818

Notes: Mica present

Sample:	SJM 1-2-13	% Gravel:	1.08
Depth:	45-50	% Sand:	49.95
Level:	XXIVb	% Silt/Clay:	48.96

PHI	Weight as Percentage of Cumulative Total
-1.00	0.00
-0.75	0.00
-0.50	0.00
-0.25	0.00
0.00	0.00
+0.25	0.17
+0.50	0.58
+0.75	1.50
+1.00	2.66
+1.25	3.99
+1.50	4.98
+1.75	5.90
+2.00	7.72
+2.25	20.18
+2.50	37.21
+2.75	56.15
+3.00	74.34
+3.25	87.96
+3.50	95.60
+3.75	99.09
+4.00	100.00

Percent Weight Error:	-1.5857

Folk-Ward Statistical Parameters		
Graphic Mean:	2.6708	:Fine Sand
Incl Graph Standard Deviation:	0.5522	:Moderately Well Sorted
Incl Graph Skewness:	-0.0864	:NEAR SYMMETRICAL
Graphic Kurtosis:	1.1711	:Leptokurtic
Normalized Kurtosis:	0.5394	

Parameter by the Method of Moments	
Mean X:	2.7550
Varience:	0.3478
Skewness:	-1.0163
Standard Deviation:	0.5897
Kurtosis:	4.2604

Notes: Mica present; clumps up to 1.6 cm; root casts

Sample:	SJM 1-2-14	% Gravel:	5.51
Depth:	45-50	% Sand:	41.74
Level:	XXIVa	% Silt/Clay:	52.74

PHI	Weight as Percentage of Cumulative Total
-1.00	0.00
-0.75	0.00
-0.50	0.00
-0.25	0.00
0.00	0.00
+0.25	0.00
+0.50	0.45
+0.75	0.89
+1.00	2.68
+1.25	4.46
+1.50	5.36
+1.75	6.47
+2.00	8.26
+2.25	17.19
+2.50	34.60
+2.75	57.14
+3.00	75.45
+3.25	88.39
+3.50	94.87
+3.75	98.66
+4.00	100.00

Percent Weight Error:	-2.0525	
Folk-Ward Statistical Parameters		
Graphic Mean:	2.6842	:Fine Sand
Incl Graph Standard Deviation:	0.5566	:Moderately Well Sorted
Incl Graph Skewness:	-0.0881	:Near Symmetrical
Graphic Kurtosis:	1.3681	:Leptokurtic
Normalized Kurtosis:	0.5777	
Parameter by the Method of Moments		
Mean X:	2.7628	
Varience:	0.3426	
Skewness:	-0.9738	
Standard Deviation:	0.5853	
Kurtosis:	5.0964	

Notes: Mica present; clumps up to 2.4 cm; root casts

Sample:	SJM 1-2-15	% Gravel:	1.00
Depth:	50-55	% Sand:	53.99
Level:	XXIVa	% Silt/Clay:	45.01

PHI	Weight as Percentage of Cumulative Total
-1.00	0.00
-0.75	0.13
-0.50	0.13
-0.25	0.13
0.00	0.13
+0.25	0.13
+0.50	0.26
+0.75	0.90
+1.00	2.06
+1.25	2.70
+1.50	3.47
+1.75	4.37
+2.00	5.66
+2.25	15.68
+2.50	35.22
+2.75	56.30
+3.00	75.32
+3.25	88.56
+3.50	96.02
+3.75	99.23
+4.00	100.00

Percent Weight Error:	-2.8332

Folk-Ward Statistical Parameters		
Graphic Mean:	2.6978	:Fine Sand
Incl Graph Standard Deviation:	0.4689	:Well Sorted
Incl Graph Skewness:	0.0332	:Near Symmetrical
Graphic Kurtosis:	1.0423	:Mesokurtic
Normalized Kurtosis:	0.5104	

Parameter by the Method of Moments	
Mean X:	2.7841
Varience:	0.2933
Skewness:	-1.1440
Standard Deviation:	0.5416
Kurtosis:	7.1457

Notes: Mica present; clumps up to 2.6 cm; root casts

Sample:	SJM 1-2-16	% Gravel:	0.00
Depth:	55-60	% Sand:	52.75
Level:	XXIVa	% Silt/Clay:	47.26

PHI	Weight as Percentage of Cumulative Total
-1.00	0.00
-0.75	0.00
-0.50	0.00
-0.25	0.00
0.00	0.00
+0.25	0.00
+0.50	0.00
+0.75	0.14
+1.00	0.57
+1.25	1.29
+1.50	2.00
+1.75	2.71
+2.00	4.14
+2.25	15.57
+2.50	33.71
+2.75	54.86
+3.00	74.57
+3.25	87.71
+3.50	95.71
+3.75	99.29
+4.00	100.00

Percent Weight Error:	-1.0986

Folk-Ward Statistical Parameters		
Graphic Mean:	2.7093	:Fine Sand
Incl Graph Standard Deviation:	0.4519	:Well Sorted
Incl Graph Skewness:	0.0653	:Near Symmetrical
Graphic Kurtosis:	0.9518	:Mesokurtic
Normalized Kurtosis:	0.4876	

Parameter by the Method of Moments	
Mean X:	2.8193
Varience:	0.2334
Skewness:	-0.4316
Standard Deviation:	0.4831
Kurtosis:	4.2282

Notes: Mica present; clumps

Sample:	SJM 1-2-17	% Gravel:	2.28
Depth:	60-65	% Sand:	60.62
Level:	XXIVa	% Silt/Clay:	37.10

PHI	Weight as Percentage of Cumulative Total
-1.00	0.14
-0.75	0.14
-0.50	0.14
-0.25	0.14
0.00	0.14
+0.25	0.42
+0.50	0.85
+0.75	1.27
+1.00	1.84
+1.25	2.55
+1.50	3.16
+1.75	3.82
+2.00	5.95
+2.25	19.41
+2.50	39.52
+2.75	59.49
+3.00	76.20
+3.25	88.53
+3.50	95.61
+3.75	99.01
+4.00	100.00

Percent Weight Error:	-4.3290

Folk-Ward Statistical Parameters		
Graphic Mean:	2.6587	:Fine Sand
Incl Graph Standard Deviation:	0.4838	:Well Sorted
Incl Graph Skewness:	0.0753	:Near Symmetrical
Graphic Kurtosis:	0.9838	:Mesokurtic
Normalized Kurtosis:	0.4959	

Parameter by the Method of Moments	
Mean X:	2.7539
Varience:	0.3149
Skewness:	-1.1686
Standard Deviation:	0.5611
Kurtosis:	3.9446

Notes: Mica present; clumps up to 0.3 cm; root casts

Sample:	SJM 1-2-18	% Gravel:	0.42
Depth:	65-70	% Sand:	62.61
Level:	XXIVa	% Silt/Clay:	36.98

PHI	Weight as Percentage of Cumulative Total
-1.00	0.00
-0.75	0.00
-0.50	0.00
-0.25	0.00
0.00	0.00
+0.25	0.00
+0.50	0.57
+0.75	1.42
+1.00	2.14
+1.25	3.13
+1.50	3.99
+1.75	5.13
+2.00	6.41
+2.25	13.39
+2.50	37.18
+2.75	57.41
+3.00	76.21
+3.25	89.03
+3.50	96.01
+3.75	99.15
+4.00	100.00

Percent Weight Error:	-4.2292

Folk-Ward Statistical Parameters		
Graphic Mean:	2.5969	:Fine Sand
Incl Graph Standard Deviation:	0.4825	:Well Sorted
Incl Graph Skewness:	0.0266	:Near Symmetrical
Graphic Kurtosis:	1.1667	:Leptokurtic
Normalized Kurtosis:	0.5385	

Parameter by the Method of Moments	
Mean X:	2.7721
Varience:	0.2988
Skewness:	-1.8676
Standard Deviation:	0.5467
Kurtosis:	6.0384

Notes: Mica present; clumps up to 0.6 cm; root casts

Sample:	SJM 1-2-19	% Gravel:	0.59
Depth:	70-75	% Sand:	61.34
Level:	XXIVa	% Silt/Clay:	38.07

PHI	Weight as Percentage of Cumulative Total
-1.00	0.00
-0.75	0.00
-0.50	0.12
-0.25	0.12
0.00	0.12
+0.25	0.12
+0.50	0.24
+0.75	0.40
+1.00	0.96
+1.25	1.32
+1.50	1.67
+1.75	2.15
+2.00	3.11
+2.25	10.41
+2.50	34.09
+2.75	59.33
+3.00	77.99
+3.25	89.71
+3.50	96.05
+3.75	99.28
+4.00	100.00

Percent Weight Error:	-3.0898	
Folk-Ward Statistical Parameters		
Graphic Mean:	2.6983	:Fine Sand
Incl Graph Standard Deviation:	0.4168	:Well Sorted
Incl Graph Skewness:	0.1491	:Fine Skewed
Graphic Kurtosis:	1.0275	:Mesokurtic
Normalized Kurtosis:	0.5068	
Parameter by the Method of Moments		
Mean X:	2.8068	
Varience:	0.2167	
Skewness:	-0.8596	
Standard Deviation:	0.4655	
Kurtosis:	8.1105	
Notes: Mica present, root casts		

Sample:	SJM 1-2-20	% Gravel:	0.52
Depth:	75-80	% Sand:	71.53
Level:	XXIVa	% Silt/Clay:	27.95

PHI	Weight as Percentage of Cumulative Total
-1.00	0.00
-0.75	0.00
-0.50	0.00
-0.25	0.00
0.00	0.00
+0.25	0.00
+0.50	0.13
+0.75	0.26
+1.00	0.65
+1.25	1.04
+1.50	1.56
+1.75	2.47
+2.00	3.78
+2.25	12.50
+2.50	40.49
+2.75	61.85
+3.00	78.12
+3.25	89.71
+3.50	96.48
+3.75	99.22
+4.00	100.00

Percent Weight Error:	-2.9553

Folk-Ward Statistical Parameters		
Graphic Mean:	2.6731	:Fine Sand
Incl Graph Standard Deviation:	0.4250	:Well Sorted
Incl Graph Skewness:	0.2010	:Fine Skewed
Graphic Kurtosis:	0.9789	:Mesokurtic
Normalized Kurtosis:	0.4947	

Parameter by the Method of Moments	
Mean X:	2.7793
Varience:	0.2124
Skewness:	0.3057
Standard Deviation:	0.4608
Kurtosis:	4.9061

Notes: Mica present; clumps up to 0.7 cm

Sample:	SJM 1-2-21	% Gravel:	8.29
Depth:	80-84	% Sand:	52.49
Level:	XXIVa	% Silt/Clay:	39.22

PHI	Weight as Percentage of Cumulative Total
-1.00	0.00
-0.75	0.00
-0.50	0.00
-0.25	0.00
0.00	0.00
+0.25	0.00
+0.50	0.15
+0.75	0.77
+1.00	1.38
+1.25	1.99
+1.50	2.60
+1.75	4.13
+2.00	5.21
+2.25	17.00
+2.50	35.68
+2.75	57.12
+3.00	75.65
+3.25	88.06
+3.50	95.41
+3.75	98.93
+4.00	100.00

Percent Weight Error:	-3.2141

Folk-Ward Statistical Parameters		
Graphic Mean:	2.6880	:Fine Sand
Incl Graph Standard Deviation:	0.4673	:Well Sorted
Incl Graph Skewness:	0.0675	Near Symmetrical
Graphic Kurtosis:	0.9917	:Mesokurtic
Normalized Kurtosis:	0.4979	

Parameter by the Method of Moments	
Mean X:	2.7898
Varience:	0.2712
Skewness:	-0.6819
Standard Deviation:	0.5208
Kurtosis:	5.0766

Notes: Mica present; clumps up to 2.6 cm; root casts

Sample:	SJM 1-2-22	% Gravel:	0.23
Depth:	84-89	% Sand:	55.18
Level:	XXVa	% Silt/Clay:	44.59

PHI	Weight as Percentage of Cumulative Total
-1.00	0.20
-0.75	0.20
-0.50	0.20
-0.25	0.20
0.00	0.39
+0.25	0.39
+0.50	0.79
+0.75	1.58
+1.00	2.76
+1.25	4.14
+1.50	5.13
+1.75	6.31
+2.00	11.64
+2.25	22.88
+2.50	41.42
+2.75	60.75
+3.00	77.51
+3.25	89.35
+3.50	95.86
+3.75	99.21
+4.00	100.00

Percent Weight Error:	-2.1430

Folk-Ward Statistical Parameters		
Graphic Mean:	2.6150	:Fine Sand
Incl Graph Standard Deviation:	0.5630	:Moderately Well Sorted
Incl Graph Skewness:	-0.0661	:Near Symmetrical
Graphic Kurtosis:	1.1982	:Leptokurtic
Normalized Kurtosis:	0.5451	

Parameter by the Method of Moments	
Mean X:	2.6977
Varience:	0.3782
Skewness:	-1.2055
Standard Deviation:	0.6150
Kurtosis:	6.9093

Notes: Mica present; clumps up to 2.8 cm; root casts

Sample:	SJM 1-2-23	% Gravel:	0.09
Depth:	89-95	% Sand:	51.22
Level:	XXVa	% Silt/Clay:	48.70

PHI	Weight as Percentage of Cumulative Total
-1.00	0.12
-0.75	0.12
-0.50	0.12
-0.25	0.12
0.00	0.12
+0.25	0.12
+0.50	0.12
+0.75	0.37
+1.00	0.87
+1.25	1.74
+1.50	2.98
+1.75	4.35
+2.00	5.22
+2.25	6.34
+2.50	16.77
+2.75	39.13
+3.00	61.86
+3.25	82.36
+3.50	94.16
+3.75	98.88
+4.00	100.00

Percent Weight Error:	-1.5718

Folk-Ward Statistical Parameters		
Graphic Mean:	2.8786	:Fine Sand
Incl Graph Standard Deviation:	0.4443	:Well Sorted
Incl Graph Skewness:	-0.0631	:Near Symmetrical
Graphic Kurtosis:	1.1590	:Leptokurtic
Normalized Kurtosis:	0.5368	

Parameter by the Method of Moments	
Mean X:	2.9602
Varience:	0.2618
Skewness:	-1.5858
Standard Deviation:	0.5116
Kurtosis:	9.5827

Notes: Mica present

Sample:	SJM 1-2-24	% Gravel:	0.45
Depth:	95-100	% Sand:	64.99
Level:	XXVd	% Silt/Clay:	34.56

PHI	Weight as Percentage of Cumulative Total
-1.00	0.00
-0.75	0.00
-0.50	0.00
-0.25	0.00
0.00	0.00
+0.25	0.00
+0.50	0.13
+0.75	0.38
+1.00	0.77
+1.25	0.89
+1.50	1.40
+1.75	1.66
+2.00	2.04
+2.25	2.93
+2.50	15.69
+2.75	37.50
+3.00	60.33
+3.25	80.36
+3.50	92.35
+3.75	98.21
+4.00	100.00

Percent Weight Error:	-4.1011

Folk-Ward Statistical Parameters		
Graphic Mean:	2.9055	:Fine Sand
Incl Graph Standard Deviation:	0.4060	:Well Sorted
Incl Graph Skewness:	0.0830	:Near Symmetrical
Graphic Kurtosis:	0.9404	:Mesokurtic
Normalized Kurtosis:	0.4846	

Parameter by the Method of Moments	
Mean X:	3.0134
Varience:	0.2031
Skewness:	-0.9070
Standard Deviation:	0.4507
Kurtosis:	6.9052

Notes: Mica present; clumps up to 1.8 cm; root casts

Sample:	SJM 1-2-25	% Gravel:	0.00
Depth:	100-105	% Sand:	68.01
Level:	XXVd	% Silt/Clay:	31.99

PHI	Weight as Percentage of Cumulative Total
-1.00	0.00
-0.75	0.00
-0.50	0.00
-0.25	0.00
0.00	0.00
+0.25	0.26
+0.50	0.26
+0.75	0.40
+1.00	0.53
+1.25	0.79
+1.50	0.79
+1.75	0.93
+2.00	1.19
+2.25	2.12
+2.50	12.19
+2.75	39.07
+3.00	64.90
+3.25	84.24
+3.50	94.17
+3.75	98.54
+4.00	100.00

Percent Weight Error:	-3.3501

Folk-Ward Statistical Parameters		
Graphic Mean:	2.8794	:Fine Sand
Incl Graph Standard Deviation:	0.3636	:Well Sorted
Incl Graph Skewness:	0.1140	:Fine Skewed
Graphic Kurtosis:	0.9823	:Mesokurtic
Normalized Kurtosis:	0.4955	

Parameter by the Method of Moments	
Mean X:	2.9990
Varience:	0.1681
Skewness:	-1.0437
Standard Deviation:	0.4100
Kurtosis:	10.0016

Notes: Mica present; clumps up to 1.2 cm; root casts

Sample:	SJM 2-1-1	% Gravel:	0.42
Depth:	0-5cm	% Sand:	5.64
Level:	IV	% Silt/Clay:	93.94

PHI	Weight as Percentage of Cumulative Total
-1.00	0.00
-0.75	0.00
-0.50	0.00
-0.25	0.00
0.00	0.00
+0.25	0.00
+0.50	0.91
+0.75	5.45
+1.00	8.18
+1.25	10.00
+1.50	13.64
+1.75	23.64
+2.00	32.73
+2.25	50.00
+2.50	61.82
+2.75	73.64
+3.00	81.82
+3.25	88.18
+3.50	92.73
+3.75	96.36
+4.00	100.00

Percent Weight Error:	-5.4146

Folk-Ward Statistical Parameters		
Graphic Mean:	2.2983	:Fine Sand
Incl Graph Standard Deviation:	0.8258	:Moderately Sorted
Incl Graph Skewness:	0.0272	:Near Symmetrical
Graphic Kurtosis:	1.1963	:Leptokurtic
Normalized Kurtosis:	0.5447	

Parameter by the Method of Moments	
Mean X:	2.4023
Varience:	0.6297
Skewness:	-0.1458
Standard Deviation:	0.7935
Kurtosis:	2.7946

Notes: Mica present; clumps up to 0.3 cm; fragments of organic material; rootcasts

Sample:	SJM 2-1-2	% Gravel:	0.16
Depth:	5-10cm	% Sand:	7.50
Level:	IV	% Silt/Clay:	92.33

PHI	Weight as Percentage of Cumulative Total
-1.00	0.00
-0.75	0.00
-0.50	0.00
-0.25	0.67
0.00	0.67
+0.25	1.34
+0.50	2.01
+0.75	2.68
+1.00	6.71
+1.25	8.72
+1.50	13.42
+1.75	18.79
+2.00	34.90
+2.25	49.66
+2.50	63.09
+2.75	73.83
+3.00	81.88
+3.25	88.59
+3.50	93.29
+3.75	97.32
+4.00	100.00

Percent Weight Error:	-3.3036	
Folk-Ward Statistical Parameters		
Graphic Mean:	2.3184	:Fine Sand
Incl Graph Standard Deviation:	0.7757	:Moderately Sorted
Incl Graph Skewness:	0.0616	:Near Symmetrical
Graphic Kurtosis:	1.1825	:Leptokurtic
Normalized Kurtosis:	0.5418	

Parameter by the Method of Moments	
Mean X:	2.4060
Varience:	0.6069
Skewness:	-0.3062
Standard Deviation:	0.7791
Kurtosis:	3.4912

Notes: Mica present; clumps up to 0.3 cm; fragments of organic material; rootcasts

Sample:	SJM 2-1-3	% Gravel:	1.93
Depth:	10-14cm	% Sand:	14.13
Level:	V	% Silt/Clay:	83.93

PHI	Weight as Percentage of Cumulative Total
-1.00	0.00
-0.75	0.00
-0.50	0.00
-0.25	0.00
0.00	0.00
+0.25	0.00
+0.50	0.91
+0.75	5.45
+1.00	8.18
+1.25	10.00
+1.50	13.64
+1.75	23.64
+2.00	32.73
+2.25	50.00
+2.50	61.82
+2.75	73.64
+3.00	81.82
+3.25	88.18
+3.50	92.73
+3.75	96.36
+4.00	100.00

Percent Weight Error:	-7.1026

Folk-Ward Statistical Parameters		
Graphic Mean:	2.4507	:Fine Sand
Incl Graph Standard Deviation:	0.0795	:Moderately Sorted
Incl Graph Skewness:	-0.0142	:Near Symmetrical
Graphic Kurtosis:	1.0638	:Mesokurtic
Normalized Kurtosis:	0.5155	

Parameter by the Method of Moments	
Mean X:	2.5430
Varience:	0.6005
Skewness:	-0.3522
Standard Deviation:	0.7749
Kurtosis:	2.9542

Notes: Mica present; clumps up to 0.5 cm; fragments of organic material; rootcasts; fine grained white concretions in gravel fractions

Sample:	SJM 2-1-4	% Gravel:	0.42
Depth:	14-24cm	% Sand:	5.64
Level:	V	% Silt/Clay:	93.94

PHI	Weight as Percentage of Cumulative Total
-1.00	0.00
-0.75	0.00
-0.50	0.00
-0.25	0.00
0.00	0.00
+0.25	0.00
+0.50	0.00
+0.75	0.00
+1.00	0.00
+1.25	1.33
+1.50	4.00
+1.75	5.33
+2.00	13.33
+2.25	21.33
+2.50	29.33
+2.75	49.33
+3.00	64.00
+3.25	76.00
+3.50	86.67
+3.75	94.67
+4.00	100.00

Percent Weight Error:	-18.8737

Folk-Ward Statistical Parameters		
Graphic Mean:	2.7607	:Fine Sand
Incl Graph Standard Deviation:	0.6534	:Moderately Well Sorted
Incl Graph Skewness:	-0.0174	:Near Symmetrical
Graphic Kurtosis:	0.9851	:Mesokurtic
Normalized Kurtosis:	0.4962	

Parameter by the Method of Moments	
Mean X:	2.8867
Varience:	0.3988
Skewness:	-0.2979
Standard Deviation:	0.6315
Kurtosis:	2.6692

Notes: Mica present; clumps up to 1 cm; fragments of organic material; rootcasts; fine grained white concretions in gravel fractions

Sample:	SJM 2-1-5	% Gravel:	2.65
Depth:	24-31.5cm	% Sand:	10.12
Level:	V	% Silt/Clay:	87.23

PHI	Weight as Percentage of Cumulative Total
-1.00	0.00
-0.75	0.00
-0.50	0.00
-0.25	0.00
0.00	0.00
+0.25	0.00
+0.50	0.91
+0.75	5.45
+1.00	8.18
+1.25	10.00
+1.50	13.64
+1.75	23.64
+2.00	32.73
+2.25	50.00
+2.50	61.82
+2.75	73.64
+3.00	81.82
+3.25	88.18
+3.50	92.73
+3.75	96.36
+4.00	100.00

Percent Weight Error:	-9.9345	
Folk-Ward Statistical Parameters		
Graphic Mean:	1.9562	:Medium Sand
Incl Graph Standard Deviation:	0.9555	:Moderately Sorted
Incl Graph Skewness:	0.0799	:Near Symmetrical
Graphic Kurtosis:	0.9154	:Mesokurtic
Normalized Kurtosis:	0.4779	

Parameter by the Method of Moments	
Mean X:	2.1087
Varience:	0.8197
Skewness:	0.1707
Standard Deviation:	0.9054
Kurtosis:	2.2069

Notes: Mica present; clumps up to 0.3 cm; fragments of organic material; rootcasts; rust colored concretions in gravel fraction

Sample:	SJM 2-1-6	% Gravel:	0.33
Depth:	31.5-41.5cm	% Sand:	14.09
Level:	VII, VIII	% Silt/Clay:	85.58

PHI	Weight as Percentage of Cumulative Total
-1.00	0.00
-0.75	0.00
-0.50	0.00
-0.25	0.00
0.00	0.00
+0.25	0.00
+0.50	0.00
+0.75	0.00
+1.00	0.32
+1.25	1.30
+1.50	2.60
+1.75	3.57
+2.00	4.87
+2.25	7.14
+2.50	11.04
+2.75	19.48
+3.00	36.69
+3.25	54.55
+3.50	74.68
+3.75	92.21
+4.00	100.00

Percent Weight Error:	-6.1010

Folk-Ward Statistical Parameters		
Graphic Mean:	3.1554	:Very Fine Sand
Incl Graph Standard Deviation:	0.5231	:Moderately Well Sorted
Incl Graph Skewness:	-0.1892	:Coarse Skewed
Graphic Kurtosis:	1.1092	:Mesokurtic
Normalized Kurtosis:	0.5259	

Parameter by the Method of Moments	
Mean X:	3.2289
Varience:	0.3137
Skewness:	-1.2372
Standard Deviation:	0.5601
Kurtosis:	5.0825

Notes: Mica present; clumps up to 0.3 cm; fragments of organic material; rootcasts

Sample:	SJM 2-1-7	% Gravel:	0.15
Depth:	41.5-49cm	% Sand:	35.45
Level:	VIII, IX	% Silt/Clay:	64.40

PHI	Weight as Percentage of Cumulative Total
-1.00	0.00
-0.75	0.00
-0.50	0.00
-0.25	0.00
0.00	0.00
+0.25	0.00
+0.50	0.00
+0.75	0.00
+1.00	0.18
+1.25	0.55
+1.50	0.55
+1.75	0.73
+2.00	1.10
+2.25	1.65
+2.50	3.30
+2.75	20.92
+3.00	43.49
+3.25	66.06
+3.50	85.14
+3.75	96.15
+4.00	100.00

Percent Weight Error:	-3.3636

Folk-Ward Statistical Parameters		
Graphic Mean:	3.0792	:Very Fine Sand
Incl Graph Standard Deviation:	0.3830	:Well Sorted
Incl Graph Skewness:	0.0563	:Near Symmetrical
Graphic Kurtosis:	0.8598	:Platykurtic
Normalized Kurtosis:	0.4623	

Parameter by the Method of Moments	
Mean X:	3.2005
Varience:	0.1654
Skewness:	-0.6520
Standard Deviation:	0.4067
Kurtosis:	5.6736

Notes: Mica present; clumps up to 0.3 cm; fragments of organic material; rootcasts

Sample:	SJM 2-1-8	% Gravel:	2.61
Depth:	49-54cm	% Sand:	31.65
Level:	X	% Silt/Clay:	65.75

PHI	Weight as Percentage of Cumulative Total
-1.00	0.00
-0.75	0.00
-0.50	0.00
-0.25	0.00
0.00	0.00
+0.25	0.00
+0.50	0.00
+0.75	0.56
+1.00	1.30
+1.25	2.61
+1.50	3.91
+1.75	5.03
+2.00	5.96
+2.25	9.12
+2.50	24.39
+2.75	43.39
+3.00	62.76
+3.25	78.96
+3.50	91.43
+3.75	98.43
+4.00	100.00

Percent Weight Error:	-3.7394

Folk-Ward Statistical Parameters		
Graphic Mean:	2.8496	:Fine Sand
Incl Graph Standard Deviation:	0.5334	:Moderately Well Sorted
Incl Graph Skewness:	-0.0561	:Near Symmetrical
Graphic Kurtosis:	1.1370	:Leptokurtic
Normalized Kurtosis:	0.5321	

Parameter by the Method of Moments	
Mean X:	2.9311
Varience:	0.3149
Skewness:	-0.9803
Standard Deviation:	0.5611
Kurtosis:	5.0341

Notes: Mica present; clumps up to 1.3 cm; fragments of organic material; rootcasts

Sample:	SJM 2-1-9	% Gravel:	5.67
Depth:	49-52.5cm	% Sand:	17.80
Level:	XI	% Silt/Clay:	76.53

PHI	Weight as Percentage of Cumulative Total
-1.00	0.00
-0.75	0.00
-0.50	0.00
-0.25	0.00
0.00	0.38
+0.25	1.15
+0.50	2.31
+0.75	3.85
+1.00	5.77
+1.25	7.31
+1.50	9.23
+1.75	11.54
+2.00	13.85
+2.25	16.92
+2.50	25.38
+2.75	51.92
+3.00	70.38
+3.25	84.23
+3.50	93.46
+3.75	98.08
+4.00	100.00

Percent Weight Error:	-2.9522

Folk-Ward Statistical Parameters		
Graphic Mean:	2.7176	:Fine Sand
Incl Graph Standard Deviation:	0.6743	:Moderately Well Sorted
Incl Graph Skewness:	-0.2027	:Coarse Skewed
Graphic Kurtosis:	1.8492	: Very Leptokurtic
Normalized Kurtosis:	0.6490	

Parameter by the Method of Moments	
Mean X:	2.7606
Varience:	0.5439
Skewness:	-1.3952
Standard Deviation:	0.7375
Kurtosis:	5.2574

Notes: Mica present; clumps up to 0.3 cm; fragments of organic material; rootcasts

APPENDIX B

INDIVIDUAL SAMPLE RESULTS OF TEXTURAL ANALYSIS AT HUACA DEL SOL

Sample:	HDS 1-1-1	% Gravel:	0.00
Depth:	0-5	% Sand:	97.15
Level:	I	% Silt/Clay:	2.85

PHI	Weight as Percentage of Cumulative Total
-1.00	0.10
-0.75	0.10
-0.50	0.10
-0.25	0.10
0.00	0.10
+0.25	0.30
+0.50	0.30
+0.75	0.79
+1.00	4.46
+1.25	7.54
+1.50	11.31
+1.75	25.69
+2.00	48.61
+2.25	71.92
+2.50	86.31
+2.75	94.05
+3.00	97.52
+3.25	99.01
+3.50	99.70
+3.75	99.90
+4.00	100.00

Percent Weight Error:	-1.9467

Folk-Ward Statistical Parameters		
Graphic Mean:	2.0188	:Fine Sand
Incl Graph Standard Deviation:	0.4885	:Well Sorted
Incl Graph Skewness:	-0.0406	:Near Symmetrical
Graphic Kurtosis:	1.2864	:Leptokurtic
Normalized Kurtosis:	0.5626	

Parameter by the Method of Moments	
Mean X:	2.1302
Varience:	0.2559
Skewness:	-0.3542
Standard Deviation:	0.5059
Kurtosis:	5.0853

Notes: Mica present

Sample:	HDS 1-1-2	% Gravel:	0.09
Depth:	8-13	% Sand:	78.41
Level:	II	% Silt/Clay:	21.50

PHI	Weight as Percentage of Cumulative Total
-1.00	0.69
-0.75	0.69
-0.50	0.69
-0.25	0.69
0.00	0.77
+0.25	0.77
+0.50	1.00
+0.75	1.08
+1.00	1.38
+1.25	1.77
+1.50	2.38
+1.75	4.84
+2.00	18.52
+2.25	44.73
+2.50	64.03
+2.75	78.25
+3.00	87.47
+3.25	93.85
+3.50	97.69
+3.75	99.54
+4.00	100.00

Percent Weight Error:	0.1173	
Folk-Ward Statistical Parameters		
Graphic Mean:	2.3927	:Fine Sand
Incl Graph Standard Deviation:	0.4762	:Well Sorted
Incl Graph Skewness:	0.2576	:Fine Sand
Graphic Kurtosis:	1.0207	:Mesokurtic
Normalized Kurtosis:	0.5051	

Parameter by the Method of Moments	
Mean X:	2.4979
Varience:	0.3301
Skewness:	-1.3394
Standard Deviation:	0.5745
Kurtosis:	11.8571

Notes: Mica present

Sample:	HDS 1-1-3	% Gravel:	0.00
Depth:	13-18	% Sand:	77.14
Level:	II	% Silt/Clay:	22.86

PHI	Weight as Percentage of Cumulative Total
-1.00	0.36
-0.75	0.36
-0.50	0.48
-0.25	0.60
0.00	0.60
+0.25	0.60
+0.50	0.84
+0.75	0.96
+1.00	1.20
+1.25	1.56
+1.50	2.28
+1.75	3.72
+2.00	16.67
+2.25	44.60
+2.50	64.03
+2.75	77.58
+3.00	86.69
+3.25	92.93
+3.50	97.36
+3.75	99.52
+4.00	100.00

Percent Weight Error:	-0.3527

Folk-Ward Statistical Parameters		
Graphic Mean:	2.4109	:Fine Sand
Incl Graph Standard Deviation:	0.4760	:Well Sorted
Incl Graph Skewness:	0.3040	:Strongly Fine Skewed
Graphic Kurtosis:	1.0393	:Mesokurtic
Normalized Kurtosis:	0.5096	

Parameter by the Method of Moments	
Mean X:	2.5177
Varience:	0.3082
Skewness:	-0.9346
Standard Deviation:	0.5552
Kurtosis:	10.0528

Notes: Mica present; small fragments of hard orange material (possible ceramic)

Sample:	HDS 1-1-4	% Gravel:	0.24
Depth:	18-23	% Sand:	75.27
Level:	II	% Silt/Clay:	24.49

PHI	Weight as Percentage of Cumulative Total
-1.00	0.00
-0.75	0.00
-0.50	0.00
-0.25	0.11
0.00	0.11
+0.25	0.11
+0.50	0.22
+0.75	0.33
+1.00	0.54
+1.25	0.87
+1.50	1.41
+1.75	2.82
+2.00	12.13
+2.25	37.92
+2.50	62.84
+2.75	77.03
+3.00	86.57
+3.25	93.50
+3.50	97.83
+3.75	99.57
+4.00	100.00

Percent Weight Error:	-2.9832

Folk-Ward Statistical Parameters		
Graphic Mean:	2.4471	:Fine Sand
Incl Graph Standard Deviation:	0.4553	:Well Sorted
Incl Graph Skewness:	0.2590	:Fine Skewed
Graphic Kurtosis:	1.0623	:Mesokurtic
Normalized Kurtosis:		0.5151

Parameter by the Method of Moments	
Mean X:	2.5653
Varience:	0.2262
Skewness:	0.1203
Standard Deviation:	0.4756
Kurtosis:	4.9252

Notes: Mica present

Sample:	HDS 1-1-5	% Gravel:	0.20
Depth:	23-28	% Sand:	73.15
Level:	II	% Silt/Clay:	26.65

PHI	Weight as Percentage of Cumulative Total
-1.00	0.00
-0.75	0.00
-0.50	0.00
-0.25	0.11
0.00	0.22
+0.25	0.33
+0.50	0.45
+0.75	0.56
+1.00	1.00
+1.25	1.34
+1.50	2.01
+1.75	3.68
+2.00	11.61
+2.25	39.51
+2.50	65.40
+2.75	81.03
+3.00	90.29
+3.25	95.65
+3.50	98.66
+3.75	99.78
+4.00	100.00

Percent Weight Error:	-2.8481

Folk-Ward Statistical Parameters		
Graphic Mean:	2.4070	:Fine Sand
Incl Graph Standard Deviation:	0.4141	:Well Sorted
Incl Graph Skewness:	0.2137	:Fine Skewed
Graphic Kurtosis:	1.0970	:Mesokurtic
Normalized Kurtosis:		0.5231

Parameter by the Method of Moments	
Mean X:	2.5209
Varience:	0.2128
Skewness:	-0.3584
Standard Deviation:	0.4613
Kurtosis:	6.7922

Notes: Mica present

Sample:	HDS 1-1-6	% Gravel:	0.08
Depth:	28-33	% Sand:	73.40
Level:	II	% Silt/Clay:	26.53

PHI	Weight as Percentage of Cumulative Total
-1.00	0.00
-0.75	0.00
-0.50	0.00
-0.25	0.00
0.00	0.17
+0.25	0.17
+0.50	0.17
+0.75	0.17
+1.00	0.17
+1.25	0.17
+1.50	0.87
+1.75	2.80
+2.00	9.97
+2.25	38.64
+2.50	61.89
+2.75	76.75
+3.00	87.06
+3.25	94.23
+3.50	98.43
+3.75	99.83
+4.00	100.00

Percent Weight Error:	-4.4698

Folk-Ward Statistical Parameters		
Graphic Mean:	2.4502	:Fine Sand
Incl Graph Standard Deviation:	0.4409	:Well Sorted
Incl Graph Skewness:	0.2628	:Fine Skewed
Graphic Kurtosis:	1.0213	:Mesokurtic
Normalized Kurtosis:		0.5053

Parameter by the Method of Moments	
Mean X:	2.5712
Varience:	0.2026
Skewness:	0.2313
Standard Deviation:	0.4502
Kurtosis:	4.6130

Notes: Mica present; small fragment of hard orange material (possible ceramic); clumps up to 1.2 cm

Sample:	HDS 1-1-7	% Gravel:	0.00
Depth:	33-38	% Sand:	76.11
Level:	II	% Silt/Clay:	23.89

PHI	Weight as Percentage of Cumulative Total
-1.00	0.00
-0.75	0.00
-0.50	0.00
-0.25	0.00
0.00	0.00
+0.25	0.00
+0.50	0.28
+0.75	0.42
+1.00	0.57
+1.25	0.99
+1.50	1.27
+1.75	3.11
+2.00	8.20
+2.25	35.64
+2.50	60.54
+2.75	76.94
+3.00	87.55
+3.25	94.34
+3.50	98.30
+3.75	99.86
+4.00	100.00

Percent Weight Error:	-3.8389

Folk-Ward Statistical Parameters		
Graphic Mean:	2.4605	:Fine Sand
Incl Graph Standard Deviation:	0.4308	:Well Sorted
Incl Graph Skewness:	0.2371	:Fine Skewed
Graphic Kurtosis:	1.0466	:Mesokurtic
Normalized Kurtosis:	0.5114	

Parameter by the Method of Moments	
Mean X:	2.5799
Varience:	0.2042
Skewness:	0.0570
Standard Deviation:	0.4519
Kurtosis:	4.6269

Notes: Mica present; small fragment of hard orange material (possibleceramic); clumps up to 1.3 cm

Sample:	HDS 1-1-8	% Gravel:	0.00
Depth:	38-43	% Sand:	76.74
Level:	II	% Silt/Clay:	23.26

PHI	Weight as Percentage of Cumulative Total
-1.00	0.00
-0.75	0.20
-0.50	0.20
-0.25	0.20
0.00	0.20
+0.25	0.20
+0.50	0.30
+0.75	0.50
+1.00	0.70
+1.25	1.00
+1.50	1.40
+1.75	2.39
+2.00	8.57
+2.25	37.19
+2.50	63.91
+2.75	79.06
+3.00	88.63
+3.25	94.32
+3.50	98.01
+3.75	99.60
+4.00	100.00

Percent Weight Error:	-4.4354

Folk-Ward Statistical Parameters		
Graphic Mean:	2.4379	:Fine Sand
Incl Graph Standard Deviation:	0.4218	:Well Sorted
Incl Graph Skewness:	0.2683	:Fine Skewed
Graphic Kurtosis:	1.0946	:Mesokurtic
Normalized Kurtosis:		0.5226

Parameter by the Method of Moments	
Mean X:	2.5586
Varience:	0.2160
Skewness:	-0.3828
Standard Deviation:	0.4647
Kurtosis:	8.8277

Notes: Mica present; clumps up to 2 cm

Sample:	HDS 1-1-9	% Gravel:	0.00
Depth:	43-48	% Sand:	71.85
Level:	II	% Silt/Clay:	28.15

PHI	Weight as Percentage of Cumulative Total
-1.00	0.00
-0.75	0.00
-0.50	0.00
-0.25	0.00
0.00	0.00
+0.25	0.00
+0.50	0.00
+0.75	0.00
+1.00	0.00
+1.25	0.00
+1.50	0.00
+1.75	1.59
+2.00	7.15
+2.25	27.98
+2.50	57.55
+2.75	74.56
+3.00	86.01
+3.25	93.32
+3.50	97.62
+3.75	99.52
+4.00	100.00

Percent Weight Error:	5.5813

Folk-Ward Statistical Parameters		
Graphic Mean:	2.4995	:Fine Sand
Incl Graph Standard Deviation:	0.4313	:Well Sorted
Incl Graph Skewness:	0.2428	:Fine Skewed
Graphic Kurtosis:	1.0856	:Mesokurtic
Normalized Kurtosis:		0.5205

Parameter by the Method of Moments	
Mean X:	2.6367
Varience:	0.1810
Skewness:	0.6541
Standard Deviation:	0.4255
Kurtosis:	3.2261

Notes: Mica present; clumps up to 2.8 cm

Sample:	HDS 1-1-10	% Gravel:	0.00
Depth:	48-54.5	% Sand:	64.00
Level:	II	% Silt/Clay:	36.00

PHI	Weight as Percentage of Cumulative Total
-1.00	0.00
-0.75	0.00
-0.50	0.00
-0.25	0.00
0.00	0.00
+0.25	0.00
+0.50	0.00
+0.75	0.00
+1.00	0.00
+1.25	0.00
+1.50	0.00
+1.75	0.17
+2.00	3.81
+2.25	20.07
+2.50	51.38
+2.75	68.51
+3.00	80.62
+3.25	89.45
+3.50	96.02
+3.75	99.31
+4.00	100.00

Percent Weight Error:	-8.1355

Folk-Ward Statistical Parameters		
Graphic Mean:	2.5907	:Fine Sand
Incl Graph Standard Deviation:	0.4457	:Well Sorted
Incl Graph Skewness:	0.3419	:Strongly Fine Skewed
Graphic Kurtosis:	0.9946	:Mesokurtic
Normalized Kurtosis:		0.4986

Parameter by the Method of Moments	
Mean X:	2.7266
Varience:	0.1921
Skewness:	0.6915
Standard Deviation:	0.4383
Kurtosis:	2.8706

Notes: Mica present; clumps up to 1.5 cm

Sample:	HDS 1-1-11	% Gravel:	0.11
Depth:	54.5-59.5	% Sand:	46.79
Level:	III	% Silt/Clay:	53.10

PHI	Weight as Percentage of Cumulative Total
-1.00	0.98
-0.75	0.98
-0.50	1.17
-0.25	1.17
0.00	1.17
+0.25	1.17
+0.50	1.37
+0.75	1.56
+1.00	1.95
+1.25	2.54
+1.50	3.13
+1.75	4.30
+2.00	8.01
+2.25	18.36
+2.50	44.92
+2.75	65.04
+3.00	78.71
+3.25	88.67
+3.50	95.31
+3.75	99.02
+4.00	100.00

Percent Weight Error:	1.0393

Folk-Ward Statistical Parameters		
Graphic Mean:	2.6296	:Fine Sand
Incl Graph Standard Deviation:	0.4911	:Well Sorted
Incl Graph Skewness:	0.1533	:Fine Skewed
Graphic Kurtosis:	1.1184	:Leptokurtic
Normalized Kurtosis:		0.5279

Parameter by the Method of Moments	
Mean X:	2.7012
Varience:	0.4058
Skewness:	-2.1591
Standard Deviation:	0.6370
Kurtosis:	14.0621

Notes: Mica present; clumps up to 2.6 cm

Sample:	HDS 1-1-12	% Gravel:	0.58
Depth:	59.5-64.5	% Sand:	47.55
Level:	IV	% Silt/Clay:	51.87

PHI	Weight as Percentage of Cumulative Total
-1.00	0.00
-0.75	0.00
-0.50	0.00
-0.25	0.41
0.00	1.03
+0.25	1.85
+0.50	3.70
+0.75	5.13
+1.00	7.39
+1.25	8.83
+1.50	10.47
+1.75	13.76
+2.00	26.08
+2.25	43.94
+2.50	62.01
+2.75	74.95
+3.00	84.19
+3.25	91.38
+3.50	96.51
+3.75	99.18
+4.00	100.00

Percent Weight Error:	1.2389

Folk-Ward Statistical Parameters		
Graphic Mean:	2.3747	:Fine Sand
Incl Graph Standard Deviation:	0.7089	:Moderately Well Sorted
Incl Graph Skewness:	-0.0441	:Near Symmetrical
Graphic Kurtosis:	1.4309	:Leptokurtic
Normalized Kurtosis:		0.5886

Parameter by the Method of Moments	
Mean X:	2.4230
Varience:	0.5564
Skewness:	-0.8403
Standard Deviation:	0.7460
Kurtosis:	4.3956

Notes: Mica present; clumps up to 2.9 cm

Sample:	HDS 1-1-13	% Gravel:	0.40
Depth:	64.5-72.5	% Sand:	60.97
Level:	IV	% Silt/Clay:	38.63

PHI	Weight as Percentage of Cumulative Total
-1.00	0.00
-0.75	0.00
-0.50	0.00
-0.25	0.17
0.00	0.50
+0.25	0.83
+0.50	1.65
+0.75	2.81
+1.00	4.30
+1.25	5.29
+1.50	6.78
+1.75	9.92
+2.00	28.43
+2.25	50.74
+2.50	69.09
+2.75	81.49
+3.00	89.59
+3.25	94.38
+3.50	97.69
+3.75	99.50
+4.00	100.00

Percent Weight Error:	-1.0330

Folk-Ward Statistical Parameters		
Graphic Mean:	2.3005	:Fine Sand
Incl Graph Standard Deviation:	0.5700	:Moderately Well Sorted
Incl Graph Skewness:	0.0864	:Near Symmetrical
Graphic Kurtosis:	1.3055	:Leptokurtic
Normalized Kurtosis:		0.5662

Parameter by the Method of Moments	
Mean X:	2.3921
Varience:	0.3761
Skewness:	-0.5880
Standard Deviation:	0.6132
Kurtosis:	5.1211

Notes: Mica present; clumps up to 1.6 cm

Sample:	HDS 1-1-14	% Gravel:	0.07
Depth:	72.5-77.5	% Sand:	58.01
Level:	V	% Silt/Clay:	41.92

PHI	Weight as Percentage of Cumulative Total
-1.00	0.15
-0.75	0.15
-0.50	0.15
-0.25	0.15
0.00	0.15
+0.25	0.15
+0.50	0.31
+0.75	0.46
+1.00	0.77
+1.25	0.92
+1.50	1.69
+1.75	2.76
+2.00	4.76
+2.25	16.59
+2.50	47.93
+2.75	69.28
+3.00	82.03
+3.25	90.94
+3.50	96.77
+3.75	99.54
+4.00	100.00

Percent Weight Error:	-1.9220

Folk-Ward Statistical Parameters		
Graphic Mean:	2.6057	:Fine Sand
Incl Graph Standard Deviation:	0.4195	:Well Sorted
Incl Graph Skewness:	0.2834	:Fine Skewed
Graphic Kurtosis:	1.0669	:Mesokurtic
Normalized Kurtosis:		0.5162

Parameter by the Method of Moments	
Mean X:	2.7108
Varience:	0.2279
Skewness:	-0.7816
Standard Deviation:	0.4774
Kurtosis:	9.5626

Notes: Mica present; clumps up to 2 cm

Sample:	HDS 1-1-15	% Gravel:	0.00
Depth:	77.5-82.5	% Sand:	74.37
Level:	V	% Silt/Clay:	25.63

PHI	Weight as Percentage of Cumulative Total
-1.00	0.11
-0.75	0.11
-0.50	0.11
-0.25	0.11
0.00	0.11
+0.25	0.11
+0.50	0.33
+0.75	0.45
+1.00	0.67
+1.25	1.34
+1.50	2.12
+1.75	3.67
+2.00	14.03
+2.25	39.20
+2.50	61.25
+2.75	78.06
+3.00	88.75
+3.25	95.21
+3.50	98.66
+3.75	99.67
+4.00	100.00

Percent Weight Error:	-3.0694

Folk-Ward Statistical Parameters		
Graphic Mean:	2.4270	:Fine Sand
Incl Graph Standard Deviation:	0.4385	:Well Sorted
Incl Graph Skewness:	0.1895	:Fine Skewed
Graphic Kurtosis:	1.0047	:Mesokurtic
Normalized Kurtosis:		0.5012

Parameter by the Method of Moments	
Mean X:	2.5398
Varience:	0.2293
Skewness:	-0.3842
Standard Deviation:	0.4788
Kurtosis:	7.0228

Notes: Mica present; clumps up to 1.4 cm

Sample:	HDS 1-1-16	% Gravel:	0.40
Depth:	82.5-90	% Sand:	80.54
Level:	V	% Silt/Clay:	19.05

PHI	Weight as Percentage of Cumulative Total
-1.00	0.00
-0.75	0.00
-0.50	0.00
-0.25	0.00
0.00	0.37
+0.25	0.86
+0.50	1.34
+0.75	2.57
+1.00	3.55
+1.25	4.89
+1.50	6.23
+1.75	10.64
+2.00	26.04
+2.25	46.82
+2.50	66.63
+2.75	79.46
+3.00	88.39
+3.25	94.38
+3.50	97.80
+3.75	99.39
+4.00	100.00

Percent Weight Error:	-2.1822

Folk-Ward Statistical Parameters		
Graphic Mean:	2.3348	:Fine Sand
Incl Graph Standard Deviation:	0.5668	:Moderately Well Sorted
Incl Graph Skewness:	0.0609	:Near Symmetrical
Graphic Kurtosis:	1.2206	:Leptokurtic
Normalized Kurtosis:		0.5497

Parameter by the Method of Moments	
Mean X:	2.4267
Varience:	0.3689
Skewness:	-0.5604
Standard Deviation:	0.6073
Kurtosis:	4.8648

Notes: Mica present; clumps up to 1 cm

Sample:	HDS 1-1-17	% Gravel:	4.08
Depth:	90-95	% Sand:	79.29
Level:	VII	% Silt/Clay:	16.63

PHI	Weight as Percentage of Cumulative Total
-1.00	0.00
-0.75	0.00
-0.50	0.50
-0.25	0.75
0.00	2.13
+0.25	4.01
+0.50	7.64
+0.75	10.65
+1.00	14.29
+1.25	16.79
+1.50	22.81
+1.75	34.96
+2.00	48.12
+2.25	62.03
+2.50	74.94
+2.75	83.83
+3.00	90.23
+3.25	94.11
+3.50	96.62
+3.75	98.37
+4.00	100.00

Percent Weight Error:	0.6244

Folk-Ward Statistical Parameters		
Graphic Mean:	1.9871	:Medium Sand
Incl Graph Standard Deviation:	0.8540	:Moderately Sorted
Incl Graph Skewness:	-0.1122	:Coarse Skewed
Graphic Kurtosis:	1.2941	:Leptokurtic
Normalized Kurtosis:		0.5641

Parameter by the Method of Moments	
Mean X:	2.0930
Varience:	0.7408
Skewness:	-0.4056
Standard Deviation:	0.8607
Kurtosis:	3.2219

Notes: Mica present; clumps up to 1.7 cm; gravel up to 2.1 cm

Sample:	HDS 1-1-18	% Gravel:	4.75
Depth:	95-100	% Sand:	79.48
Level:	VII	% Silt/Clay:	15.78

PHI	Weight as Percentage of Cumulative Total
-1.00	0.00
-0.75	0.00
-0.50	0.12
-0.25	0.36
0.00	1.31
+0.25	3.46
+0.50	6.68
+0.75	10.86
+1.00	14.44
+1.25	19.45
+1.50	28.04
+1.75	42.96
+2.00	57.40
+2.25	71.72
+2.50	82.34
+2.75	89.38
+3.00	94.27
+3.25	97.26
+3.50	99.05
+3.75	99.88
+4.00	100.00

Percent Weight Error:	0.5096

Folk-Ward Statistical Parameters		
Graphic Mean:	1.8362	:Medium Sand
Incl Graph Standard Deviation:	0.7781	:Moderately Sorted
Incl Graph Skewness:	-0.0943	:Near Symmetrical
Graphic Kurtosis:	1.2045	:Leptokurtic
Normalized Kurtosis:		0.5464

Parameter by the Method of Moments	
Mean X:	1.9526
Varience:	0.5951
Skewness:	-0.3175
Standard Deviation:	0.7714
Kurtosis:	3.0732

Notes: Mica present; clumps up to 2.2 cm

Sample:	HDS 1-1-19	% Gravel:	2.45
Depth:	100-104	% Sand:	77.30
Level:	VII	% Silt/Clay:	20.24

PHI	Weight as Percentage of Cumulative Total
-1.00	0.00
-0.75	0.00
-0.50	0.00
-0.25	0.00
0.00	0.28
+0.25	1.69
+0.50	3.38
+0.75	6.75
+1.00	10.83
+1.25	15.47
+1.50	20.39
+1.75	30.52
+2.00	52.74
+2.25	67.93
+2.50	78.48
+2.75	86.78
+3.00	92.83
+3.25	96.48
+3.50	98.59
+3.75	99.72
+4.00	100.00

Percent Weight Error:	-0.5207

Folk-Ward Statistical Parameters		
Graphic Mean:	1.9708	:Medium Sand
Incl Graph Standard Deviation:	0.7304	:Moderately Sorted
Incl Graph Skewness:	-0.0318	:Near Symmetrical
Graphic Kurtosis:	1.2891	:Leptokurtic
Normalized Kurtosis:		0.5631

Parameter by the Method of Moments	
Mean X:	2.0928
Varience:	0.5153
Skewness:	-0.2614
Standard Deviation:	0.7178
Kurtosis:	3.2142

Notes: Mica present; clumps up to 1.9 cm

Sample:	HDS 1-1-20	% Gravel:	2.03
Depth:	104-108	% Sand:	68.76
Level:	VII	% Silt/Clay:	29.21

PHI	Weight as Percentage of Cumulative Total
-1.00	0.15
-0.75	0.15
-0.50	0.30
-0.25	0.30
0.00	0.91
+0.25	2.58
+0.50	4.56
+0.75	7.60
+1.00	11.25
+1.25	15.65
+1.50	20.52
+1.75	33.74
+2.00	53.34
+2.25	67.63
+2.50	77.51
+2.75	85.56
+3.00	91.64
+3.25	95.90
+3.50	98.48
+3.75	99.70
+4.00	100.00

Percent Weight Error:	1.2468

Folk-Ward Statistical Parameters		
Graphic Mean:	1.9756	:Medium Sand
Incl Graph Standard Deviation:	0.7616	:Moderately Sorted
Incl Graph Skewness:	-0.0150	:Near Symmetrical
Graphic Kurtosis:	1.2804	:Leptokurtic
Normalized Kurtosis:		0.5615

Parameter by the Method of Moments	
Mean X:	2.0813
Varience:	0.5794
Skewness:	-0.3741
Standard Deviation:	0.7612
Kurtosis:	3.5315

Notes: Mica present; clumps up to 2.3 cm

Sample:	HDS 1-1-21	% Gravel:	0.79
Depth:	108-113	% Sand:	58.64
Level:	VIII	% Silt/Clay:	40.57

PHI	Weight as Percentage of Cumulative Total
-1.00	0.00
-0.75	0.00
-0.50	0.00
-0.25	0.00
0.00	0.00
+0.25	0.38
+0.50	1.34
+0.75	2.48
+1.00	4.77
+1.25	7.06
+1.50	10.88
+1.75	17.56
+2.00	34.92
+2.25	60.50
+2.50	74.05
+2.75	83.40
+3.00	90.27
+3.25	95.04
+3.50	98.28
+3.75	99.62
+4.00	100.00

Percent Weight Error:	-1.5598

Folk-Ward Statistical Parameters		
Graphic Mean:	2.2037	:Fine Sand
Incl Graph Standard Deviation:	0.6069	:Moderately Well Sorted
Incl Graph Skewness:	0.0733	:Near Symmetrical
Graphic Kurtosis:	1.3631	:Leptokurtic
Normalized Kurtosis:		0.5768

Parameter by the Method of Moments	
Mean X:	2.2987
Varience:	0.3862
Skewness:	-0.2175
Standard Deviation:	0.6215
Kurtosis:	3.8036

Notes: Mica present; clumps up to 1.5 cm

Sample:	HDS 1-1-22	% Gravel:	0.00
Depth:	113-118	% Sand:	51.32
Level:	VIII	% Silt/Clay:	48.68

PHI	Weight as Percentage of Cumulative Total
-1.00	0.00
-0.75	0.00
-0.50	0.00
-0.25	0.00
0.00	0.00
+0.25	0.39
+0.50	0.78
+0.75	1.36
+1.00	1.95
+1.25	3.31
+1.50	5.84
+1.75	10.89
+2.00	25.10
+2.25	50.58
+2.50	68.68
+2.75	79.96
+3.00	88.52
+3.25	93.97
+3.50	97.86
+3.75	99.61
+4.00	100.00

Percent Weight Error:	0.0401

Folk-Ward Statistical Parameters		
Graphic Mean:	2.3174	:Fine Sand
Incl Graph Standard Deviation:	0.5447	:Moderately Well Sorted
Incl Graph Skewness:	0.1711	:Fine Skewed
Graphic Kurtosis:	1.2126	:Leptokurtic
Normalized Kurtosis:		0.5480

Parameter by the Method of Moments	
Mean X:	2.4280
Varience:	0.3217
Skewness:	-0.1637
Standard Deviation:	0.5672
Kurtosis:	4.2181

Notes: Mica present; clumps up to 1.6 cm

Sample:	HDS 1-1-23	% Gravel:	0.28
Depth:	118-123	% Sand:	58.66
Level:	VII	% Silt/Clay:	41.07

PHI	Weight as Percentage of Cumulative Total
-1.00	0.00
-0.75	0.00
-0.50	0.00
-0.25	0.14
0.00	0.28
+0.25	0.42
+0.50	0.83
+0.75	1.53
+1.00	2.77
+1.25	4.44
+1.50	8.18
+1.75	14.29
+2.00	35.23
+2.25	58.25
+2.50	69.76
+2.75	79.47
+3.00	87.52
+3.25	93.34
+3.50	97.23
+3.75	99.17
+4.00	100.00

Percent Weight Error:	-2.4461

Folk-Ward Statistical Parameters		
Graphic Mean:	2.2738	:Fine Sand
Incl Graph Standard Deviation:	0.5936	:Moderately Well Sorted
Incl Graph Skewness:	0.2301	:Fine Skewed
Graphic Kurtosis:	1.1204	:Leptokurtic
Normalized Kurtosis:		0.5284

Parameter by the Method of Moments	
Mean X:	2.3679
Varience:	0.3861
Skewness:	-0.0336
Standard Deviation:	0.6213
Kurtosis:	3.9078

Notes: Mica present; clumps up to 2.4 cm

Sample:	HDS 1-1-24	% Gravel:	0.42
Depth:	123-128	% Sand:	49.90
Level:	VII	% Silt/Clay:	49.68

PHI	Weight as Percentage of Cumulative Total
-1.00	0.00
-0.75	0.00
-0.50	0.00
-0.25	0.00
0.00	0.43
+0.25	0.87
+0.50	1.52
+0.75	2.38
+1.00	3.90
+1.25	6.28
+1.50	9.74
+1.75	15.37
+2.00	29.65
+2.25	51.73
+2.50	70.56
+2.75	80.74
+3.00	87.45
+3.25	92.86
+3.50	96.32
+3.75	99.13
+4.00	100.00

Percent Weight Error:	1.2754

Folk-Ward Statistical Parameters		
Graphic Mean:	2.2877	:Fine Sand
Incl Graph Standard Deviation:	0.6244	:Moderately Well Sorted
Incl Graph Skewness:	0.0905	:Near Symmetrical
Graphic Kurtosis:	1.3585	:Leptokurtic
Normalized Kurtosis:		0.5760

Parameter by the Method of Moments	
Mean X:	2.3777
Varience:	0.4252
Skewness:	-0.2999
Standard Deviation:	0.6521
Kurtosis:	4.1586

Notes: Mica present; clumps up to 2 cm

Sample:	HDS 1-1-25	% Gravel:	0.00
Depth:	128-133	% Sand:	35.19
Level:	VIII	% Silt/Clay:	64.81

PHI	Weight as Percentage of Cumulative Total
-1.00	0.00
-0.75	0.00
-0.50	0.00
-0.25	0.00
0.00	0.00
+0.25	0.00
+0.50	0.45
+0.75	1.36
+1.00	2.26
+1.25	3.17
+1.50	5.43
+1.75	9.50
+2.00	17.65
+2.25	38.01
+2.50	64.71
+2.75	81.45
+3.00	89.59
+3.25	93.21
+3.50	96.83
+3.75	99.10
+4.00	100.00

Percent Weight Error:	-0.9292

Folk-Ward Statistical Parameters		
Graphic Mean:	2.3800	:Fine Sand
Incl Graph Standard Deviation:	0.5108	:Moderately Well Sorted
Incl Graph Skewness:	0.0566	:Near Symmetrical
Graphic Kurtosis:	1.3973	:Leptokurtic
Normalized Kurtosis:		0.5829

Parameter by the Method of Moments	
Mean X:	2.4932
Varience:	0.3020
Skewness:	-0.2467
Standard Deviation:	0.5495
Kurtosis:	4.6035

Notes: Mica present; clumps up to 2 cm

Sample:	HDS 1-1-26	% Gravel:	0.41
Depth:	133-138	% Sand:	43.26
Level:	VII	% Silt/Clay:	56.33

PHI	Weight as Percentage of Cumulative Total
-1.00	1.22
-0.75	1.22
-0.50	1.22
-0.25	1.46
0.00	2.20
+0.25	3.17
+0.50	4.63
+0.75	6.59
+1.00	8.78
+1.25	10.73
+1.50	14.15
+1.75	20.73
+2.00	40.98
+2.25	62.68
+2.50	75.61
+2.75	84.18
+3.00	90.00
+3.25	94.39
+3.50	97.32
+3.75	99.27
+4.00	100.00

Percent Weight Error:	2.3604

Folk-Ward Statistical Parameters		
Graphic Mean:	2.1400	:Fine Sand
Incl Graph Standard Deviation:	0.7113	:Moderately Sorted
Incl Graph Skewness:	-0.0191	:Near Symmetrical
Graphic Kurtosis:	1.6472	:Very Leptokurtic
Normalized Kurtosis:		0.6222

Parameter by the Method of Moments	
Mean X:	2.1988
Varience:	0.6266
Skewness:	-1.0294
Standard Deviation:	0.7916
Kurtosis:	5.9003

Notes: Mica present; clumps up to 4 cm, most smaller than 2 cm

Sample:	HDS 1-1-27	% Gravel:	0.32
Depth:	138-143	% Sand:	48.11
Level:	VIII	% Silt/Clay:	51.56

PHI	Weight as Percentage of Cumulative Total
-1.00	0.00
-0.75	0.00
-0.50	0.00
-0.25	0.19
0.00	0.57
+0.25	1.15
+0.50	1.72
+0.75	3.07
+1.00	4.41
+1.25	7.28
+1.50	10.92
+1.75	16.67
+2.00	34.87
+2.25	57.47
+2.50	71.65
+2.75	80.84
+3.00	88.51
+3.25	93.68
+3.50	97.32
+3.75	99.43
+4.00	100.00

Percent Weight Error:	-0.7170

Folk-Ward Statistical Parameters		
Graphic Mean:	2.2471	:Fine Sand
Incl Graph Standard Deviation:	0.6298	:Moderately Well Sorted
Incl Graph Skewness:	0.1183	:Fine Skewed
Graphic Kurtosis:	1.2910	:Leptokurtic
Normalized Kurtosis:		0.5635

Parameter by the Method of Moments	
Mean X:	2.3257
Varience:	0.4409
Skewness:	-0.3610
Standard Deviation:	0.6640
Kurtosis:	4.1806

Notes: Mica present; clumps up to 3.6 cm

Sample:	HDS 1-1-28	% Gravel:	0.30
Depth:	143-148	% Sand:	53.05
Level:	VIII	% Silt/Clay:	46.65

PHI	Weight as Percentage of Cumulative Total
-1.00	0.00
-0.75	0.00
-0.50	0.00
-0.25	0.23
0.00	0.93
+0.25	1.40
+0.50	2.79
+0.75	4.65
+1.00	5.81
+1.25	8.37
+1.50	11.63
+1.75	18.84
+2.00	38.60
+2.25	62.79
+2.50	77.91
+2.75	86.05
+3.00	91.16
+3.25	94.88
+3.50	97.67
+3.75	99.30
+4.00	100.00

Percent Weight Error:	1.2516

Folk-Ward Statistical Parameters		
Graphic Mean:	2.1522	:Fine Sand
Incl Graph Standard Deviation:	0.6279	:Moderately Well Sorted
Incl Graph Skewness:	0.0190	:Near Symmetrical
Graphic Kurtosis:	7.5996	:Very Leptokurtic
Normalized Kurtosis:		0.6153

Parameter by the Method of Moments	
Mean X:	2.2424
Varience:	0.4428
Skewness:	-0.4632
Standard Deviation:	0.6654
Kurtosis:	4.6379

Notes: Mica present; clumps up to 2.4 cm

Sample:	HDS 1-1-29	% Gravel:	1.10
Depth:	148-153	% Sand:	62.56
Level:	VIII	% Silt/Clay:	36.34

PHI	Weight as Percentage of Cumulative Total
-1.00	0.00
-0.75	0.00
-0.50	0.00
-0.25	0.00
0.00	0.23
+0.25	1.15
+0.50	2.29
+0.75	3.67
+1.00	4.82
+1.25	6.88
+1.50	11.01
+1.75	16.74
+2.00	35.55
+2.25	64.68
+2.50	78.44
+2.75	86.47
+3.00	91.97
+3.25	95.64
+3.50	98.17
+3.75	99.54
+4.00	100.00

Percent Weight Error:	0.7930

Folk-Ward Statistical Parameters		
Graphic Mean:	2.1716	:Fine Sand
Incl Graph Standard Deviation:	0.5698	:Moderately Well Sorted
Incl Graph Skewness:	0.0702	:Near Symmetrical
Graphic Kurtosis:	1.5493	:Very Leptokurtic
Normalized Kurtosis:		0.6077

Parameter by the Method of Moments	
Mean X:	2.2569
Varience:	0.3830
Skewness:	-0.3944
Standard Deviation:	0.6189
Kurtosis:	4.6718

Notes: Mica present; clumps up to 2.6 cm

Sample:	HDS 1-1-30	% Gravel:	0.00
Depth:	153-158	% Sand:	63.33
Level:	VIII	% Silt/Clay:	36.67

PHI	Weight as Percentage of Cumulative Total
-1.00	0.00
-0.75	0.00
-0.50	0.00
-0.25	0.00
0.00	0.00
+0.25	0.28
+0.50	0.83
+0.75	1.53
+1.00	2.78
+1.25	4.31
+1.50	6.53
+1.75	15.00
+2.00	32.50
+2.25	55.83
+2.50	71.67
+2.75	82.08
+3.00	89.44
+3.25	94.31
+3.50	97.78
+3.75	99.58
+4.00	100.00

Percent Weight Error:	-0.2871

Folk-Ward Statistical Parameters		
Graphic Mean:	2.2556	:Fine Sand
Incl Graph Standard Deviation:	0.5615	:Moderately Well Sorted
Incl Graph Skewness:	0.1614	:Fine Skewed
Graphic Kurtosis:	1.1761	:Leptokurtic
Normalized Kurtosis:		0.5405

Parameter by the Method of Moments	
Mean X:	2.3639
Varience:	0.3438
Skewness:	-0.0522
Standard Deviation:	0.5863
Kurtosis:	3.9143

Notes: Mica present; clumps up to 2 cm

Sample:	HDS 1-2-31	% Gravel:	0.31
Depth:	158-163	% Sand:	74.99
Level:	IX	% Silt/Clay:	24.70

PHI	Weight as Percentage of Cumulative Total
-1.00	0.00
-0.75	0.00
-0.50	0.00
-0.25	0.00
0.00	0.00
+0.25	0.13
+0.50	0.65
+0.75	1.04
+1.00	1.03
+1.25	3.39
+1.50	5.48
+1.75	15.25
+2.00	34.03
+2.25	58.02
+2.50	77.84
+2.75	87.74
+3.00	93.22
+3.25	96.61
+3.50	98.83
+3.75	99.74
+4.00	100.00

Percent Weight Error:	-0.7295

Folk-Ward Statistical Parameters		
Graphic Mean:	2.1940	:Fine Sand
Incl Graph Standard Deviation:	0.4797	:Well Sorted
Incl Graph Skewness:	0.1176	:Fine Skewed
Graphic Kurtosis:	1.1839	:Leptokurtic
Normalized Kurtosis:		0.5421

Parameter by the Method of Moments	
Mean X:	2.3155
Varience:	0.2665
Skewness:	0.0104
Standard Deviation:	0.5162
Kurtosis:	4.4141

Notes: Mica present; clumps up to 2.2 cm

Sample:	HDS 1-2-32	% Gravel:	0.58
Depth:	163-168	% Sand:	84.13
Level:	IX	% Silt/Clay:	15.29

PHI	Weight as Percentage of Cumulative Total
-1.00	0.00
-0.75	0.18
-0.50	0.18
-0.25	0.18
0.00	0.37
+0.25	0.46
+0.50	0.65
+0.75	1.02
+1.00	1.57
+1.25	2.59
+1.50	4.62
+1.75	14.87
+2.00	42.47
+2.25	65.37
+2.50	78.86
+2.75	88.55
+3.00	94.18
+3.25	97.23
+3.50	98.98
+3.75	99.63
+4.00	100.00

Percent Weight Error:	-1.5677

Folk-Ward Statistical Parameters		
Graphic Mean:	2.1584	:Fine Sand
Incl Graph Standard Deviation:	0.4541	:Well Sorted
Incl Graph Skewness:	0.2633	:Fine Skewed
Graphic Kurtosis:	1.0880	:Mesokurtic
Normalized Kurtosis:		0.5211

Parameter by the Method of Moments	
Mean X:	2.2701
Varience:	0.2644
Skewness:	-0.1392
Standard Deviation:	0.5142
Kurtosis:	6.4536

Notes: Mica present; clumps up to 2.2 cm

Sample:	HDS 1-2-33	% Gravel:	0.95
Depth:	168-173	% Sand:	90.80
Level:	IX	% Silt/Clay:	8.25

PHI	Weight as Percentage of Cumulative Total
-1.00	0.00
-0.75	0.00
-0.50	0.09
-0.25	0.09
0.00	0.09
+0.25	0.09
+0.50	0.36
+0.75	0.44
+1.00	0.80
+1.25	1.60
+1.50	3.64
+1.75	24.71
+2.00	59.82
+2.25	79.64
+2.50	91.20
+2.75	96.44
+3.00	98.67
+3.25	99.38
+3.50	99.91
+3.75	100.00
+4.00	100.00

Percent Weight Error:	-0.7040

Folk-Ward Statistical Parameters		
Graphic Mean:	1.9736	:Medium Sand
Incl Graph Standard Deviation:	0.5509	:Well Sorted
Incl Graph Skewness:	0.2384	:Fine Skewed
Graphic Kurtosis:	1.0868	:Mesokurtic
Normalized Kurtosis:		0.5208

Parameter by the Method of Moments	
Mean X:	2.1076
Varience:	0.1465
Skewness:	0.2248
Standard Deviation:	0.3828
Kurtosis:	6.6292

Notes: Mica present; clumps up to 2.4 cm; small fragemts of hard rust colored material

Sample:	HDS 1-2-34	% Gravel:	0.28
Depth:	173-178	% Sand:	90.35
Level:	IX	% Silt/Clay:	9.37

PHI	Weight as Percentage of Cumulative Total
-1.00	0.00
-0.75	0.00
-0.50	0.00
-0.25	0.00
0.00	0.00
+0.25	0.57
+0.50	0.92
+0.75	1.49
+1.00	2.40
+1.25	3.55
+1.50	5.95
+1.75	19.34
+2.00	52.75
+2.25	75.06
+2.50	88.22
+2.75	94.85
+3.00	97.48
+3.25	98.86
+3.50	99.54
+3.75	99.89
+4.00	100.00

Percent Weight Error:	-2.6154

Folk-Ward Statistical Parameters		
Graphic Mean:	2.0290	:Fine Sand
Incl Graph Standard Deviation:	0.3896	:Well Sorted
Incl Graph Skewness:	0.1773	:Fine Skewed
Graphic Kurtosis:	1.2223	:Leptokurtic
Normalized Kurtosis:		0.5500

Parameter by the Method of Moments	
Mean X:	2.1479
Varience:	0.2047
Skewness:	-0.1596
Standard Deviation:	0.4525
Kurtosis:	6.1158

Notes: Mica present; clumps up to 2.3 cm; small fragemts of hard rust colored material

Sample:	HDS 1-2-35	% Gravel:	0.57
Depth:	178-182	% Sand:	89.03
Level:	IX	% Silt/Clay:	10.40

PHI	Weight as Percentage of Cumulative Total
-1.00	0.00
-0.75	0.00
-0.50	0.09
-0.25	0.19
0.00	0.19
+0.25	0.46
+0.50	0.93
+0.75	1.94
+1.00	3.89
+1.25	5.83
+1.50	9.07
+1.75	25.65
+2.00	54.63
+2.25	74.72
+2.50	87.69
+2.75	94.72
+3.00	97.69
+3.25	98.89
+3.50	99.63
+3.75	99.91
+4.00	100.00

Percent Weight Error:	-0.6949

Folk-Ward Statistical Parameters		
Graphic Mean:	1.9978	:Medium Sand
Incl Graph Standard Deviation:	0.4532	:Well Sorted
Incl Graph Skewness:	0.0675	:Near Symmetrical
Graphic Kurtosis:	1.2973	:Leptokurtic
Normalized Kurtosis:		0.5647

Parameter by the Method of Moments	
Mean X:	2.1097
Varience:	0.2440
Skewness:	-0.3475
Standard Deviation:	0.4939
Kurtosis:	5.5719

Notes: Mica present; small fragemts of hard rust colored material

Sample:	HDS 1-2-36	% Gravel:	5.09
Depth:	182-187	% Sand:	74.41
Level:	X	% Silt/Clay:	20.50

PHI	Weight as Percentage of Cumulative Total
-1.00	0.18
-0.75	0.18
-0.50	0.46
-0.25	0.55
0.00	0.91
+0.25	2.56
+0.50	5.57
+0.75	8.77
+1.00	11.69
+1.25	15.80
+1.50	25.66
+1.75	44.84
+2.00	65.94
+2.25	80.00
+2.50	89.50
+2.75	94.25
+3.00	96.71
+3.25	98.26
+3.50	99.27
+3.75	99.82
+4.00	100.00

Percent Weight Error:	

Folk-Ward Statistical Parameters		
Graphic Mean:		
Incl Graph Standard Deviation:		
Incl Graph Skewness:		
Graphic Kurtosis:		
Normalized Kurtosis:		

Parameter by the Method of Moments	
Mean X:	
Varience:	
Skewness:	
Standard Deviation:	
Kurtosis:	

Notes:

Sample:	HDS 1-2-37	% Gravel:	1.40
Depth:	187-192	% Sand:	55.94
Level:	X	% Silt/Clay:	42.66

PHI	Weight as Percentage of Cumulative Total
-1.00	0.14
-0.75	0.14
-0.50	0.14
-0.25	0.14
0.00	1.10
+0.25	3.17
+0.50	6.48
+0.75	11.03
+1.00	15.59
+1.25	20.41
+1.50	29.52
+1.75	44.55
+2.00	59.59
+2.25	69.93
+2.50	79.31
+2.75	86.76
+3.00	92.14
+3.25	95.72
+3.50	98.07
+3.75	99.59
+4.00	100.00

Percent Weight Error:	1.7392

Folk-Ward Statistical Parameters		
Graphic Mean:	1.8398	:Medium Sand
Incl Graph Standard Deviation:	0.8350	:Moderately Sorted
Incl Graph Skewness:	-0.0174	:Near Symmetrical
Graphic Kurtosis:	1.1418	:Leptokurtic
Normalized Kurtosis:		0.5331

Parameter by the Method of Moments	
Mean X:	1.9662
Varience:	0.6611
Skewness:	-0.1421
Standard Deviation:	0.8131
Kurtosis:	2.9506

Notes: Mica present; clumps up to 3.3 cm

Sample:	HDS 1-2-38	% Gravel:	1.60
Depth:	192-197	% Sand:	54.06
Level:	X	% Silt/Clay:	44.34

PHI	Weight as Percentage of Cumulative Total
-1.00	0.00
-0.75	0.00
-0.50	0.00
-0.25	0.42
0.00	2.32
+0.25	5.05
+0.50	8.42
+0.75	14.74
+1.00	19.79
+1.25	27.79
+1.50	39.58
+1.75	53.26
+2.00	63.79
+2.25	72.42
+2.50	80.63
+2.75	86.74
+3.00	91.79
+3.25	95.16
+3.50	97.68
+3.75	99.37
+4.00	100.00

Percent Weight Error:	1.8439

Folk-Ward Statistical Parameters		
Graphic Mean:	1.7136	:Medium Sand
Incl Graph Standard Deviation:	0.9099	:Moderately Sorted
Incl Graph Skewness:	0.0362	:Near Symmetrical
Graphic Kurtosis:	1.0523	:Mesokurtic
Normalized Kurtosis:		0.5127

Parameter by the Method of Moments	
Mean X:	1.8526
Varience:	0.7643
Skewness:	0.0545
Standard Deviation:	0.8743
Kurtosis:	2.6396

Notes: Mica present

Sample:	HDS 1-2-39	% Gravel:	2.33
Depth:	197-202	% Sand:	55.03
Level:	X	% Silt/Clay:	42.64

PHI	Weight as Percentage of Cumulative Total
-1.00	0.00
-0.75	0.00
-0.50	0.00
-0.25	0.17
0.00	0.87
+0.25	3.47
+0.50	8.51
+0.75	12.33
+1.00	18.40
+1.25	27.95
+1.50	42.71
+1.75	52.95
+2.00	63.72
+2.25	73.44
+2.50	79.69
+2.75	85.42
+3.00	90.45
+3.25	94.62
+3.50	97.57
+3.75	99.31
+4.00	100.00

Percent Weight Error:	1.1171

Folk-Ward Statistical Parameters		
Graphic Mean:	1.7558	:Medium Sand
Incl Graph Standard Deviation:	0.8947	:Moderately Sorted
Incl Graph Skewness:	0.1080	:Fine Skewed
Graphic Kurtosis:	1.0631	:Mesokurtic
Normalized Kurtosis:		0.5153

Parameter by the Method of Moments	
Mean X:	1.8711
Varience:	0.7472
Skewness:	0.1920
Standard Deviation:	0.8644
Kurtosis:	2.5716

Notes: Mica present

Sample:	HDS 1-2-40	% Gravel:	1.44
Depth:	202-207	% Sand:	54.68
Level:	X	% Silt/Clay:	43.88

PHI	Weight as Percentage of Cumulative Total
-1.00	0.00
-0.75	0.00
-0.50	0.16
-0.25	0.31
0.00	0.93
+0.25	4.04
+0.50	7.76
+0.75	14.60
+1.00	19.72
+1.25	29.97
+1.50	42.70
+1.75	54.50
+2.00	64.75
+2.25	73.60
+2.50	81.99
+2.75	88.20
+3.00	92.55
+3.25	95.65
+3.50	98.14
+3.75	99.53
+4.00	100.00

Percent Weight Error:	0.6956	
Folk-Ward Statistical Parameters		
Graphic Mean:	1.6847	:Medium Sand
Incl Graph Standard Deviation:	0.8774	:Moderately Sorted
Incl Graph Skewness:	0.0608	:Near Symmetrical
Graphic Kurtosis:	1.0160	:Mesokurtic
Normalized Kurtosis:		0.5040
Parameter by the Method of Moments		
Mean X:		1.8273
Varience:		0.7171
Skewness:		0.1408
Standard Deviation:		0.8468
Kurtosis:		2.6139

Notes: Mica present; clumps up to 3.1 cm

Sample:	HDS 1-2-41	% Gravel:	3.25
Depth:	207-212	% Sand:	53.01
Level:	X	% Silt/Clay:	43.73

PHI	Weight as Percentage of Cumulative Total
-1.00	0.00
-0.75	0.00
-0.50	0.11
-0.25	0.22
0.00	1.74
+0.25	4.78
+0.50	8.36
+0.75	13.03
+1.00	18.89
+1.25	25.19
+1.50	40.28
+1.75	52.23
+2.00	62.11
+2.25	71.88
+2.50	80.46
+2.75	86.32
+3.00	91.21
+3.25	95.01
+3.50	97.94
+3.75	99.57
+4.00	100.00

Percent Weight Error:	0.6324

Folk-Ward Statistical Parameters		
Graphic Mean:	1.7437	:Medium Sand
Incl Graph Standard Deviation:	0.8957	:Moderately Sorted
Incl Graph Skewness:	0.0522	:Near Symmetrical
Graphic Kurtosis:	1.1133	:Leptokurtic
Normalized Kurtosis:		0.5268

Parameter by the Method of Moments	
Mean X:	1.8768
Varience:	0.7458
Skewness:	0.0415
Standard Deviation:	0.8636
Kurtosis:	2.6320

Notes: Mica present; clumps up to 5.1 cm

Sample:	HDS 1-2-42	% Gravel:	12.02
Depth:	212-217	% Sand:	47.87
Level:	X	% Silt/Clay:	40.11

PHI	Weight as Percentage of Cumulative Total
-1.00	0.00
-0.75	0.00
-0.50	0.16
-0.25	0.16
0.00	0.98
+0.25	3.09
+0.50	7.15
+0.75	13.01
+1.00	18.05
+1.25	24.88
+1.50	32.52
+1.75	47.48
+2.00	61.79
+2.25	71.71
+2.50	80.49
+2.75	87.32
+3.00	91.06
+3.25	94.63
+3.50	97.56
+3.75	99.35
+4.00	100.00

Percent Weight Error:	0.2985

Folk-Ward Statistical Parameters		
Graphic Mean:	1.7737	:Medium Sand
Incl Graph Standard Deviation:	0.8740	:Moderately Sorted
Incl Graph Skewness:	-0.0072	:Near Symmetrical
Graphic Kurtosis:	1.0958	:Mesokurtic
Normalized Kurtosis:		0.5229

Parameter by the Method of Moments	
Mean X:	1.9215
Varience:	0.7080
Skewness:	0.0269
Standard Deviation:	0.8414
Kurtosis:	2.7313

Notes: Mica present; clumps up to 3.8 cm; possible FCR in gravel fraction

Sample:	HDS 1-2-43	% Gravel:	3.47
Depth:	217-222	% Sand:	51.02
Level:	X	% Silt/Clay:	45.52

PHI	Weight as Percentage of Cumulative Total
-1.00	0.12
-0.75	0.12
-0.50	0.12
-0.25	0.36
0.00	1.68
+0.25	4.93
+0.50	9.63
+0.75	15.28
+1.00	20.82
+1.25	27.80
+1.50	41.28
+1.75	53.55
+2.00	62.21
+2.25	71.60
+2.50	79.54
+2.75	85.92
+3.00	90.61
+3.25	94.71
+3.50	97.95
+3.75	99.76
+4.00	100.00

Percent Weight Error:	0.0168

Folk-Ward Statistical Parameters		
Graphic Mean:	1.7116	:Medium Sand
Incl Graph Standard Deviation:	0.9305	:Moderately Sorted
Incl Graph Skewness:	0.0552	:Near Symmetrical
Graphic Kurtosis:	1.0250	:Mesokurtic
Normalized Kurtosis:		0.5062

Parameter by the Method of Moments	
Mean X:	1.8550
Varience:	0.7949
Skewness:	0.0385
Standard Deviation:	0.8915
Kurtosis:	2.5283

Notes: Mica present

Sample:	HDS 1-2-44	% Gravel:	3.31
Depth:	222-227	% Sand:	46.46
Level:	X	% Silt/Clay:	50.23

PHI	Weight as Percentage of Cumulative Total
-1.00	0.13
-0.75	0.13
-0.50	0.26
-0.25	0.78
0.00	2.46
+0.25	6.21
+0.50	12.03
+0.75	19.66
+1.00	26.00
+1.25	32.34
+1.50	44.76
+1.75	60.54
+2.00	67.66
+2.25	73.22
+2.50	78.78
+2.75	84.86
+3.00	90.17
+3.25	94.44
+3.50	97.54
+3.75	99.35
+4.00	100.00

Percent Weight Error:	0.4821

Folk-Ward Statistical Parameters		
Graphic Mean:	1.6425	:Medium Sand
Incl Graph Standard Deviation:	0.9947	:Moderately Sorted
Incl Graph Skewness:	0.0906	:Near Symmetrical
Graphic Kurtosis:	0.9355	:Mesokurtic
Normalized Kurtosis:		0.4833

Parameter by the Method of Moments	
Mean X:	1.7717
Varience:	0.8887
Skewness:	0.1680
Standard Deviation:	0.9427
Kurtosis:	2.4569

Notes: Mica present; clumps up to 4 cm

Sample:	HDS 1-2-45	% Gravel:	3.32
Depth:	227-233	% Sand:	52.12
Level:	X	% Silt/Clay:	44.57

PHI	Weight as Percentage of Cumulative Total
-1.00	0.00
-0.75	0.00
-0.50	0.00
-0.25	0.49
0.00	3.16
+0.25	6.44
+0.50	12.03
+0.75	17.50
+1.00	23.69
+1.25	29.65
+1.50	38.15
+1.75	53.22
+2.00	64.64
+2.25	71.93
+2.50	78.13
+2.75	84.33
+3.00	89.55
+3.25	94.17
+3.50	97.57
+3.75	99.39
+4.00	100.00

Percent Weight Error:	0.7673

Folk-Ward Statistical Parameters		
Graphic Mean:	1.7050	:Medium Sand
Incl Graph Standard Deviation:	0.9943	:Moderately Sorted
Incl Graph Skewness:	0.0153	:Near Symmetrical
Graphic Kurtosis:	0.9853	:Mesokurtic
Normalized Kurtosis:		0.4963

Parameter by the Method of Moments	
Mean X:	1.8399
Varience:	0.8797
Skewness:	0.0298
Standard Deviation:	0.9379
Kurtosis:	2.4192

Notes: Mica present; clumps up to 4.9 cm

Sample:	HDS 1-2-46	% Gravel:	0.14
Depth:	233-234.5	% Sand:	58.26
Level:	XI	% Silt/Clay:	41.60

PHI	Weight as Percentage of Cumulative Total
-1.00	0.16
-0.75	0.16
-0.50	0.16
-0.25	0.16
0.00	0.49
+0.25	0.81
+0.50	1.47
+0.75	1.79
+1.00	2.77
+1.25	4.07
+1.50	6.35
+1.75	11.56
+2.00	32.08
+2.25	57.98
+2.50	72.80
+2.75	83.55
+3.00	90.07
+3.25	94.14
+3.50	97.39
+3.75	99.35
+4.00	100.00

Percent Weight Error:	-0.4138

Folk-Ward Statistical Parameters		
Graphic Mean:	2.2481	:Fine Sand
Incl Graph Standard Deviation:	0.5384	:Moderately Well Sorted
Incl Graph Skewness:	0.1990	:Fine Skewed
Graphic Kurtosis:	1.2630	:Leptokurtic
Normalized Kurtosis:		0.5581

Parameter by the Method of Moments	
Mean X:	2.3567
Varience:	0.3579
Skewness:	-0.3911
Standard Deviation:	0.5983
Kurtosis:	5.9514

Notes: Mica present; clumps up to 1.7 cm

Sample:	HDS 1-2-47	% Gravel:	0.20
Depth:	233-240	% Sand:	64.69
Level:	XIII	% Silt/Clay:	35.11

PHI	Weight as Percentage of Cumulative Total
-1.00	0.10
-0.75	0.10
-0.50	0.21
-0.25	0.21
0.00	0.31
+0.25	0.31
+0.50	0.42
+0.75	0.83
+1.00	1.14
+1.25	2.19
+1.50	3.85
+1.75	7.91
+2.00	20.50
+2.25	49.22
+2.50	69.41
+2.75	81.58
+3.00	89.39
+3.25	94.38
+3.50	97.61
+3.75	99.48
+4.00	100.00

Percent Weight Error:	-0.8870

Folk-Ward Statistical Parameters		
Graphic Mean:	2.3326	:Fine Sand
Incl Graph Standard Deviation:	0.4909	:Well Sorted
Incl Graph Skewness:	0.2205	:Fine Skewed
Graphic Kurtosis:	1.2296	:Leptokurtic
Normalized Kurtosis:		0.5515

Parameter by the Method of Moments	
Mean X:	2.4521
Varience:	0.2839
Skewness:	-0.2939
Standard Deviation:	0.5328
Kurtosis:	6.5713

Notes: Mica present; clumps up to 5.8 cm

Sample:	HDS 1-2-48	% Gravel:	0.00
Depth:	240-248	% Sand:	37.34
Level:	XIV	% Silt/Clay:	62.66

PHI	Weight as Percentage of Cumulative Total
-1.00	0.00
-0.75	0.00
-0.50	0.00
-0.25	0.00
0.00	0.00
+0.25	0.23
+0.50	0.23
+0.75	0.94
+1.00	1.87
+1.25	3.98
+1.50	7.73
+1.75	13.35
+2.00	23.65
+2.25	43.33
+2.50	65.34
+2.75	77.75
+3.00	85.95
+3.25	92.27
+3.50	96.49
+3.75	98.83
+4.00	100.00

Percent Weight Error:	-0.3155

Folk-Ward Statistical Parameters		
Graphic Mean:	2.3602	:Fine Sand
Incl Graph Standard Deviation:	0.5988	:Moderately Well Sorted
Incl Graph Skewness:	0.0645	:Near Symmetrical
Graphic Kurtosis:	1.2667	:Leptokurtic
Normalized Kurtosis:		0.5588

Parameter by the Method of Moments	
Mean X:	2.4701
Varience:	0.3625
Skewness:	-0.0709
Standard Deviation:	0.6021
Kurtosis:	3.5583

Notes: Mica present; clumps up to 4.4 cm, redder in color than the non-clumped portion of sample

Sample:	HDS 1-2-49	% Gravel:	0.32
Depth:	248-251	% Sand:	40.11
Level:	XIII	% Silt/Clay:	59.57

PHI	Weight as Percentage of Cumulative Total
-1.00	0.00
-0.75	0.00
-0.50	0.34
-0.25	0.34
0.00	0.34
+0.25	0.51
+0.50	0.51
+0.75	0.51
+1.00	0.51
+1.25	0.68
+1.50	1.53
+1.75	3.24
+2.00	7.67
+2.25	23.34
+2.50	48.21
+2.75	63.88
+3.00	76.66
+3.25	86.37
+3.50	93.87
+3.75	98.30
+4.00	100.00

Percent Weight Error:	-1.1916

Folk-Ward Statistical Parameters		
Graphic Mean:	2.6168	:Fine Sand
Incl Graph Standard Deviation:	0.5238	:Moderately Well Sorted
Incl Graph Skewness:	0.2293	:Fine Skewed
Graphic Kurtosis:	1.0026	:Mesokurtic
Normalized Kurtosis:		0.5007

Parameter by the Method of Moments	
Mean X:	2.7330
Varience:	0.3055
Skewness:	-0.5106
Standard Deviation:	0.5527
Kurtosis:	6.7252

Notes: Mica present; clumps up to 1.5 cm

Sample:	HDS 1-2-50	% Gravel:	0.00
Depth:	251-256	% Sand:	10.83
Level:	XV	% Silt/Clay:	89.17

PHI	Weight as Percentage of Cumulative Total
-1.00	0.00
-0.75	0.00
-0.50	0.00
-0.25	0.00
0.00	0.00
+0.25	0.00
+0.50	0.00
+0.75	0.00
+1.00	1.19
+1.25	1.19
+1.50	1.79
+1.75	4.17
+2.00	10.12
+2.25	18.45
+2.50	42.26
+2.75	66.07
+3.00	77.38
+3.25	85.71
+3.50	92.86
+3.75	97.02
+4.00	100.00

Percent Weight Error:	1.1679

Folk-Ward Statistical Parameters		
Graphic Mean:	2.6521	:Fine Sand
Incl Graph Standard Deviation:	0.5349	:Moderately Well Sorted
Incl Graph Skewness:	0.1720	:Fine Skewed
Graphic Kurtosis:	1.2019	:Leptokurtic
Normalized Kurtosis:		0.5459

Parameter by the Method of Moments	
Mean X:	2.7545
Varience:	0.2950
Skewness:	-0.0020
Standard Deviation:	0.5431
Kurtosis:	3.6487

Notes: Mica present; clumps up to 4.5 cm

Sample:	HDS 1-2-51	% Gravel:	0.00
Depth:	256-261	% Sand:	3.58
Level:	XV	% Silt/Clay:	96.42

PHI	Weight as Percentage of Cumulative Total
-1.00	0.00
-0.75	0.00
-0.50	0.00
-0.25	0.00
0.00	0.00
+0.25	0.00
+0.50	0.00
+0.75	0.00
+1.00	0.00
+1.25	0.00
+1.50	0.00
+1.75	2.33
+2.00	13.95
+2.25	25.58
+2.50	41.86
+2.75	58.14
+3.00	74.42
+3.25	86.05
+3.50	90.70
+3.75	97.67
+4.00	100.00

Percent Weight Error:	-14.6107

Folk-Ward Statistical Parameters		
Graphic Mean:	2.6250	:Fine Sand
Incl Graph Standard Deviation:	0.5703	:Moderately Well Sorted
Incl Graph Skewness:	0.0573	:Near Symmetrical
Graphic Kurtosis:	0.9766	:Mesokurtic
Normalized Kurtosis:		0.4941

Parameter by the Method of Moments	
Mean X:	2.7733
Varience:	0.2989
Skewness:	0.2548
Standard Deviation:	0.5467
Kurtosis:	2.3763

Notes: Sand fraction consists almost entirely of mica and hard rust colored material; hard clumps up to 3.2 cm; unable to improve percent error, sand fraction too small

Sample:	HDS 1-2-52	% Gravel:	0.00
Depth:	261-267	% Sand:	6.97
Level:	XV	% Silt/Clay:	93.03

PHI	Weight as Percentage of Cumulative Total
-1.00	0.00
-0.75	0.00
-0.50	0.00
-0.25	0.00
0.00	0.00
+0.25	0.00
+0.50	0.00
+0.75	0.00
+1.00	1.16
+1.25	4.65
+1.50	10.47
+1.75	19.77
+2.00	32.56
+2.25	58.14
+2.50	79.07
+2.75	87.21
+3.00	90.70
+3.25	93.02
+3.50	95.35
+3.75	98.84
+4.00	100.00

Percent Weight Error:	-1.7177

Folk-Ward Statistical Parameters		
Graphic Mean:	2.1569	:Fine Sand
Incl Graph Standard Deviation:	0.5836	:Moderately Well Sorted
Incl Graph Skewness:	0.0677	:Near Symmetrical
Graphic Kurtosis:	1.5032	:Very Leptokurtic
Normalized Kurtosis:		0.6005

Parameter by the Method of Moments	
Mean X:	2.3227
Varience:	0.3385
Skewness:	0.5432
Standard Deviation:	0.5818
Kurtosis:	3.7427

Notes: Mica present; clumps up to 2.7 cm

Sample:	HDS 1-2-53	% Gravel:	0.00
Depth:	267-270	% Sand:	75.80
Level:	XVI	% Silt/Clay:	24.20

PHI	Weight as Percentage of Cumulative Total
-1.00	0.00
-0.75	0.00
-0.50	0.00
-0.25	0.07
0.00	0.07
+0.25	0.07
+0.50	0.15
+0.75	1.05
+1.00	4.20
+1.25	11.69
+1.50	31.63
+1.75	60.34
+2.00	76.99
+2.25	86.51
+2.50	91.38
+2.75	94.30
+3.00	96.40
+3.25	97.90
+3.50	99.10
+3.75	99.78
+4.00	100.00

Percent Weight Error:	0.7179

Folk-Ward Statistical Parameters		
Graphic Mean:	1.7160	:Medium Sand
Incl Graph Standard Deviation:	0.4937	:Well Sorted
Incl Graph Skewness:	0.2451	:Fine Skewed
Graphic Kurtosis:	1.3379	:Leptokurtic
Normalized Kurtosis:		0.5723

Parameter by the Method of Moments	
Mean X:	1.8709
Varience:	0.2799
Skewness:	1.0414
Standard Deviation:	0.5291
Kurtosis:	5.0451

Notes: Mica present; clumps up to 2.1 cm

Sample:	HDS 1-2-54	% Gravel:	0.00
Depth:	270-272	% Sand:	56.13
Level:	XVII	% Silt/Clay:	43.87

PHI	Weight as Percentage of Cumulative Total
-1.00	0.00
-0.75	0.00
-0.50	0.12
-0.25	0.12
0.00	0.36
+0.25	0.36
+0.50	0.36
+0.75	0.60
+1.00	1.79
+1.25	5.02
+1.50	12.32
+1.75	25.96
+2.00	40.55
+2.25	52.39
+2.50	63.16
+2.75	73.92
+3.00	83.01
+3.25	89.95
+3.50	95.45
+3.75	98.56
+4.00	100.00

Percent Weight Error:	-0.2459

Folk-Ward Statistical Parameters		
Graphic Mean:	2.2675	:Fine Sand
Incl Graph Standard Deviation:	0.7051	:Moderately Well Sorted
Incl Graph Skewness:	0.1431	:Fine Skewed
Graphic Kurtosis:	0.8733	:Platykurtic
Normalized Kurtosis:		0.4662

Parameter by the Method of Moments	
Mean X:	2.3900
Varience:	0.4963
Skewness:	0.1006
Standard Deviation:	0.7045
Kurtosis:	2.7970

Notes: Mica present; clumps up to 2.7 cm

Sample:	HDS 1-2-55	% Gravel:	0.00
Depth:	272-274	% Sand:	17.22
Level:	XIX	% Silt/Clay:	82.78

PHI	Weight as Percentage of Cumulative Total
-1.00	0.00
-0.75	0.00
-0.50	0.00
-0.25	0.00
0.00	0.00
+0.25	0.46
+0.50	0.91
+0.75	0.91
+1.00	1.37
+1.25	3.20
+1.50	7.31
+1.75	14.16
+2.00	21.46
+2.25	31.05
+2.50	45.21
+2.75	58.90
+3.00	72.15
+3.25	82.19
+3.50	90.87
+3.75	96.80
+4.00	100.00

Percent Weight Error:	1.3150

Folk-Ward Statistical Parameters		
Graphic Mean:	2.5676	:Fine Sand
Incl Graph Standard Deviation:	0.7229	:Moderately Sorted
Incl Graph Skewness:	-0.0506	:Near Symmetrical
Graphic Kurtosis:	0.9691	:Mesokurtic
Normalized Kurtosis:		0.4921

Parameter by the Method of Moments	
Mean X:	2.6826
Varience:	0.5003
Skewness:	-0.3641
Standard Deviation:	0.7073
Kurtosis:	3.0061

Notes: Sand fraction consists almost entirely of mica and hard rust colored material

Sample:	HDS 1-2-56	% Gravel:	0.00
Depth:	272-280	% Sand:	8.50
Level:	XX	% Silt/Clay:	91.50

PHI	Weight as Percentage of Cumulative Total
-1.00	0.00
-0.75	0.00
-0.50	0.00
-0.25	0.00
0.00	0.00
+0.25	0.52
+0.50	0.52
+0.75	1.05
+1.00	3.66
+1.25	6.81
+1.50	13.61
+1.75	24.08
+2.00	31.41
+2.25	39.79
+2.50	55.50
+2.75	68.59
+3.00	76.44
+3.25	84.82
+3.50	93.19
+3.75	97.38
+4.00	100.00

Percent Weight Error:	-0.5271

Folk-Ward Statistical Parameters		
Graphic Mean:	2.3984	:Fine Sand
Incl Graph Standard Deviation:	0.7962	:Moderately Well Sorted
Incl Graph Skewness:	-0.0349	:Near Symmetrical
Graphic Kurtosis:	0.8741	:Platykurtic
Normalized Kurtosis:		0.4664

Parameter by the Method of Moments	
Mean X:	2.5065
Varience:	0.5841
Skewness:	-0.1578
Standard Deviation:	0.7642
Kurtosis:	2.4941

Notes: Sand fraction consists almost entirely of mica and hard rust colored material; clumps up to 4 cm

Sample:	HDS 1-2-57	% Gravel:	0.00
Depth:	280-282.5	% Sand:	3.00
Level:	XXI	% Silt/Clay:	97.00

PHI	Weight as Percentage of Cumulative Total
-1.00	0.00
-0.75	0.00
-0.50	0.00
-0.25	0.00
0.00	0.00
+0.25	0.00
+0.50	0.00
+0.75	0.00
+1.00	0.00
+1.25	2.78
+1.50	5.56
+1.75	11.11
+2.00	13.89
+2.25	19.44
+2.50	36.11
+2.75	44.67
+3.00	50.00
+3.25	61.11
+3.50	72.22
+3.75	97.22
+4.00	100.00

Percent Weight Error:	-7.9641

Folk-Ward Statistical Parameters		
Graphic Mean:	2.9043	:Fine Sand
Incl Graph Standard Deviation:	0.7258	:Moderately Sorted
Incl Graph Skewness:	-0.2748	:Coarse Skewed
Graphic Kurtosis:	0.7815	:Platykurtic
Normalized Kurtosis:		0.4387

Parameter by the Method of Moments	
Mean X:	2.9722
Varience:	0.5409
Skewness:	-0.5784
Standard Deviation:	0.7355
Kurtosis:	2.3207

Notes: Sand fraction consists almost entirely of mica and hard rust colored material

BIOGRAPHY OF THE AUTHOR

Paul M. Pluta was born in Phoenixville, Pennsylvania in 1988. He graduated from Phoenixville Area High School in 2006 before moving to Philadelphia, Pennsylvania to attend Temple University. In college Paul began study of anthropological archaeology and gained archaeological field and laboratory experience on a variety of projects in Pennsylvania and New Jersey. He graduated in 2010 with a B.A. in anthropology and a B.A. in philosophy.

Following his graduation from Temple, Paul worked full-time as an archeological technician for The University of Wyoming, Metcalf Archaeological Consultants, Environmental Planning Group and The State Museum of Pennsylvania, participating in projects in Wyoming, Montana, Oregon and Pennsylvania. Paul entered the graduate program in The Climate Change Institute at The University of Maine in the Fall of 2012, where he began research on geoarchaeology and climate change in coastal Peru. He is a candidate for the Master of Science degree in Quaternary and Climate Studies from The University of Maine in December, 2015.